University of Hohenheim

Institute of Nutritional Medicine and Prevention

Director: Prof. Dr. med. Stephan C. Bischoff

Role of plasminogen activator inhibitor (PAI-1) in the pathogenesis of fructose-induced non-alcoholic fatty liver disease (NAFLD)

Dissertation

Submitted in fulfilment of the requirements for the degree

"Dr. rer. nat." / Ph.D in Natural sciences to the

Faculty of Natural Sciences at University of Hohenheim

Submitted by

Giridhar Kanuri

born in Kovvali, India

2012

Date of oral examination : 23.07.12

Examiners:
Dean: Prof. H Breer
Supervisor: Prof. S C Bischoff
Co-supervisor: Prof. L Graeve
Additional examiner: PD. I Bergheim

Abbreviations

NAFLD	Non-alcoholic fatty liver disease
TNF α	Tumor necrosis factor α
TNFR1	Tumor necrosis factor receptor 1
PAI-1	Plasminogen activator inhibitor 1
Akt	Protein kinase B
SREBP-1	Sterol regulatory element-binding protein 1
ALT	Alanine aminotransferase
FAS	Fatty acid synthase
ATP	Adenosine triphosphate
AMPK	Adenosine monophosphate activated protein kinase
CCL2	Chemokine (C-C motif) ligand 2
CCL19	Chemokine (C-C motif) ligand 19
ICAM-1	Inter-cellular adhesion molecule 1
PEPCK	Phosphoenolpyruvate carboxykinase
ApoB	Apolipoprotein B
CD1d	Cluster of differentiation 1d
HGF	Hepatic growth factor
IFN γ	Interferon gamma γ
IL15	Interleukin 15
MTTP	Microsomal triglyceride transfer protein
NK1.1	Natural killer 1.1
PI3K	Phosphoinositide 3-kinase
RBP4	Retinol binding protein-4
VLDL	Very low density lipoprotein
BCL XL	B-cell lymphoma-extra large
GLUT 4	Glucose transporter type 4
AML 12	Alpha mouse liver 12
uPA	Urokinase-type plasminogen activator
iNKT cells	invariant natural killer T cells

CD3ζ	Cluster of differentiation 3ζ
LPS	Lipopolysaccharide
RNA	Ribose nucleic acid
PCR	Polymerase chain reaction
RT-PCR	reverse transcription polymerase chain reaction
iNOS	Inducible nitric oxide synthase
FCS	Foetal calf serum
SDS	Sodium dodecyl sulfate
DTT	1,4 Dithiothreit
TEMED	Tetramethylethylenediamine,
EDTA	Ethylenedinitrilotetraacetic acid
dNTP	Deoxyribonucleotide triphosphate
BSA	Bovine serum albumin
HCl	Hydrochloric acid
APS	Ammonium persulfate
PBS	Phosphate buffer saline
NO	Nitric oxide
µM	Micro molar
ng	Nano gram
mM	Milli molar
h	Hours
OD	Optical density

Index

1 Introduction

1.1 Prevalence and mechanism of non-alcoholic fatty liver disease (NAFLD)

Non-alcoholic fatty liver disease (NAFLD) is one of most common liver disease worldwide, affecting almost 30% of the general population in developed countries (data from US) and 10% of the general population in developing countries (1). NAFLD, as the name indicates occurs in the absence of significant alcohol consumption (<20 g ethanol/d) or other known causes of steatosis such as abuse of drugs or toxins. Histologically, the first stage of NAFLD is steatosis and this can continue to steatohepatitis finally leading to fibrosis and cirrhosis. Historically, steatosis was thought to be benign state of liver disease; however, recent studies (2) have indicated that fatty livers are more vulnerable to injury from various causes and can progress to steatohepatitis, increasing the probability of further liver-related morbidity and mortality (3). Worldwide, the prevalence and incidence of NAFLD is increasing as the worldwide prevalence of overweight and obesity increased and the developing countries shifting towards a western lifestyle. In general NAFLD affects substantial proportion of general population from several countries. The prevalence of NAFLD in the selected study populations in different countries is summarized in Table 1.

Table 1: Recent studies on prevalence of NAFLD in different countries in the selected study population

Author	**Country**	**Prevalence of NAFLD %**
Browing 2004 [4]	USA	31%
Bedogni 2005 [5]	Italy	23%
Luyckx 1998 [6]	Belgium	74%
Fan 2005 [7]	China	15%
Dixon 2001 [8]	Australia	71%
Park 2006 [9]	South Korea	16%
Kamikowski 2007 [10]	Brazil	35%
Das 2010 [11]	India	10%

In the past 30 years, the prevalence of NAFLD has increased paralleling that of obesity, type 2 diabetes and metabolic syndrome. However, recent epidemiological studies suggest that certain dietary patterns (e.g. diet rich in fructose) may also be associated with an increased risk to develop NAFLD (for overview see (12)).

Mechanism of NAFLD

Several animal and human studies suggest that an increased intestinal permeability and endotoxemia may be involved in the pathogenesis of NAFLD (13-15). Indeed, Bode *et al.* were the first to report that endotoxemia is not only associated with alcoholic cirrohsis patients but also in non-alcoholic cirrohsis patients (16). Moreover, results of Wigg *et al.* suggest that the prevalence of intestinal bacterial growth, intestinal permeability and endotoxemia is increased in NASH patients (17). Recent studies in 35 biopsy proven NAFLD patients and health volunteers by Miele *et al.* revealed that NAFLD is associated with increased intestinal permeability due to an increased prevalence of small intestinal bacterial overgrowth (18). Furthermore, we recently showed that NAFLD patients have an altered intestinal permeability, higher endotoxin levels and that this was associated with an elevated expression of the endotoxin receptor toll like receptor-4 (TLR-4) (19, 20).

In support of these human studies, we also recently reported that chronic fructose consumption in mice (30% fructose solution) is associated with an increased intestinal translocation of bacterial endotoxin into the portal vein (21). Furthermore, in various settings of liver diseases (e.g. alcoholic liver disease) it was shown that endotoxin binds to the lipopolysaccharide binding protein (LBP) which is produced by hepatocytes (22). The binding of endotoxin to LBP facilitates the transfer of endotoxin to the membrane bound cluster of differentiation (CD14) thereby activating Kupffer cells (22). The activation of Kupffer cells is then mediated through Toll like receptor (TLR 4). The activation of TLR 4 turns on to an intracellular signalling cascade, which is mediated via MyD88 (23). MyD88 associates with interleukin-1 receptor-associated kinase (IRAK) and tumour necrosis factor (TNF) - activated factor-6 (TRAF 6). This in turn results in the translocation of nuclear factor-κB (NF-κB) into the nucleus and the production of proinflammatory cytokines (e.g. TNF-α) (24, 25).

Furthermore, results of Lida *et al*. showed that stimulation of Kupffer cells with endotoxin produce large amounts of the free radical nitric oxide ($NO^{\cdot}$) synthesized by the inducible form of nitric oxide synthase (iNOS) (26). The role of TNFα in the pathogenesis of NAFLD has been suggested before. For instance, animal studies have shown that antibodies against TNF improved NAFLD in obese mice. Furthermore, in diet induced (e.g. MCD diet, high fat diet) animal models of NAFLD an increased expression of TNFα has repeatedly been shown to be involved in the progression of the disease (27, 28). In line with these findings results of human studies have also shown an increased expression of TNFα in NAFLD patients (29). Additionally, we and others reported that patients with NAFLD have elevated hepatic and plasma levels of plasminogen activator inhibitor-1 (PAI-1) in comparison to controls (19, 30). Moreover, it was also shown that plasma PAI-1 levels and hepatic PAI-1 expression was increased in genetically obese mice (31). It has further been shown in animal models of acute alcohol-induced liver steatosis and in *in vitro* experiments that TNFα induced PAI-1 is involved in mediating the pivotal effect of TNFα on the liver (32). PAI-1 is an acute phase protein that inhibits fibrinolysis by inactivating urokinase-type and tissue-type plasminogen activator (33). PAI-1 has also lately been linked to the onset but also to the progression of liver diseases of various etiologies (e.g. alcohol, endotoxin) (for overview see (34)). For instance, in settings of alcohol-induced liver damage PAI-1 was shown to impair HGF/c-Met signaling cascade, which in turn impairs hepatic lipid export (32). However, how TNFα is involved in the onset of PAI-1 and progression of NAFLD has not yet been determined.

1.2 Fructose

Fructose Intake

Fructose is one of the main sugars consumed in diet besides glucose and sucrose. Sucrose is made of glucose and fructose to equal parts. Since 1970 sucrose (refined sugar) has more and more been replaced by High Fructose Corn Syrup (HFCS), a sugar derived from corn which contains 42-90% fructose in the United States (35, 36). In recent years sucrose is also more and more frequently replaced by fructose-glucose syrup containing at least 50% of fructose or plain fructose syrup in Europe.

Indeed in the US fructose consumption has increased five fold over the last century and in the last 30 years it's doubled. Recent data from Vos *et al.* indicate that fructose consumption was ~ 15g/day before 1900. However, this had increased to ~24g/day before World War II and to ~55g/day by 1994. Today the daily intake is estimated to be ~73 g/day (37). Reasons for this markedly increased intake may be the increased consumption of soft drinks and juice beverages containing sucrose or high fructose corn syrup (HFCS). For instance, food consumption studies (1965-1996) involving US adolescents revealed that there were large increases in the intake of soft drinks and non-citrus juices (38). In line with these findings results of Bray *et al.* indicate that the consumption of HFCS-55 (sweetener used in soft drinks) in the US has increased by 1000% between 1970 and 1990 (39). Recent results of an Italian survey on over 3300 subjects revealed that the mean daily consumption of soft drinks in Italy is as follows: 132g/day female adolescents, 203g/d in male adolescents, 114g/d in female adults, 147g/d in adult males (40)

Fructose consumption and health

Results of various studies in humans suggest that an excessive consumption of fructose is associated with clinical and biochemical symptoms of abdominal obesity, insulin resistance, dyslipidemia and the occurrence of metabolic as well as cardiovascular disorders (41). For instance, a cross-sectional study using data collected from the National Health and Nutrition Examination Survey (NHANES 2003 to 2006) involving 4528 adults without a history of hypertension revealed that a consumption of 74g/d fructose was associated with significantly higher blood pressure levels (42). Furthermore, the data analysis from the National Health and Nutrition Examination Survey over 6000 US adults revealed a significant correlation between consumption of caloric sweeteners (e.g. HFCS 55) and blood lipid levels (43). The dietary and life style information collected by Finnish Mobile Clinic Health Examination Survey in Finland from 51522 non-diabetic men and women suggest that consumption of sweetened fruit juices and soft drinks is associated with an increased risk to develop diabetes (44). Furthermore, the results of Framingham Heart Study conducted in 6039 participants suggest that consumption of more than one can of soft drink per day is associated with occurrence of metabolic syndrome (e.g. high blood pressure, waist circumference >35 cm females, >40 cm males, increased plasma triglycerides, increased fasting glucose, low HDL cholesterol) (45).

Additionally, weight gain was also observed in 14 diabetic men (11 with type 2 diabetes mellitus, 3 with type 1 diabetes mellitus) who consumed a diet supplemented with 50-60g fructose/d for 24 weeks (46). In a randomized controlled trail including 74 adult men consumption of 200g fructose/day for 2 weeks was associated with increased blood pressure levels and decreased high density lipoprotein levels (47). Consumption of fructose sweetened beverages for 10 weeks in 32 overweight or obese subjects resulted in the development of visceral obesity and increased lipoprotein levels in comparison to glucose consuming subjects. In addition, fasting plasma glucose levels, insulin levels and insulin resistance increased in subjects consuming fructose but not in subjects consuming glucose (48). Recently, results of Le *et al.* indicated that consumption of high fructose diet for one week in healthy young men increased fat deposition in the liver as well as in skeletal muscle (49). Taken together, the question if fructose intake is a general risk factor for the development of obesity has not been fully clarified; however, results of intervention studies, where excessive additional fructose was offered to participants indicate that elevated fructose intake is associated with the development of abdominal obesity. However, molecular mechanisms involved have not been fully understood.

Cellular metabolism of fructose

In the small intestine uptake of fructose is mediated through glucose transporter-5 (GLUT5), located at both the apical lumen facing side of the intestine and the basolateral enterocytes facing membranes (Figure 1) (50).

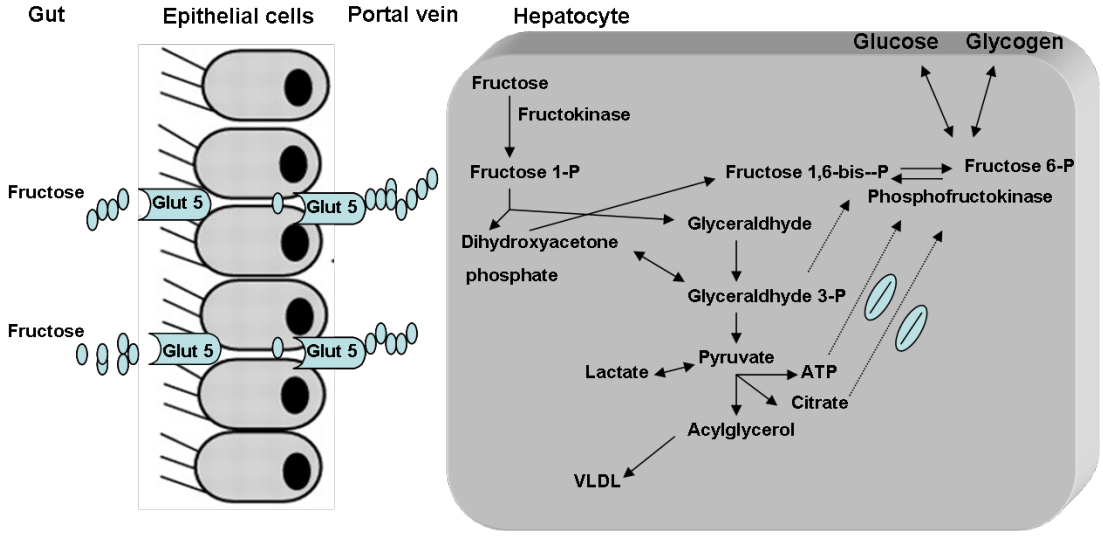

Figure 1: Fructose and its hepatic metabolism. Glut 5 located at the intestinal membranes mediates fructose transport to portal blood. In the liver fructose is phospohorylated to fructose-1-phosphate, which is then further metabolized into glyceraldehyde, dihydroxyacetone phosphate. Thus, fructose enters the glyolytic pathway at the glyceraldehyde or dihydroxyacetone phosphate level respectively, thereby by-passing the major step of the glycolysis, which are controlled through insulin. Glut 5: glucose transporter 5, VLDL: very low density lipoprotein, ATP: adenosine tri-phosphate.

The absorbed fructose is taken up by the liver with help of glucose transporter 2 (GLUT 2) (51, 52) so that only a modest escapes hepatic metabolism and enters systemic circulation. In the liver, fructose is phosphorylated by fructokinase to fructose-1-phosphate, which is then further metabolized into glyceraldehyde, dihydroxyacetone phosphate and glyceraldehyde-3-phosphate, respectively. Dihydroxyacetone phosphate and glyceraldehyde-3-phosphate may either be converted to glucose or triglycerides. Fructose thereby bypasses the major step in glycolysis, which is catalysed by the rate-limiting enzyme phosphofructokinase and is tightly regulated by insulin. Therefore, fructose can continuously enter the glycolytic/gluconeogenic pathway and produce glucose, glycogen, lactate and pyruvate without the control of insulin (Figure 1) (41, 53, 53). Pyruvate and lactate are then converted to acyl-glycerol, a molecule which is esterified leading to the formation of triglycerides and subsequently very-low-density lipoprotein (VLDL).

Fructose and NAFLD

Emerging evidences suggest that consumption of carbohydrate rich diet and herein particularly a fructose rich diet may be involved in the development of liver damage. Indeed, results of recent human studies carried out in the US in 427 adults revealed a link between increased consumption of fructose and hepatic inflammation and fibrosis (54). Zelber-Sagi *et al.* found a significant difference between the dietary patterns of NAFLD patients and controls in Israel. Specifically, NAFLD patients consumed larger amounts of sugar-sweetened soft drinks than the controls (55).

These results were also confirmed in two small studies of our own group where we found that the total carbohydrate intake of patients with NAFLD did not differ from that of controls; however, fructose intake of patients with various stages of NAFLD (e.g. steatosis and steatohepatitis) was higher in comparison to controls (19, 20). Indeed, Thuy *et al.* reported that the total fructose intake was markedly higher by ~10g/day in NAFLD patients than in controls (19). In the US the assessment of dietary fructose intake in NAFLD patients revealed that NAFLD patients consumed ~2.1-fold more HFCS containing sweets and beverages than controls (56). In support of these human studies, studies in rodents of our own group and others have also shown that increased consumption of fructose (e.g. 30-60 % of daily calories derived from fructose) may result in an increased lipid accumulation in the liver accompanied with insulin resistance, elevated plasma triglycerides levels and oxidative stress as well as hepatic tumor necrosis factor (TNFα) expression (21, 57-59). This effect was not found in mice concomitantly treated with antibiotics or deletion of TLR 4 or deletion of iNOS (21, 60, 61). Additionally, this protective effect of antibiotic treatment or deletion of iNOS is also associated with decreased phosphorylation of IκB.

Taken together, these studies suggest that chronic fructose consumption is associated with an increased lipid accumulation in the liver, inflammation and insulin resistance suggesting that besides de novo lipogenesis of fructose other mechanisms might also be involved in the pathogenesis of fructose-induced NAFLD.

1.3 Aims

Worldwide the prevalence of overweight and obesity as well as insulin resistance associated diseases like NAFLD has increased throughout the last decades (41). Alterations of diet like an increased intake of refined sugar and herein particularly fructose are discussed as risk factors for the development of NAFLD (62). In recent years our own group has shown that chronic fructose intake in rodents is associated with an increased translocation of bacterial endotoxin from the gut and subsequently an activation of the TLR-4 signaling cascade in the liver (21, 60). However, molecular mechanisms involved in the damaging effects of fructose on the liver have not been clarified. Therefore, the aim of the present study is to investigate the role TNFα and PAI-1 in the onset of fructose-induced NAFLD in a mouse model as well as in human NAFLD patients. The specific aims were:

1) Are TNFR1-/- mice protected from fructose-induced NAFLD? If yes, what are the molecular mechanisms involved?

2) Are PAI-1-/- mice protected from fructose-induced NAFLD? And if so, what are the molecular mechanisms involved?

3) Are molecular mechanisms identified in mouse studies in regards to the development of NAFLD also relevant to human situation?

2 Materials and Methods

2.1 Materials

2.1.1 Animals and treatments

C57BL/6J mice	Jackson, Main, USA
TNFR1 -/- mice (Tnfrsf1a$^{tm1Mak/J}$)	Jackson, Main, USA
PAI-1 -/- mice (Serpine1^{tm1Mlg})	Jackson, Main, USA
Feed (Chow)	ssniff® Spezialdiäten GmbH, Soest, Germany
Cages 360cm^2	Techniplast Deutschland GmbH, Hohenpeißenberg, Germany
Ketamine	BelaPharm GmbH, Fechta, Germany
Xylazine	Bayer AG, Leverkusen, Germany
Fragmin® P Forte	Pfizer Pharma GmbH, Karlsruhe, Germany
Sodium chloride ≥99,8%	CarlRoth GmbH & Co, Karlsruhe, Germany
Syringes 1ml	B/Braun Melsungen, Melsungen, Germany
Needles	B/Braun Melsungen, Melsungen, Germany

2.1.2 Cell culture and treatments

AML-12 cells	LGC Promochem, Wesel
PAI-1	Sigma, Steinheim, Germany
DMEM/F12 medium	PAN Biotech GmbH, Aidenbach
ITS	PAA-Laboratories, Colbe, Germany
Dexamethasone	PAA-Laboratories, Colbe, Germany
BSA	Sigma, Steinheim, Germany
FCS	Biochrom AG, Berlin
Penicillin/ Streptomycin (10.000 U Penicillin/ml) 10mg Streptomycin/ml)	PAN Biotech GmbH, Aidenbach
PBS	PAN Biotech GmbH, Aidenbach
HGF	Sigma, Steinheim, Germany
Trypsin/EDTA solution	PAA-Laboratories, Colbe, Germany

2.1.2 Human subjects and tissue collection

RNA-later	Ambion, England
Aprotinin	CarlRoth GmBH & Co, Karlsruhe, Germany
EDTA tubes	Sarstedt, Nümbrecht, Germany
Li-heparin tubes	Sarstedt, Nümbrecht, Germany

2.1.3 Real time RT-PCR

RNA isolation

peqGOLD TriFast™	Pequlab Biotechnologie GmbH, Erlangen, Germany
Chloroform >99%	CarlRoth GmBH & Co, Karlsruhe, Germany
Isoproponal >99.5%	CarlRoth GmBH & Co, Karlsruhe, Germany
Ethanol absolute	Merk, Darmstadt, Germany
RNase free water	Gibco/In vitrogen Corp., Karlsruhe, Germany

cDNA synthesis

5x MulV Buffer	Fermantas GmbH, St. Leon-Rot, Germany
DNase (1U/µl)	Fermantas GmbH, St. Leon-Rot, Germany
EDTA	CarlRoth GmBH & Co, Karlsruhe, Germany
Oligo dT	Genaxxon Bioscience GmBH, Biberach, Germany
dNTP	Genaxxon Bioscience GmBH, Biberach, Germany
MulV reverse transcriptase (20U/µl)	Fermantas GmbH, St. Leon-Rot, Germany

cDNA synthesis for PAI-1

Baseline-Zero DNase	Epicentre Biotechnologies, Madison, USA
MMLV cDNA Synthesis Kit (No.: M5-70702)	Epicentre Biotechnologies, Madison, USA

PCR

SYBR Green	Applied Biosystems, Darmstadt, Germany
All the primers used	MWG-Biotech, Ebersberg, Germany
12-well-Strips, 200µl Thin wall	Bio-Rad Laboratories, Munich, Germany
RT-PCR-i cycler	Bio-Rad Laboratories, Munich, Germany

2.1.4 Western Blotting

Cytosolic protein isolation

HEPES	CarlRoth GmBH & Co, Karlsruhe, Germany
$MgCl_2$	CarlRoth GmBH & Co, Karlsruhe, Germany
KCl	CarlRoth GmBH & Co, Karlsruhe, Germany
Glycerol	CarlRoth GmBH & Co, Karlsruhe, Germany
EDTA	CarlRoth GmBH & Co, Karlsruhe, Germany
DTT	CarlRoth GmBH & Co, Karlsruhe, Germany

RIPA protein isolation

MOPS	CarlRoth GmBH & Co, Karlsruhe, Germany
Nacl	CarlRoth GmBH & Co, Karlsruhe, Germany
Nonidet P-40	CarlRoth GmBH & Co, Karlsruhe, Germany
SDS	CarlRoth GmBH & Co, Karlsruhe, Germany
Proteinase inhibitor cocktail	Sigma Aldrich, Steinheim, Germany
Tyrosine inhibitor cocktail	Sigma Aldrich, Steinheim, Germany
Ser/Thr phosphates inhibitor cocktail	Sigma Aldrich, Steinheim, Germany

Bradford assay

Biorad dye	Bio-Rad Laboratories, Munich, Germany
BSA	CarlRoth GmBH & Co, Karlsruhe, Germany

Gel preparation and blotting

SDS	CarlRoth GmBH & Co, Karlsruhe, Germany
Tris –Base	CarlRoth GmBH & Co, Karlsruhe, Germany
HCL	CarlRoth GmBH & Co, Karlsruhe, Germany
Ammoniumpersulfate	CarlRoth GmBH & Co, Karlsruhe, Germany
Glycine	CarlRoth GmBH & Co, Karlsruhe, Germany
Methanol	CarlRoth GmBH & Co, Karlsruhe, Germany
Rainbow marker	GE Healthcare Europe, Frieburg, Germany
Acrylamide/Bis- solution (30 %)	Bio-Rad Laboratories, Munich, Germany
10% SDS	Gibco/In vitrogen Corp., Karlsruhe, Germany
TEMED	Sigma Aldrich, Steinheim, Germany
Ponceau S Solution	Sigma Aldrich, Steinheim, Germany
β-actin, Akt, AMPK, c-Met, phospho Akt, AMPK, c-Met, TNFα	Cell Signaling Technology, USA
Super signalling western dura kit	Amersham Biosciences Europe GmBH, Frieburg, Germany

2.1.5 Oil Red O staining

Oil Red O	Sigma-Aldrich, Steinheim, Germany
Isopropanol ≥99,5%	CarlRoth GmbH , Karlsruhe, Germany
Hematoxylin	medite Medizintechnik, Burgdorf, Germany
Immersion medium	medite Medizintechnik, Burgdorf, Germany
OCT	medite Medizintechnik, Burgdorf, Germany
Glass slides	Menzel GmbH & Co, Braunschweig, Germany
Cryomold	Sakura Finetek, Zoeterwoude, NL
Microtome Leica CM3050J	Leica Camera AG, Solms, Germany

2.1.6 Naphthol AS-D chloroacetate esterase staining

Naphthol AS-D Chloroacetate-Esterase-Kit (No.: 017K4339)	Sigma-Aldrich Chemie GmbH, Steinheim, Germany
Formalin 37%	Merck, Darmstadt, Germany

Paraffin Histowax, 56-58°C	Histolab Products, Göteborg, Schweden
Filter paper for embedding cassette	Vogel GmbH & Co. KG, Giessen, Germany
Roti-Histol	CarlRoth GmbH & Co, Karlsruhe, Germany
Ethanol absolute	Merk, Darmstadt, Germany
Aceton ≥99,8%	CarlRoth GmbH & Co, Karlsruhe, Germany
Immersion medium	medite Medizintechnik, Burgdorf, Germany
Paraffin station Leica EG1150H	Leica Camera AG, Solms, Germany
Cool plate Leica EG1150C	Leica Camera AG, Solms, Germany
Microtome RM2255	Leica Camera AG, Solms, Germany
Embedding cassette	Leica Camera AG, Solms, Germany
Heater	Thermo Electron Co., Langenselbold, Germany
Glass slides	Menzel GmbH & Co., Braunschweig, Germany
Water bath	MS Laborgeräte Schroeder OHG, Wiesloch

2.1.7 Immunohistochemical staining

Dako envision staining kit (Cat #K1390)	Dako, Hamburg, Germany
iNOS antibody	Affinity Bioreagents, USA
CD3ζ antibody	Santa cruz Biotechnology, Heidelberg, Germany
4-HNE antibody	Cell Signaling Technology, USA
PA1-1 antibody	Santa cruz Biotechnology, Heidelberg, Germany
Formalin 37%	Merck, Darmstadt, Germany
Paraffin Histowax, 56-58°C	Histolab Products, Göteborg, Schweden
Filter paper for embedding cassette	Vogel GmbH & Co. KG, Giessen, Germany
Roti-Histol	CarlRoth GmbH & Co, Karlsruhe, Germany
Ethanol absolute	Merk, Darmstadt, Germany
Aceton ≥99,8%	CarlRoth GmbH & Co, Karlsruhe, Germany
Immersion medium	medite Medizintechnik, Burgdorf, Germany
Paraffin station Leica EG1150H	Leica Camera AG, Solms, Germany
Cool plate Leica EG1150C	Leica Camera AG, Solms, Germany
Microtome RM2255	Leica Camera AG, Solms, Germany

Embedding cassette	Leica Camera AG, Solms, Germany
Heater	Thermo Electron Co., Langenselbold
Glass slides	Menzel GmbH & Co., Braunschweig, Germany
Water bath	MS Laborgeräte Schroeder OHG, Wiesloch

2.1.8 Hematoxylin & Eosin staining

Hematoxylin	medite Medizintechnik, Burgdorf, Germany
Eosin	medite Medizintechnik, Burgdorf, Germany
Paraffin Histowax, 56-58°C	Histolab Products, Göteborg, Schweden
Filter paper for embedding cassette	Vogel GmbH & Co. KG, Giessen, Germany
Roti-Histol	CarlRoth GmbH & Co, Karlsruhe, Germany
Ethanol absolute	Merk, Darmstadt, Germany
Immersion medium	medite Medizintechnik, Burgdorf, Germany
Paraffin station Leica EG1150H	Leica Camera AG, Solms, Germany
Cool plate Leica EG1150C	Leica Camera AG, Solms, Germany
Microtome RM2255	Leica Camera AG, Solms, Germany
Embedding cassette	Leica Camera AG, Solms, Germany
Heater	Thermo Electron Co., Langenselbold
Glass slides	Menzel GmbH & Co., Braunschweig, Germany
Water bath	MS Laborgeräte Schroeder OHG, Wiesloch

2.1.9 Triglyceride isolation

Chloroform	CarlRoth & Co, Karlsruhe, Germany
Methanol	CarlRoth & Co, Karlsruhe, Germany
BSA	CarlRoth & Co, Karlsruhe, Germany
PBS	
NaCl	CarlRoth & Co, Karlsruhe, Germany
Na_2HPO_4	CarlRoth & Co, Karlsruhe, Germany
KH_2PO_4	CarlRoth & Co, Karlsruhe, Germany

Randox TRIGS Triglyceride-Kit (Nr.: 121047)	Randox Laboratories LTD., Crumlin, UK
Triglyceride-Kit for cell culture	Biovision, California, USA
Polytron homogenizer	Kinematica AG, Switzerland
Sonicator	Bandelin, Berlin, Germany
96-well-plate	BD Bioscience, Heidelberg, Germany

2.1.10 Endotoxin assay

Charles river Endosafe kit	Charles River, L'ARBRESLE Cedex, France
Glass tubes	Sarsted AG & Co, Nümbercht, Germany
Endosafe microtiter plate	Greiner BioOne GmbH, Frickenhausen, Germany
Endosafe pipette tips	Sarsted AG & Co, Nümbercht, Germany

2.1.11 Microsomal triglyceride transfer protein (MTTP) assay

MTTP assay kit	Chylos Inc. USA
Tris	CarlRoth & Co, Karlsruhe, Germany
EGTA	CarlRoth & Co, Karlsruhe, Germany
$MgCl_2$	CarlRoth & Co, Karlsruhe, Germany
Isopropanol	CarlRoth & Co, Karlsruhe, Germany
96-well black microtiter plate	Greiner BioOne GmbH, Frickenhausen, Germany

2.1.12 Adenosine 5’-triphosphate (ATP) assay

EnzyLight ^{TM} ATP assay kit (EATP-100)	BioAssay systems, CA, USA
96-well black white plate	Greiner BioOne GmbH, Frickenhausen, Germany

2.1.13 Alanine aminotransferase (ALT) assay

Alanine Aminotransferase EC 2.6.1.2 kit	Randox Laboratories LTD., Crumlin, UK

2.1.14 Miscellaneous

Disposable plastic pippetes	Greiner BioOne GmbH, Frickenhausen, Germany
Micropippetes	Eppendrof, Hamburg, Germany
Micropippete tips	Sarsted AG & Co, Nümbercht, Germany
Reaction tubes	Eppendrof, Hamburg, Germany
Falcons (15 ml, 50 ml)	Greiner BioOne GmbH, Frickenhausen, Germany
96 –Well-round-bottom –plates	Greiner BioOne GmbH, Frickenhausen, Germany

2.1.15 Preparation of working solutions and buffers

1.5 M Tris HCl (pH 8.8): 90.75 g tris base was dissolved in 500 ml nano pure water and the pH was adjusted to 8.8 with concentrated HCl.

0.5M Tris HCl (pH 6.8): 30 g tris base was dissolved in 500 ml nano pure water and the pH was adjusted to 6.8 with concentrated HCl.

10 % APS: 1 g ammoniumpersulfate was dissolved in 10 ml nano pure water and stored at 4 ^{0}C.

10X Electrophoresis buffer: 30 g tris base, 144 g glycine, 10 g SDS was dissolved in 1000 ml nano pure water and stored at room temperature.

Transfer buffer: 2.9 g glycine, 5,8 g tris buffer, 0.37 g SDS, 200 ml methanol was dissolved in 1000 ml nano pure water.

Dignum A: Dignum A was prepared as follows

Reagents	Volume
1M HEPES (pH 7.6)	100 µl
1 M $MgCl_2$	15 µl
2 M KCl	50 µl
1 M DTT	5 µl
protease inhibitor cocktail	10µl
ser/thr inhibitor cocktail	100µl
tyrosine inhibitor cocktail	100µl
final volume was adjusted to 10 ml with nano pure water	

RIPA buffer: 0.418g MOPS (20mM MOPS pH7.0), 0.816g Nacl (150mM Nacl), 0.029g EDTA (1mM EDTA), 1ml Nonidet P-40 (1% v/v), 0.1g SDS (0.1 % w/v) were dissolved in 100ml of distilled water. From this stock solution 10ml was taken and protease inhibitor cocktails (10µl protease inhibitor cocktail, 100µl ser/thr inhibitor cocktail, 100µl tyrosine inhibitor cocktail) were added before protein isolation.

Oil Red O stock solution: Oil red O stock solution was prepared by dissolving 300mg of Oil Red O powder in 100ml of isopropanol and stirred this thoroughly that no clumps are evident. Then the solution was filtered three times using Whatmann filter paper.

Oil Red O working solution: 24ml of Oil Red O stock solution was dissolved in 16ml of distilled water and stirred thoroughly and set aside for 10 min.

Fixative for Naphthol AS-D chloroacetate esterase staining: Fixative solution was prepared according to the instructions of manufacturer by mixing 2.5ml of citrate solution in 6.5ml of acetone and 0.8ml of 37% formalin.

Naphthol AS-D chloroacetate esterase staining solution: To 40 ml of warm distilled water 1ml of sodium nitrite solution and 1ml Fast Red Violet LB Base were added and mixed thoroughly: In this mixture 5ml of TRIZMAL and 1ml of Naphthol AS-D Chloroacetate Solution were added and stirred thoroughly. All the reagents used were in part of the kit.

Phosphate buffer saline tween solution (PBST): In 1liter water 8g Nacl, 1.44g Na_2HPO_4, 0.2g KCl, 0.24g KH_2PO_4 and 0.4ml Tween were dissolved and the pH was adjusted to 7.4.

DMEM/F12 working medium: 450 ml DMEM/F12 medium was supplemented with 10 % inactivated FCS (50 ml), 5ml of Penicillin/Streptomycin, 5ml of ITS, 500µl of dexamethasone and stored at 4 ^{0}C.

DMEM/F12 stravation medium: 450 ml DMEM/F12 medium was supplemented with 0.01% BSA (50 ml), 5 ml of Penicillin/Streptomycin, 5ml of ITS, and stored at 4 ^{0}C

2.2 Methods

2.2.1 Animals and treatments

Six week old C57BL/6J, TNFR1 -/- mice (Tnfrsf1a$^{tm1Mak/J}$) or PAI-1 -/- mice (Serpine1^{tm1Mlg}) (n=5-6 per group) were used for the experiments. All procedures were approved by the local Institutional Animal Care and Use Committee (IACUC). During the experimental period the mice were kept under controlled lighting and air conditions in the specific-pathogen-free area (SPF-range) of the animal facility at the University of Hohenheim. Mice were randomly divided into 4 groups and either fed plain water or water containing 30% fructose for a period of 8 weeks (Table 2) *ad libitum*.

Table 2: Animal groups and feeding

Experimental group	**Drinking solution**	**Feed**
Wild-type control	Water	Standard chow
Knockout control (e.g, PAI-1, TNFR1)	Water	Standard chow
Wild-type fructose	30% fructose solution	Standard chow enriched with protein
Knockout fructose (e.g, PAI-1, TNFR1)	30% fructose solution	Standard chow enriched with protein

It has been previously shown by our own group that the mice chronically exposed to 30% fructose solution reduced their food intake in comparison to water fed mice (21). Therefore, in this study mice exposed to fructose were fed a protein and micronutrients enriched chow to prevent malnutrition. Body weight was assessed weekly over the 8 weeks feeding period.

2.2.2 Tissue collection

After the 8 week long feeding period animals were anesthetized with 80 mg ketamin/ kg and 6 mg xylazin/ kg body weight by i.p. injection. Blood was collected just prior to sacrifice from the portal vein in heparinised syringes, which was then transferred to tubes containing 15µl heparin and immediately placed on ice. Blood was centrifuged for plasma at 700 rpm for 14min at 10°C and then stored until further processing at -80°C. For histological evaluation

portions of liver were either fixed in 4% PBS-buffered formalin for at least 24hrs or frozen-fixed in OCT mounting media. For molecular analysis portions of liver tissue were frozen immediately in liquid nitrogen.

2.2.3 Human subjects and tissue collection

The samples used in the present study were obtained in the due course of the master thesis of S.Thuy. Characteristics of patients as well as exclusion criteria have been described before in that master thesis and in Thuy *et al.*(19). In brief, patients included in the study underwent partial liver resection (e.g. because of liver metastasis) or liver biopsies for medical reasons (n=18). Characteristics of study participants are summarized in Table 3.

Table 3: Characteristics of patients with NAFLD and controls[1]

	Control	NAFLD patients
N	6	12
Sex, % female	66	25
Age, y	47 ± 7	55 ± 4
BMI, kg/m^2	22.5 ± 1.2	27.8 ± 0.7*
Leisure physical activity, yes/no	6/0	6/6
Plasma ALT, U/L (0–40 U/L) [2]	40 ± 10	59 ± 12
Plasma AST, U/L (0–38 U/L) [2]	39 ± 10	39 ± 5
Plasma g-GT, U/L (0–40 U/L) [2]	57 ± 19	173 ± 50
Liver resection, n	6	7
Liver biopsy, [3] n	0	5
Basic illness[4]		
Malignancy, n Other, n	5 1	6 1
Liver pathology		
Without NAFLD, n Steatosis, n Steatohepatitis, n Steatohepatitis with fibrosis, n	6	 2 3 7

[1] Values are means of ± SEM. *Different from controls, P<0.05. [2] Normal range (27). [3]Biopsy taken for staging of NAFLD. [4]Basic illness of subjects underwent liver resection. (Table adapted from Thuy *et al.(19)*)

Exclusion criteria was as follows: 1) consuming lipid-lowering drugs or drugs affecting lipid metabolism; 2) altered lipid and glucose metabolism (e.g. diabetes); 3) alcohol abuse and alcohol intake >15 g/d ethanol; 4) drug-induced hepatotoxicity; 5) infection with hepatitis B or C virus; and 6) impaired nutritional status. Blood samples were drawn from fasted patients and controls before surgical intervention or liver biopsy in special Li-heparin tubes containing 0.1mg of aprotinin/ml of blood. The collected blood was centrifuged at 3000rpm for 10min and the plasma was stored at -80^{0}C. Liver tissue obtained through biopsy or during hepatectomy were immediately placed in RNAlater and stored at -80^{0}C or fixed in 10% buffered formalin until later analysis

2.2.4 Cell culturing and treatments

All experiments were performed using AML-12 cells purchased from LGC Promochem GmbH, Germany. The cells were cultured in a 25 cm^2 flask containing DMEM/F12 medium supplemented with 10 % FCS, ITS, dexamethasone and antibiotics.

Sub-cultivation of cells

After attaining 70 % confluence the cells were splitted and transferred into a new flask (75 cm^2) as follows:

a) Media and PBS were pre-warmed in 37 ^{0}C warm water bath.
b) The media was discarded and cells were washed with 10 ml of PBS twice.
c) Cells were incubated with 3ml of 1X trypsin/EDTA solution for couple of minutes at 37 ^{0} C.
d) After the cells detached, fresh media was added into the flask and cells were span at 1200xg for 5 min
e) The cells were transferred into a new culture flask and the volume of the medium was adjusted to 12 ml.
f) The culture flask was incubated at 37 ^{0} C in an incubator with CO_2.

For incubation experiments cells were plated in 6 well plates as follows:

a) The cells were splitted as mentioned above; however, after spinning the cells 10 ml of fresh media was added and the cells were separated carefully by pipetting up and down.
b) 400 µl of the cell suspension and 2 ml of fresh medium was pipetted into each well and incubated at 37 ^{0} C in an incubator with CO_2.

Cell treatments

At 70 % confluence cells were serum starved for 18 hrs in starvation medium supplemented with 0.01% BSA, ITS as well as antibiotics. Cells were then challenged with 10 ng/mL PAI-1 for 24 h. In addition, some cells were concomitantly treated with 20 ng/mL hepatocyte growth factor (HGF). Cells were rinsed twice with phosphate buffer saline (PBS) and either used for triglyceride isolation or measurements of microsomal triglyceride transfer protein (MTTP) activity as detailed below (see section 2.2.12 & 2.2.14).

2.2.5 Real time – polymerase chain reaction

RNA isolation

Total RNA was extracted from liver tissue samples using Trifast reagent according to the instructions of the manufacturer. In brief, the phenol-based reagent used for RNA isolation disrupts the tissue and the lysate is mixed with chloroform followed by centrifugation. Centrifugation separates the mixture into three phases, RNA is precipitated by isopropanol in aqueous phase.

Liver tissue was homogenised in 1 ml of Trifast reagent and incubated for 5 minutes at room temperature. After shaking samples vigorously for 15 sec, 0.2 ml of chloroform was added and the lysates were kept at room temperature for 3-10 minutes. During centrifugation at 12000 xg and 4 ^{0}C the mixture separates into the lower red (phenol-chloroform phase), the interphase and the colourless upper aqueous phase. The aqueous phase was transferred into a fresh tube and 0.5 ml of isopropanol was added to precipitate the RNA. Samples were placed on ice for 15 minutes, followed by a centrifugation for 10 minutes at 4 ^{0}C and 12000 xg. The supernatant was carefully removed and the RNA pellet was washed twice with 75 % ethanol by vortexing and subsequent centrifugation for 8 minutes at 7500 x g (4 ^{0}C). Excess ethanol was removed and the RNA pellet was air-dried. The pellet was resuspended in 10 µl of DNase and RNase free water and the samples were incubated at 55 ^{0}C for 10 minutes. RNA was then stored at –80 ^{0}C until further use.

Determination of RNA concentration and purity: To determine concentration, RNA was diluted (1:50) in a 96-well coaster UV plate with RNase and DNase free water. The absorbance was measured at a wavelength of 260/280 nm. The concentration was calculated as follows:

Dilution = 2 µl of RNA sample + 98 µl distilled water (1:50 dilution).

Concentration of RNA sample = 40* A_{260}* Dilution factor

RNA purity and integrity was determined by running 1% agarose gel. 28S and 18S rRNA bands were inspected to judge the quality.

c-DNA Synthesis

To determine mRNA concentration, mRNA is transcribed into cDNA using of special enzyme called reverse transcriptase. In brief, the oligo(dT) primer anneals selectively on the poly(A) tail of mRNA, which acts as the anchor for reverse transcriptase. One µg of total RNA was diluted to a final volume of 20 µl using RNase and DNase free water. Five µl of 5X MuLV buffer and 1 µl of DNase was added to the RNA samples and the samples were incubated for 15 minutes at 37 ^{0}C. The reaction was stopped by adding 2.5 µl of 25 mmol EDTA followed by an incubation at 70 ^{0}C for 10 minutes. To each sample 5 µl 5X MuLV buffer, 2.5 µl oligo(dt), 4 µl dNTP, 1 µl MuLV reverse transcriptase, 9 µl H_2O were added and the mix was incubated for 1 h at 37 ^{0}C. After the incubation 50 µl of H_2O was added to have a final volume of 100 µl of cDNA. cDNA synthesis for measuring PAI-1 mRNA expression was performed by using Epicentre cDNA synthesis kit as follows:

1µg RNA/ µl in	8,11 µl
Dnase-mix:	
10xBuffer Zero B.	0,96 µl
DNase Zero B	0,84 µl
Incubation: 20 min at 37°C	
Stopping the reaction:	
Stop Solution	0,95 µl
Incubation: 10 min at 65°C	
cDNA-Synthesis:	
OligodT Primer	2 µl
Incubation: 2 min at 65°C and 1 min on ice	

10xMMLV RT Buffer	2 µl
DTT	2 µl
dNTP	2 µl
RNase Inhibitor	0,5 µl
Reverse transcriptase	1 µl
Incubation: 5 min at 85°C and 1 min on ice	
RNase-free Water	20 µl

Real time Polymerase Chain Reaction

The concentration of PAI-1, Apo B, SREBP-1, FAS, CCL2, CCL19, ICAM-1, PEPCK Glut-4, RBP-4, glucokinase, NK1.1, CD1d, CD3ε, IL-15, IFNγ, BCL XL, 18S mRNA human IRS-1, human CD1d, human CD3ε, human MTP, human cMet, human IL-15, human IL-4, human BCL2l and human ß-actin mRNA in the liver tissue was determined by real time PCR using an I cycler (BioRad). The comparative threshold method was used to analyse the data obtained. The comparative C_t method is also known as the $2^{-[\delta][\delta]\ Ct}$ method, where

$$[\delta][\delta]C_t = [\delta]C_{t,sample} - [\delta]C_{t,reference}$$

With $[\delta]C_{t,\ reference}$ being the C_t value of the endogenous housekeeping gene.

The PCR reaction mixture was prepared as follows:

10 µl Sybr-Green

3µl H_2O

1 µl forward primer

1 µl reverse primer

5 µl of sample

The sequences of the primers used in the reaction mixture are summarized in Table 4.

Table 4: Primer sequences used for the detection of hepatic mRNA expression in mouse or human liver samples

	Forward (5'-3')	Reverse (5'-3')	Conc. nmol/L
PAI-1	5' TCC AAG GGG CAA CGG ATA GA 3'	5' GAC GAA GAG CCA GGC ACA CA 3'	300
ß-actin	5'-GGC TCC CAG CAC CAT GAA-3'	5'-AGC CAC CGA TCC ACA CAG A-3'	300
Apo B	5' TCA CCA TTT GCC CTC AAC CT 3'	5' CAG GTC AAC ATC GGC AAT CA 3'	300
SREBP-1	5' ACC GGC TAC TGC TGG ACT GC 3'	5'AGA GCA AGA GGG TGC CAT CG 3'	300
FAS	5' GGG GGT GGG AGG ACA GAG AT 3'	5' CAC ATG GGC TGA CAG CTT GG 3'	300
CCL2	5' GCC AGA CGG GAG GAA GGC CA 3'	5' TGG ATG CTC CAG CCG GCA AC 3'	300
CCL19	5' GTC GGA GCC TCG GCC TCT CA 3'	5' CCA CCC AGG GCT GGT CTG GA 3'	300
ICAM-1	5' ACT GGA TCT CAG GCC GCA AG 3'	5' GCC CTC CCA GCT CCA GGT AT 3'	300
PEPCK	5' CCC TGG GAG ATG GGG AGT TC 3'	5' CCC ACC ATA TCC GCT TCC AA 3'	300
18S	5' GTA ACC CGT TGA ACC CCA TT 3'	5' CCA TCC AAT CGG TAG TAG CG 3'	300
NK1.1	5' GGC AGC TGT GCC TCC ATC TT 3'	5' CAC AGA TCT GGT GCG GAT GG3'	300
CD 1d	5' TGT GTA CCA GTC CGG GAG CA 3'	5' GTG CGG GAC CAG CTT CTG TT 3'	300
CD 3ε	5' ATG GCC AAG AGC TGC CTC AG 3'	5' TGA CCA TCA GCA AGC CCA GA3'	300
IL-15	5' ATG TGA GGA GCT GGA GGA GA 3'	5' ACG TTA GTT TGC CCA GCA GA3'	400
IFNγ	5' CAA GCG GCT GAC TGA ACT CA 3'	5' CAC TGC AGC TCT GAA TGT TTC TTA TT 3'	300
BCL XL	5' ATG GCA GCA GTG AAG CA AG 3'	5' GCA ATC CGA CTC ACC AAT ACC 3'	300
RBP-4	5' TGC AGA CAT GGT GGG CAC TT 3'	5' ACC AGC CTC CGT GTC TCT GG 3'	300
GLUT-4	5' ACC CCT CAT TCC CCC TGT GT 3'	5' ACA CAC CCA CCC CTG CTG TT 3'	300
Glucokinase	5'ACT TTC CAG GCC ACA AAC A 3'	5' TCC CAG AAC TGT AAG CCA CTC 3'	300

Human IRS 1	5’ GTC TGG CCC GGT GGC TTT CC 3’	5’ GTG CTC TCC TGC CAG GCT GC 3’	300
Human CD1d	5’ CCA GGT GTC CGC TGG CTG TG 3’	5’ TGG GGC CTC TTG GGT TGG CT 3’	300 F 400 R
Human BCL 2l	5’ AAACTGGGTCGCATTGTGG 3’	5’ TCTCGCCTGCTGCATTGTTC 3’	300
Human MTTP	5’ CGG GGC GGG GTC TGG AGT TA 3’	5’ TGG CAG CCA GTG AGG GAG TGA 3’	300
Human cMet	5’ CCC AGC CCC TCT GCT TTC TT 3’	5’ ATG GCT CCT CTG CAC CAA GG 3’	300
Human ß actin	5’ GCA AGA GAG GCA TCC TCA CC 3’	5’ CGT AGA TGG GCA CAG TGT GG 3’	300
Human IL 4	5’ GCC GGCAACTTTGTCCAC GG 3’	5’ TCT GTT ACG GTC AAC TCG GTG CA 3’	300
Human IL 15	5’ CTG CAG CCA GGA CTC GAT GGA GAA 3’	5’ GCT CCA TGT GAC GTC AGC AGC A 3’	300

2.2.6 Western Blotting

Cytosolic protein isolation

To obtain the cytosolic protein fraction liver tissue was homogenised in 400 µl of dignum A solution by using a glass homogenizer. The suspension was transferred to a 1.5 ml reaction tube and was incubated on ice for 15 minutes. Thirty µl of a 10 % NP-40 solution was added to each tube and the tubes were vortexed vigorously for 10 sec. The samples were then centrifuged at 4 ^{0}C for 30 sec and the supernatant with cytosolic protein was transferred into a fresh tube.

RIPA protein isolation

To obtain total protein lysate liver tissue was homogenised in 1ml of RIPA buffer with a polytron until no visible tissue chunks are left. The samples were sonicated for 10 sec and vortexed at full speed. Samples were centrifuged at full speed (4^0C) for 5 min. The supernatant was stored in a fresh tube at-80^0C until further use.

Bradford assay

Bradford assay was used to determine protein concentration. The assay is based on the binding of G-250 dye to proteins at arginine, tryptophan, tyrosine, histidine and phenylalanine residues. The dye binds to these residues in the anionic form, which has an absorbance maximum at 595 nm (blue). A standard reference curve for the protein was prepared as follows:

Dignum A or RIPA solution was diluted in H_2O (ratio1: 50), Biorad dye 5ml was diluted with 20 ml of dH_2O. Protein standard stock solution (BSA, 1 mg BSA/ml) was thawed and different standards were prepared as described in Table 5.

Table 5: Preparation of the standard curve for the Bradford assay

S: NO	Concentration	Dilution
S1	1 mg BSA/ml	2 µl BSA stock+198 µl diluted dignum A/RIPA
S2	0.5 mg BSA/ml	100 µl S1+100 µl diluted dignum A/RIPA
S3	0.25 mg BSA/ml	100 µl S2 + 100 µl diluted dignum A/RIPA
S4	0.125 mg BSA/ml	100 µl S3 + 100 µl diluted dignum A/RIPA
S5	0.0625 mg BSA/ml	100 µl S4 +100 µl diluted dignum A/RIPA
S6	0	100 µl diluted dignum A/RIPA

Samples were diluted with water (1:50). In a 96-well plate 5 µl of sample or standard per well and 200 µl of diluted dye were mixed and incubated for 5 minutes at room temperature. Protein concentration of standard and samples were determined in triplicates. The plate was incubated for 5 minutes and measurements were carried out at 595 nm. A standard curve was generated and average absorbance value of each concentration of the protein standard was determined as a function of X with protein concentration as a function of Y

According to the concentration, the samples were diluted with 2 x sample buffer (without DTT) and dignum A or RIPA so that the final concentration in each sample was 4 or 6µg protein/µl sample. The samples were stored at –80 ^{0}C until further use.

Gel preparation for Western blotting

To determine the protein concentration of phospho Akt, phospho cMet, phospho AMPK, Akt, AMPK, cMet, TNFα and β-actin protein samples were separated in a sodium dodecyl sulfate polyacrylamide gel electrophoresis (SDS-PAGE) and transferred from the gel to a polyvinylidene (PVDF) membrane using the semi-dry method (63). The transferred protein was subsequently detected by immunological methods.

SDS-PAGE

Glass plates, spacers and combs (15 wells) of the electrophoresis unit were thoroughly cleaned with isoproponal. The gel mix was prepared as described in Table 6.

Table 6: Preparation of separation gel

Reagents	8%	10 %	12%	15%
Nano pure water	4.5 ml	4.17 ml	3.5 ml	2.35 ml
Acrylamide/Bis- solution (30 %)	2.7 ml	3.33 ml	4 ml	5 ml
1.5 Tris HCl (pH 8.8)	2.6 ml	2.6 ml	2.6 ml	2.6 ml
10 % SDS	0.1 ml	0.1 ml	0.1 ml	0.1 ml
10 % APS	0.1 ml	0.1 ml	0.1 ml	0.1 ml
TEMED	0.006 ml	0.006 ml	0.006 ml	0.006 ml

The gel was poured with a disposable pipette and covered with isoproponal. When the separation gel was polymerized, isoproponal was washed off 3 times with nano pure water. The stacking gel was prepared as described in Table 7 and poured on top using a disposable pipette.

Table 7: Preparation of stacking gel.

Reagents	**4 %**
Nano pure water	1.575 ml
Acrylamide/Bis-solution (30 %)	0.250 ml
0.5Tris HCl (pH6.8)	0.625 ml
10 % SDS	0.025 ml
10 % APS	0.025 ml
TEMED	0.003 ml

The comb was placed carefully in the gel. After the gel was polymerized, it was wrapped in wet paper towels soaked in water, kept in a foil and stored in the refrigerator overnight. Protein samples diluted with sample buffer were thawed on ice and 10 µl of the protein samples were transferred into a fresh tube. Two µl of a 100 mM DTT solution was added. Samples were heated at 95 ^{0}C for 5 minutes and immediately placed on ice. A coloured protein marker was also heated simultaneously. Samples and marker were centrifuged shortly at 4 ^{0}C. One x electrophoresis buffer (50 ml 10 x buffer + 450 ml water) was poured in the electrophoresis apparatus and the gel was loaded with the protein samples or the marker proteins, respectively. Proteins were separated at 110 V for 1 h 20 minutes.

Blotting

Whatman paper and the PVDF membrane were cut to the size of the gel (5 x 8 cm^2). The PVDF membrane was activated with methanol for 10 sec and the activated membrane was equilibrated in transfer buffer for 10 minutes on a shaking table. Simultaneously, whatman papers were also soaked in transfer buffer and placed on the shaking table for 10 minutes. The gel was transferred into transfer buffer and gently shaked for a couple of minutes and then a gel-paper-membrane sandwich was arranged on the semi-dry-blotter as follows:

whatman membrane - gel - PVDF membrane - whatman membrane.

The proteins were transferred to the membrane at 1 mA/cm^2 of membrane for 55 minutes. The membrane was removed from the sandwich assembly and dried for 1 h. Then the membrane was activated again with methanol and washed with nano pure water. The PVDF membrane was stained with Ponceau S solution and washed with water thoroughly to check the protein transfer. The marker band was marked according to the respective colours and the membrane was blocked with 2.5% BSA in Tris-buffered saline-Tween (TBST) for 45 minutes. The membrane was incubated with primary antibody (dilutions of all primary antibodies 1:500 in 2.5 % BSA) overnight at 4 ^{0}C on a rocking table.After the overnight incubation the membrane was washed 3-times with TBST for 5 minutes and treated with the secondary antibody for 45 minutes (depending on the primary antibody (e.g. anti-mouse or anti-rabbit) on a rocking table at room temperature. After the incubation with the secondary antibody (dilutions of all secondary antibodies; 1:5000 in 2.5% BSA) the membrane was washed again with TBST 3 times for 10 minutes. The membrane was incubated with Super Signal Western Dura solutions (1:1 dilution,) for 5 minutes protected from light. A picture was taken under the gel documentation system (Alpha Innotech, USA) after incubation

Densitometric analysis of blots

Protein bands were densitometrically analyzed using the Flurochem Software. In this method the band of interest and the background were selected and analyzed for the specific protein concentration as follows:

Protein concentration (e.g. TNFα) = Average of TNFα band- Auto-background/ Average of β actin band- Auto-background.

Protein concentration of phosphorylated protein = Average of phosphorylated protein band – Auto-background/ Average of total protein band – Auto-background.

2.2.7 Oil red O staining

Oil red O is a lipid soluble dye which is soluble in the tissue lipid than in the solvent it's dissolved. Oil red O staining was done to reveal the lipid accumulation in liver. The lipid droplets appear red in colour after the staining. Frozen OCT mounted liver sections were cut at 10µm thickness with help of cryostat, dried for 2 min and immediately frozen at -20^0 C. The stock dye solution was prepared as described in section 2.1; stirred for an hour and filtered twice. Forty eight ml of filtered stock solution was diluted with 32 ml ddH_2O and added directly to just thawed liver sections in the cuvette. After 15 min in the cuvette the sections were washed twice with ddH_2O and checked for colour intensity under the microscope. Then the specimens were rinsed 5 min under running cold tap water and counter stained with hematoxylin for 45 sec. Excess staining was washed off under running tap water for 2-3 minutes. Nuclei in stained sections appear blue. Subsequently, the sections were briefly dipped in ddH2O and covered with one to two drops aqueous mount. Representative 400x microscopic pictures were made by using Zeiss microscope in combination with AxioVision software release 4.5.

2.2.8 Paraffin embedding of liver sections

A formalin fixed paraffin embedded tissue is a piece of tissue which is immobilized and preserved for the purpose of staining. Fixation makes tissue permeable to staining reagents and cross-links its macromolecules so that they are stabilized and locked in position. Table 8 summarizes fixing and paraffin embedding of liver tissue.

Table 8: Paraffin embedding of tissue

Treatment	Incubation time
4% Formalin	≥ 24 h
Cold running tap water	
75% EtOH	1 h
85% EtOH	1 h
95% EtOH	Over night

100% EtOH	1 h
100% EtOH	1 h
100% EtOH	1 h
100% EtOH : Roti-Histol (1:1)	30 min
Roti-Histol	1 h
Roti-Histol	1 h
Paraffin	30 min
Paraffin	30 min
Paraffin	30 min
Embedding of tissue sections in paraffin	
Storage at -20 ° C	10 min

2.2.9 Naphthol AS-D chloroacetate esterase staining to detect neutrophils

For staining of neutrophils in the liver a commercially available kit from Sigma-Aldrich was used following the instructions of the manufacturer. The kit has Naphthol AS-D Chloroacetate which is enzymatically hydrolyzed by "specific esterase," liberating a free naphthol compound. This then couples with a diazonium salt, forming highly colored deposits at sites of enzyme activity. This enzyme is usually considered specific for cells of granulocytic lineage (e.g. neutrophils). The staining was performed in paraffin embedded liver sections as summarized in Table 9

Table 9: Staining of tissue sections with naphthol AS-D chloroacetate esterase

Cutting the tissue at 5µm thickness	
Drying the sections at 37°C	72 h
Roti-Histol	10 min
100% EtOH	5 min
96% EtOH	5 min
70% EtOH	5 min
ddH2O	5 min
ddH2O	5 min
1-4 drops of fixative	30 sec
ddH2O	60 sec
Incubation of the sections at 37 ° C in the staining solution	15 min

Staining was checked under microscope	
Counter stain with hematoxylin	15 sec
Mount the sections with aqueous mount	

Using a Zeiss Axiovert 200M microscope and the AxioVision software release 4.5, neutrophil numbers in liver specimens were counted in 5 randomly selected fields (200x).

2.2.10 Immunohistochemical staining of iNOS, 4-hydroxynoneal adducts (4 -HNE), CD3ζ, human 4 HNE, human PAI-1, human 4-HNE and human CD3ζ

Immunohistochemical staining of iNOS, CD3 ζ, 4-HNE and PAI-1 was performed in the respective paraffin embedded liver tissue. The tissue was embedded, cut and deparaffinised as described previously in Table 8 and 9. The deparaffinised tissue sections were washed twice with PBS-tween. The tissue sections were blocked with peroxidase for 5 minutes and then washed once again with PBS-tween for 5 minutes. The tissue sections were stained either for 4-hydroxynonenal-protein adducts or iNOS or CD3ζ or PAI-1 using respective polyclonal antibodies for 30 minutes at room temperature (Dilutions of primary antibodies; 1:500 in 2.5% BSA). To detect specific binding of primary antibody, tissue sections were incubated with a peroxidase linked secondary antibody for 15 minutes and diaminobenzidine for 8 minutes. The sections were washed under slow running tap water for 6 minutes and then stained with hematoxylin staining for 30 sec and sections were once again washed under running tap water. The sections were dehydrated and cover slips were mounted. Using a Zeiss Axiovert 200M microscope and the AxioVision software release 4.5, the extent of staining in liver sections was defined as percent of the field area within the default colour range as determined by the software. To determine means, data from 8 fields (200 x for 4-HNE, 630x with oil immersion for iNOS, CD3ζ and PAI-1) of each tissue section were used.

2.2.11 Hematoxylin and Eosin staining

Hematoxylin and Eosin staining is the standard staining method used in histology and gives an overview of the structure of the tissue. It was used to evaluate liver pathology. The staining protocol is summarized in Table 10.

Table 10: Staining of tissue sections with H & E

Cut and deparaffinised the sections in the usual way (see Table 10, 11)	
Hemotoxylin solution	2-5 min
Staining was checked under microscope	
Running tap water	10 min
ddH2O	
40% EtOH	2 min
Eosin aqueous solution	60-75 sec
Staining was checked under microscope	
70% EtOH	30 sec
96% EtOH	30 sec
100% EtOH	30 sec
Roti-Histol	10 min
Mount the sections with aqueous mount	

2.2.12 Triglycerides (TG) isolation

Hepatic triglycerides were isolated using a method modified from that of Folch *et al.(64)* and the concentration of triglycerides was measured by using a commercially available kit following the instructions of the manufacturer. In brief, ~50mg of liver tissue was homogenized with 'polytron' in 1 ml of ice-cold 2x PBS. The homogenate was sonicated for 20 sec at full speed. Five hundred µl of the homogenate was aliquoted and 750µl of a pre-made chloroform/methanol mixture (2:1) was added to it. Then each sample was vortexed for 10 sec in a span of 10 min. Samples were then incubated at room temperature for 2 hrs followed by a full speed centrifugation at 4^0C for 5 min. The bottom phase (400µl) was transferred into a new tube and dried in a centrifugation concentrator for 12 min.

The samples were resuspended in 5% BSA, sonicated for 10 sec at full speed and frozen at -80^{0}C over night. To further breakup left over particles the samples were once again sonicated for 10 sec at full speed and warmed up to 37^{0}C. The enzyme reagent and standard were thawed at room temperature, two µl of standard or sample and 200µl of enzyme reagent was pipetted into 96 well round bottom plate. The plate was incubated at 37^{0}C for 5min.The spectrophotometer was also pre-warmed at 37^{0}C and then the plate was measured at 500nm. Hepatic triglycerides concentration was normalized with hepatic protein content. Accordingly, Bradford assay was performed as described in section 2.2.5.3 with the remaining liver tissue homogenate. The final hepatic triglyceride content was calculated as follows:

$$\text{Triglyceride [mg/dl]} = \text{Concentration}_{(\text{Standard})} * \frac{\text{Absorbance}_{(\text{Sample})}}{\text{Absorbance}_{(\text{Standard})}}$$

$$\text{Final triglyceride (µg/mg) of protein} = \text{TG concentration}_{(\text{Sample})} / \text{Protein concentration}_{(\text{Sample})}$$

Triglycerides isolation from cells

Triglyceride levels in cell cultures were determined using a kit from Biovision following the instructions of the manufacturer. In brief, cells were homogenized in 5% NP-40 solution and the samples were heated at 100^{0}C in a water bath for 5 min until NP-40 became cloudy, then the samples were cooled down to room temperature. The heating step was repeated once again to solublize all triglyceride. The samples were centrifuged at top speed for 2 min to remove any insoluable material. The samples were then diluted with triglyceride assay buffer in 1:1 ratio to final volume of 50µl/well. Triglyceride standard solution was prepared by adding 40µl 1mM TG in 160µl assay buffer. A standard reference curve was pipetted as follows:

Table11: Pipetting of standards for triglyceride assay

S: NO	Concentration	Dilution
S1	0mM	50µl of TG assay buffer
S2	2mM	10µl 0 2mM TG + 40µl TG assay buffer
S3	4mM	20µl 0 2mM TG + 30µl TG assay buffer
S4	6mM	30µl 0 2mM TG + 20µl TG assay buffer
S5	8mM	40µl 0 2mM TG + 10µl TG assay buffer
S6	10mM	50µl 0 2mM TG

Two µl of lipase was added to each sample and standard wells. The plate was incubated at room temperature for 20 min to convert triglyceride to fatty acid and glycerol. Meanwhile, a reaction mix of 50µl/well was prepared by adding 46µl Triglyceride assay buffer, 2µl Triglyceride probe and 2µl Triglyceride enzyme mix. Reaction mix was added to each well and incubated at room temperature for 60 min in the dark. The reaction was measured at 570nm in a microtiter plate. TG concentration was calculated as follows:

Concentration of TG = Ts/Sv µmol/ml or mM
Ts is triglyceride amount from the standard curve (nmol)
Sv sample volume added in the sample wells (µl)

2.2.13 Endotoxin assay

Plasma endotoxin levels were determined using a commercially available endpoint Limulus Amebocyte Lysate assay kit which is dependent on a direct relationship between endotoxin concentration and colour development. In brief, plasma samples were diluted in 1:5 ratio to get an end volume of 70µl and heated at 70^{o}C for 20 min. Meanwhile, different standards were prepared as follows:

Table12: Preparation of standards for endotoxin assay

S: NO	Concentration	Dilution
S1	0 EU/ml	250µl Endosafe water
S2	0.00195 EU/ml	250µl S3 + 250µl Endosafe water
S3	0.00390 EU/ml	250µl S4 + 250µl Endosafe water
S4	0.00781 EU/ml	250µl S5 + 250µl Endosafe water
S5	0.01560 EU/ml	250µl S6 + 250µl Endosafe water
S6	0.0312 EU/ml	250µl S7 + 250µl Endosafe water
S7	0.0625 EU/ml	250µl S8 + 250µl Endosafe water
S8	0.125 EU/ml	1.25µl (50EU/ml) + 498.75 Endosafe water

Twenty five µl of standards or samples were pipetted in duplicates into a special endoasfe microtiter plate and incubated at 37^0C for 5 min. Then 25µl of Limulus-Amoebocyte-Lysate (LAL) was added and incubated at 37^0C for 5 min. After the incubation, 50µl of chromogen substrate/Buffer (1:1) mixture was added and once again incubated at 37^0C for 5 min. The colour reaction was stopped by adding 50µl of 20% acetic acid followed by reading the plate at 405nm. A standard curve was generated and average absorbance value of each concentration of the endotoxin standard was determined as a function of X with endotoxin concentration as a function of Y. The recovery rate of the assay was around ~70%.

2.2.14 Microsomal triglyceride transfer protein (MTTP) activity

Hepatic MTTP activity was determined using a commercially available MTTP assay kit following the instructions of the manufacturer. In brief, purified MTTP or cellular homogenates were incubated with donor vesicles containing fluorescent lipids and acceptor vesicles containing phosphatidylcholine and triacylglycerols. Increases in fluorescence were measured and credited to MTP-mediated lipid transfer. Liver tissue was homogenised in 1ml of ice-cold buffer containing 1mM Tris pH7.6, 1mM EGTA and 1mM $MgCl_2$ and 50µl of protease inhibitors cocktail. Homogenisation was followed by a centrifugation of the samples at 7400xg for 30 min at 4^0C and the supernatant was transferred into fresh 1.5ml microcentrifuge tubes for protein measurement. 100µg was taken for determining the MTTP activity. Measurements were performed in triplicate in a black microtiter plate by pipetting the components provided in the kit and samples as shown in Table 13.

Table 13: Pipetting of different components and samples for MTTP assay

	Vesicles	Water	Sample	Buffer	Isopropanol	MTP
A. Blank	5µl	90µl		5µl		
B. Total	5µl				95µl	
C. Positive control	5µl	85µl		5µl		5µl
D. Test	5µl	90µl	5µl			

After pipetting, the plate was incubated for 30 min at room temperature and the fluorescence units were measured using excitation and emission wavelengths of 460-470 and 530-550nm, respectively. Following calculations were used to calculate the MTTP activity in samples.

1) % Transfer in controls (C): (Control $_{FU}$ - Blank $_{FU}$)/(Total $_{FU}$ - Blank $_{FU}$)*100

2) % Transfer in controls (D): (Test $_{FU}$ - Blank $_{FU}$)/(Total $_{FU}$- Blank $_{FU}$)*100

MTTP assay in cells

Cells were washed twice with 1ml of ice cold PBS and rinsed with ice cold MTTP assay buffer. Then the cells were incubated with MTTP assay buffer at 37^0C for couple of minutes and the buffer was aspirated. Hundred µl of ice cold MTTP assay buffer containing protease inhibitors was added. The cells were scrapped and homogenized by passing through a 21 gauge syringe needle. Homogenized cell suspension was centrifuged at top speed for 1h at 4^0C.The supernatant was used for lipid transfer assay as described above.

2.2.15 Adenosine 5'-triphosphate (ATP) assay

ATP levels in liver tissue were determined by using a commercially available ATP assay kit. Tissue was lysated with assay buffer to release ATP. The released ATP reacts with D-luciferin in presence of luciferase to produce light. The light intensity is a direct measure of intracellular ATP concentration. Liver tissue was homogenized in ice cold PBS and centrifuged at 12000 g for 5 min. The supernatant was diluted with PBS (1:5) to an end volume of 100µl and pipetted into a white opaque 96-well plate in triplicates. Simultaneously, 1000µl of 30µM ATP premix was prepared by mixing 10µl of 3mM ATP standard in 990µl distilled water and diluted to generate a standard curve as shown in Table 14. Hundred µl of the standards was also pipetted in triplicates into the plate followed by 90µl of reconstituted reagent (reconstituted reagent: 95µl assay buffer + 1µl substrate + 1µl ATP enzyme). The plate was incubated at room temperature for 10 min and luminescence was measured at 125 nm.

Table 14: Preparation of standard curve for ATP assay

No	Premix + water	Vol (µl)	ATP (µM)
1	150µl+0µl	150	30
2	120µl+30µl	150	24
3	90µl+60µl	150	18
4	60µl+90µl	150	12
5	45µl+105µl	150	9
6	30µl+120µl	150	6
7	15µl+135µl	150	3
8	0µl+150µl	150	0

2.2.16 Alanine aminotransferase (ALT) assay

Plasma ALT levels of mice were determined by using a commercially available Randox ALT assay kit following the instructions of the manufacturer. In brief, ALT enzymatic assay kit uses a coupled enzymatic reaction scheme in which alanine and α-ketoglutarate are first converted to glutamate and pyruvate after which the pyruvate is converted by lactate dehydrogenase to generate lactate and NAD+. The conversion of the NADH chromophore to NAD+ was measured at 340 nm, which is proportional to the level of ALT enzyme in the sample. Plasma was diluted 1:10 with water. 10µl of the diluted plasma and 100µl of reconstituted buffer containing substrate and enzyme were pipetted into the microtiter plate. The initial absorbance was measured at 1, 2 and 3min and the values of the first 2min were used for the calculation.

ALT activity of sample (U/L) = 1746*δ A 340nm/min.

2.2.17 Retinol binding protein 4(RBP-4) ELISA

RBP-4 levels were determined using a commercially available ELISA kit following the instructions of the manufacturer. In brief, RBP/RBP4 in the samples is bound to polyclonal rabbit anti RBP/RBP4 antibodies, immobilized on the microtitre plate. A peroxidase-conjugated anti RBP/RBP4 antibody is used for detection and quantification, and tetramethylbenzidine (TMB) as a peroxidase substrate.

The precoated microtiter plate was washed 5 times with 250µl wash buffer. Hundred µl of standard, controls and samples were pipetted into the wells in duplicates. The plate was incubated for 1hr at room temperature on a horizontal mixer. The content of the plate was decanted and the wells were washed 5 times with 250µl of wash buffer followed by addition of 100µl of conjugate into each well. The plate was incubated for 1hr at room temperature and decanted, washed 5 times with 250µl of wash buffer. Hundred µl of substrate solution was added to each well and incubated for 20 minutes at room temperature by slightly shaking until colour differences are sufficient. Fifty µl of stop solution was added into each well and mixed shortly. The absorption was determined at 450nm against 620nm as a reference. A standard curve was generated and average absorbance value of each concentration of the RBP-4 standard was determined as a function of X with RBP-4 concentration as a function of Y.

2.2.18 Statistical analysis

All results are expressed as means $\pm$ SEM (Mice samples n=5-6) (Human subjects n=18). Results were statistically analysed using the analysis of variance test (ANOVA) or student t-test included in the Graph pad prism software or SPSS. Normal distribution of the data was tested out with the Kolmogorov-Smirnov test and homogeneity of variances was tested with the Bartlett's test. Logarithmic transformation of raw data was performed in cases of unequal variances. Statistically significant differences were determined using Tukey’s post hoc test. P value < 0.05 was considered to be significant

.

3 Results

3.1 Studies in TNFR 1-/- mice fed fructose

3.1.1 Effect of fructose feeding on weight gain and liver to body weight ratio in TNFR 1-/- mice

The body weight of mice was measured weekly. In table 17 absolute weight gain of mice throughout the 8 weeks of feeding is summarized. Absolute weight gain of wild-type controls was significantly lower than that of TNFR 1-/- mice fed water (~1.4g, $p<0.05$). When compared with their respective controls, absolute body weight gain of both fructose fed groups were significantly higher (wild-type: +~2g, TNFR 1-/-: +~3g both $p<0.05$, in comparison to respective controls). In both fructose fed groups not only absolute liver weight but also liver to body weight ratio was significantly higher than their respective controls (wild-type liver weight: +~0.3-fold, liver to body weight ratio: +~1-fold; TNFR 1-/- liver weight: +~0.16-fold, liver to body weight ratio: +~1-fold, all $p<0.05$) (Table 15)

Table 15 Effect of fructose feeding on body weight, liver weight and liver to body weight ratio in TNFR 1-/- mice

	Control + Water	TNFR1 -/- + Water	Control + Fructose	TNFR1 -/- + Fructose
Weight gain (g)	3.1 ± 0.1	4.5 ± 0.3	5.1 ± 0.7 [a]	7.6 ± 0.5 [a,b,c]
Liver to body weight ratio (%)	4.8 ± 0.1	5.12 ± 0.1	5.9 ± 0.1 [a,b]	6.2 ± 0.1 [a,b]
Absolute liver weight (g)	0.99 ± 0.01	1.16 ± 0.03 [a]	1.33 ± 0.14 [a,b]	1.63 ± 0.07 [a,b,c]

[1] Values represent means ± SEM. [a]$p < 0.05$ compared with wild-type mice fed with plain water. [b]$p < 0.05$ compared with TNFR1 -/- mice fed with plain water. [c]$p< 0.05$ compared with wild-type fructose fed mice.

3.1.2 Effect fructose feeding on liver steatosis, inflammation and ATP levels in TNFR1-/- mice

Liver steatosis

Hepatic lipid accumulation was assessed by oil red O staining and quantitative analysis of hepatic triglyceride concentration. Liver pathology was assessed by hematoxylin and eosin (H&E) staining. Figure 2 depicts representative photomicrographs of hepatic hematoxylin and eosin (H & E), oil red O staining and quantitative analysis of hepatic triglyceride concentration in TNFR1 -/- and wild-type mice either fed water or water sweetened with 30% fructose for 8 weeks. H & E staining revealed no significant pathological changes between wild-type and TNFR1 -/- mice fed water (Figure 2A upper panel). In line with these findings lipid staining as well as hepatic triglyceride concentration was minimal in wild-type and TNFR1 -/- mice fed water (Figure 2A lower panel & B). In contrast, in wild-type mice chronic fructose feeding caused an ~5-fold increase in hepatic triglyceride levels in comparison to wild-type water fed mice (Figure 2B) ($p < 0.05$) whereas in TNFR1-/- mice it caused only an ~2-fold increase in hepatic triglyceride levels in comparison to water fed TNFR1-/- mice (Figure 2B) ($p < 0.05$). In the present study, plasma ALT levels were found to be significantly increased by ~6-fold in wild-type mice fed fructose in comparison to water fed wild-type mice. In contrast, plasma ALT levels of TNFR1 -/- mice fed fructose did not differ from that of the respective control mice fed water (Table 16).

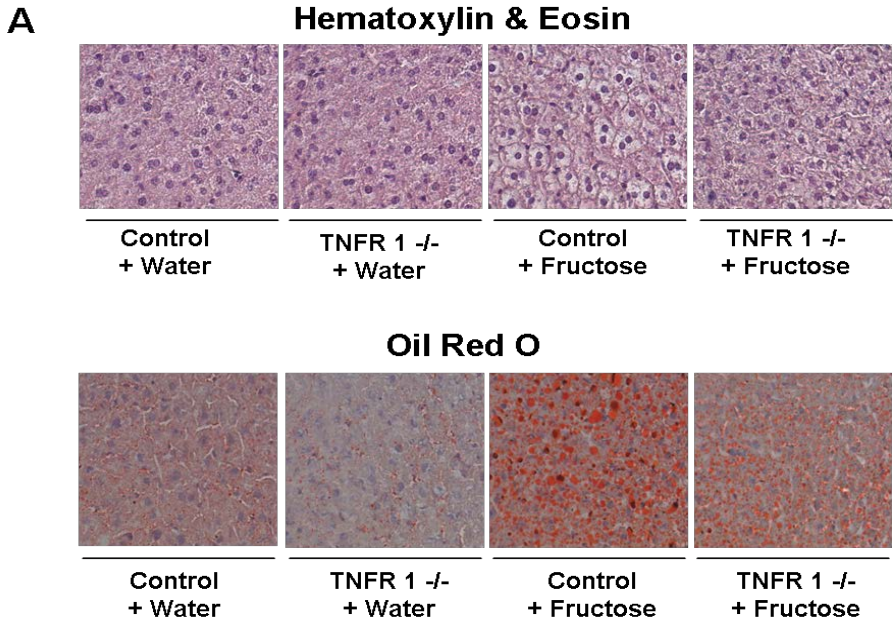

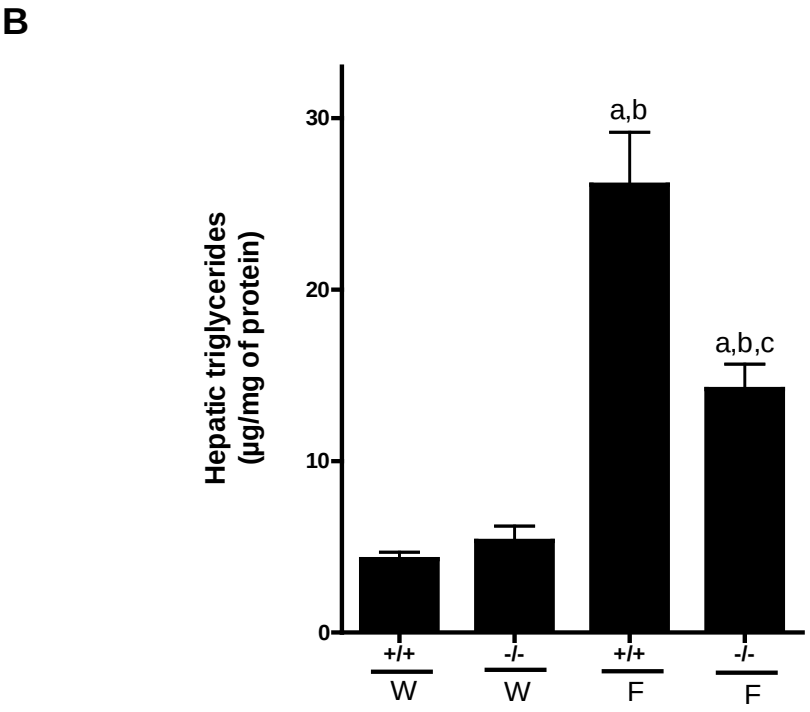

Figure 2 Effect of fructose feeding on hepatic pathology, lipid accumulation and triglyceride levels. (A) Representative photomicrographs of hematoxylin and eosin (upper panel) and oil red O staining (lower panel) of liver sections (400x). (B) Quantitation of hepatic triglyceride content. Data are expressed as means ± SEM (n = 4-6). W – water; F – 30% fructose solution. [a]$p < 0.05$ compared with wild-type mice fed with plain water. [b]$p < 0.05$ compared with TNFR1 -/- mice fed with plain water. [c]$p < 0.05$ compared with wild-type fructose fed mice.

Liver inflammation and ATP levels

In settings of steatosis and steatohepatitis TNFα may potentially induce chemokine secretion (like CCL2 and CCL19) and inflammation (for review see (65)) thus, number of neutrophils as well as expression of ICAM-1, CCL2 and 19 were determined (Table 16). Chronic fructose feeding in wild-type mice was associated with an increased number of neutrophils and expression of ICAM-1 in comparison to water controls (neutrophils: +~5.5-fold, ICAM-1: +~1.8-fold in comparison to wild-type water contols) (Table 16). Similarly, CCL2 and CCL19 mRNA expression in livers of fructose fed wild-type mice was also increased; however, as expression varied considerable between animals, differences did not reach a level of significance (CCL2; p=0.38, CCL19; p=0.11 in comparison to wild-type water controls) (CCL2; p<0.05, CCL19; p=0.07 in comparison to TNFR 1-/- water controls) (see Table 16). In contrast, these effects of fructose feeding were not found in TNFR1-/- mice.

In addition, ATP concentrations were also determined in the present study, as it has been shown in humans and rodents that acute intravenous exposure to fructose can lead to a depletion of ATP (66) in the livers and this may be associated with alteration of both apoptotic and necrotic TNFR1-mediated liver damage. However, in the present study hepatic ATP concentration did not differ between the groups (see Table 16).

Table 16 Effect of fructose feeding on ALT levels, inflammatory infiltration and expression patterns of chemokines as well as hepatic ATP concentrations[1]

	Control + Water	TNFR1 -/- + Water	Control + Fructose	TNFR1 -/- + Fructose
ALT (U/L)	2.7 + 0.8	3.4 + 0.9	16.1 + 4.1 [a,b]	5.4 + 0.9 [c]
Neutrophil count	0.2 ± 0.03	0.2 ± 0.08	1.1 ± 0.09 [a,b,d]	0.33 ± 0.05
ICAM-1 (% of control)	100 ± 16	126 ± 3	182 ± 16 [a,d]	118 ± 18
CCL2 (% of control)	100 ± 15	36 ± 2	156 ± 58 [b]	38 ± 6
CCL19 (% of control)	100 ± 16	99 ± 13	207 ± 57	82 ± 13 [c]
ATP (µM)	0.94 + 0.2	1.17 + 0.1	1.02 + 0.1	1.08 + 0.1

[1] Values represent means ± SEM. [a]$p < 0.05$ compared with wild-type mice fed with plain water. [b]$p < 0.05$ compared with TNFR1 -/- mice fed with plain water. [c]$p< 0.05$ compared with wild-type fructose fed mice. [d]$p< 0.05$ compared with TNFR1 -/- fructose fed mice

3.1.3 Effect of fructose feeding on hepatic iNOS protein levels and lipid peroxidation in livers of TNFR1-/- mice

Studies of our own group and those of other groups have shown that chronic fructose intake is associated with elevated levels of reactive oxygen species and lipid peroxidation (21, 59, 60) Therefore, hepatic iNOS levels and 4-hydroxynonenal adducts were determined in wild-type and TNFR1 -/- mice fed plain water or 30% fructose solution. Results are summarized in Figure 3. Hepatic iNOS protein levels were minimal and similar in wild-type and TNFR1 -/- mice fed water (Figure 3A). In contrast, iNOS protein levels of the liver were significantly higher by ~3.2-fold in fructose fed wild-type mice in comparison to water fed controls (Figure 3A). A similar effect of fructose feeding on hepatic iNOS protein levels was also found in TNFR1-/- mice. In line with these findings levels of 4-hydroxynonenal protein adducts were significantly increased by ~3-fold in livers of both fructose fed wild-type mice and TNFR1 -/- mice ($p<0.05$ in comparison to their respective water controls) (Figure 3B). Conversely, levels of 4-hydroxynonenal protein adducts in the liver were minimal and remained similar in wild-type and TNFR1 -/- mice fed water (Figure 3B).

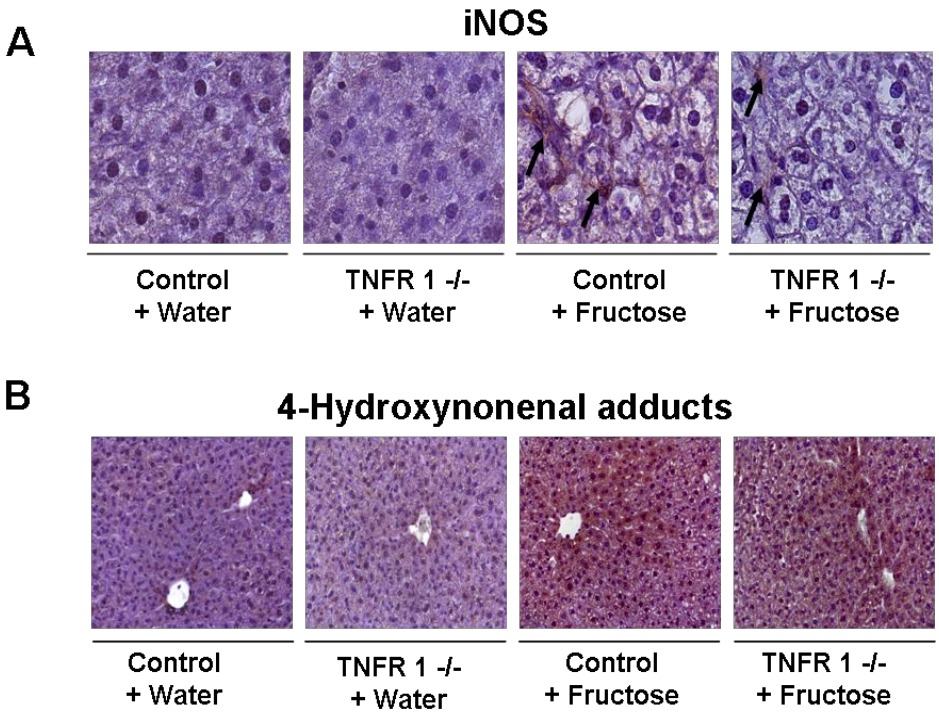

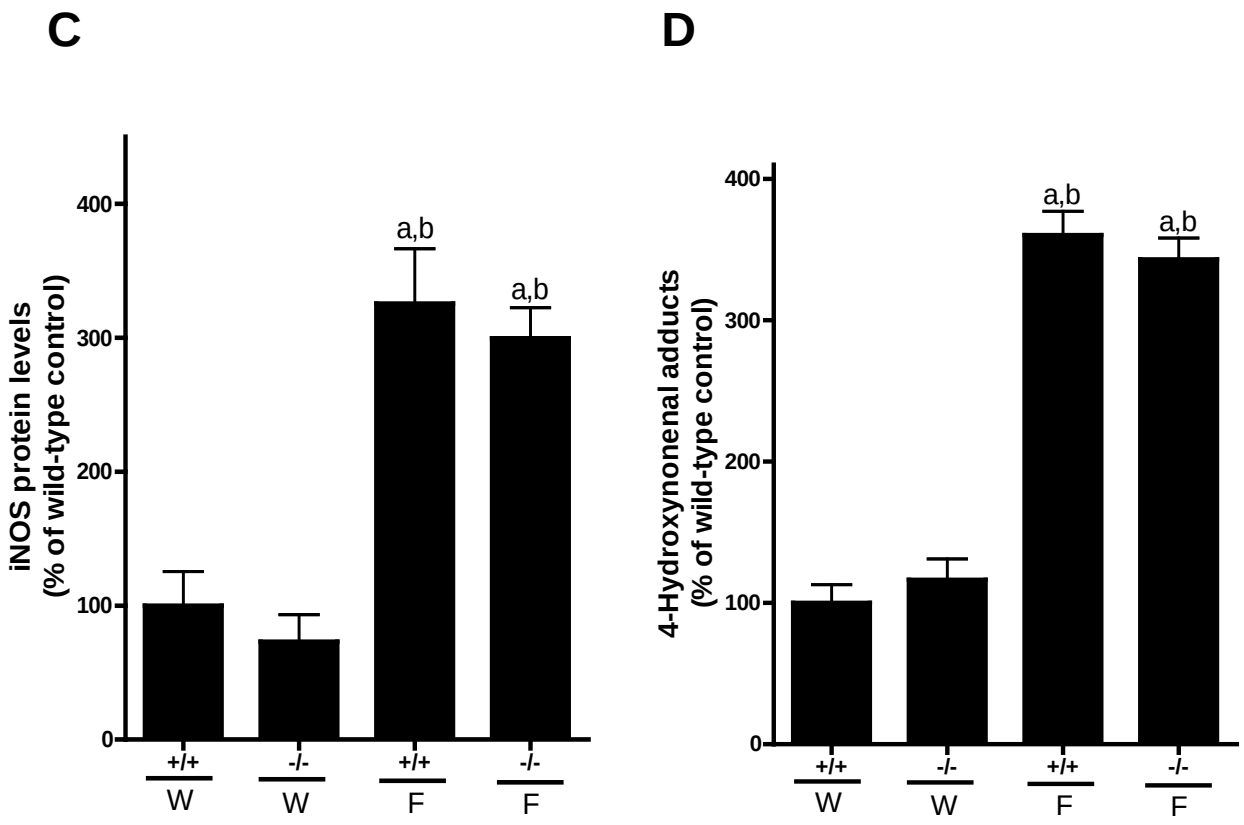

Figure 3 Effect of fructose feeding on iNOS protein levels and markers of lipid peroxidation in livers of TNFR 1-/- mice. (A) Representative photomicrographs of immunostaining of iNOS in liver sections (630x). (B) Photomicrographs of immunostaining of 4-hydroxynonenal protein adducts in liver sections (200x). (C&D) Densitometric analysis of the respective staining. Data are shown as means ± SEM (n = 4-6) and are normalized to percent of wild-type control. W – water; F – 30% fructose solution. [a]$p < 0.05$ compared with wild-type mice fed with plain water. [b]$p < 0.05$ compared with TNFR1 -/- mice fed with plain water

3.1.4 Effect of fructose feeding on hepatic glucose metabolism and insulin signaling in TNFR 1-/- mice

Results of our own group and those of other groups have indicated that alterations in glucose metabolism and hepatic insulin signalling may be associated with chronic fructose intake and induction of TNFα in the liver (21, 60, 67). Thus, in the present study markers of insulin resistance (e.g. RBP-4, Akt) as well as the expression of gluconeogenic enzyme PEPCK were determined in the livers of mice either fed with water or 30% fructose solution. Results are summarized in Figure 4.

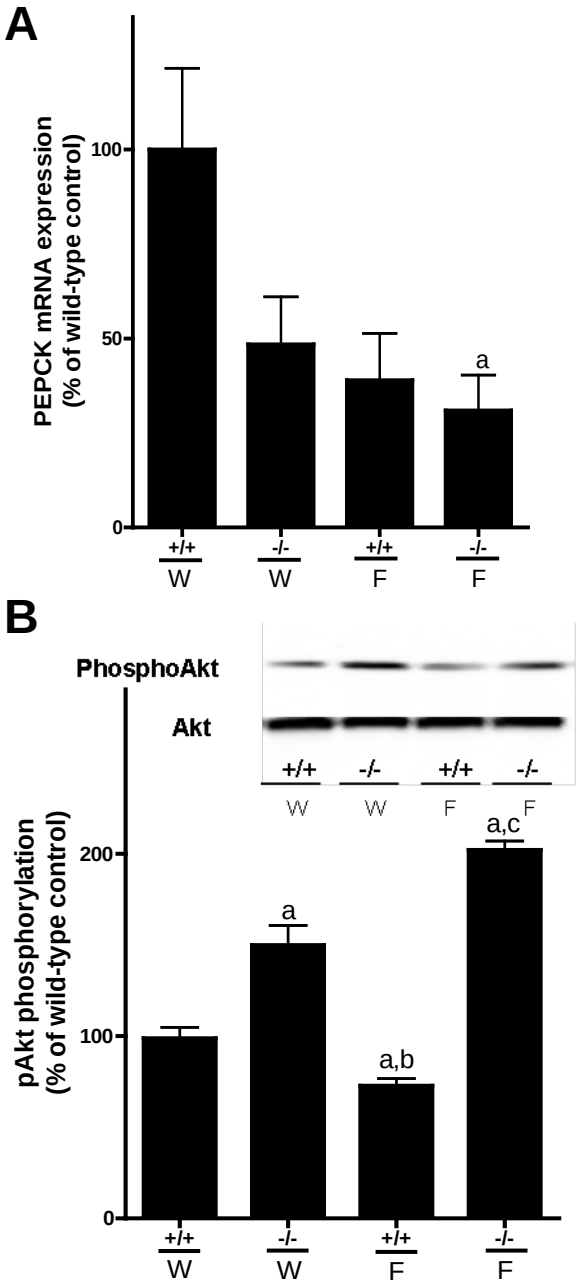

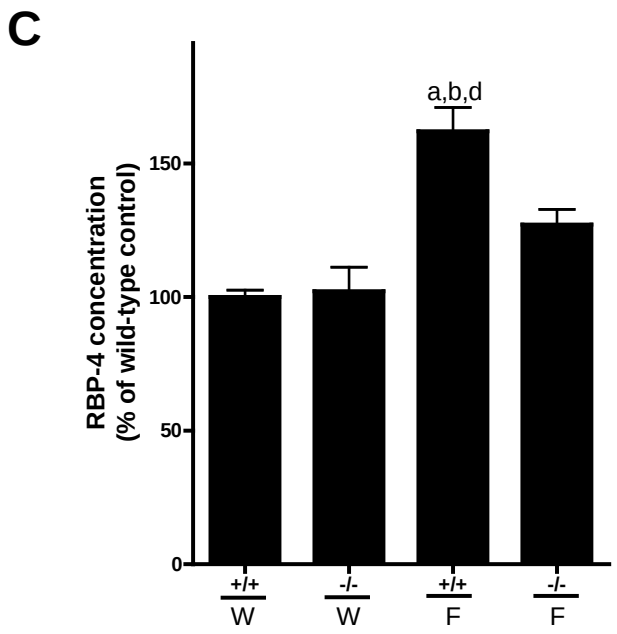

Figure 4 Effect of fructose feeding on hepatic PEPCK mRNA expression, plasma levels of RBP4 and phosphorylation status of Akt in livers of TNFR1-/- mice. (A) PEPCK mRNA expression in the liver. (B) Representative photographs of western blots of phospho Akt and total Akt and quantitative analysis of blots. (C) Plasma RBP4 levels. Data are expressed as means ± SEM (n=4-6) and are normalized to percent of wild-type control. W – water; F – 30% fructose solution. [a] $p < 0.05$ compared with wild-type mice fed with plain water. b $p < 0.05$ compared with TNFR1 -/- mice fed with plain water. [C] $p< 0.05$ compared with wild-type fructose fed mice. [d] $p< 0.05$ compared with TNFR1 -/- fructose fed mice.

Hepatic PEPCK mRNA expression did not differ between water fed TNFR1-/- and fructose fed TNFR1-/- mice. However, in fructose fed wild-type mice PEPCK mRNA expression in the liver was lower by -~61% ($p=0.06$) in comparison to wild-type water controls (Figure 4 A). As expected, phosphorylation of Akt was significantly lower by -~35% in livers of fructose fed wild-type mice in comparison to water fed wild-type mice. Interestingly, this effect of fructose feeding was not observed in the livers of TNFR1-/- mice, rather, the phosphorylation of Akt was higher and similar to that of water fed TNFR1-/- mice. (Figure 4 B). In line with these findings, plasma RBP4 levels were significantly increased by +~1.6-fold in plasma of fructose fed wild-type mice in comparison to water fed wild-type mice. Conversely, similar effect of fructose feeding was not found in TNFR1 -/- mice

3.1.5 Effect of fructose feeding on hepatic AMPK phosphorylation and lipogenesis in livers of TNFR1-/- mice

Markers of hepatic lipid metabolism (e.g. SREBP-1, FAS and PAI-1) and AMPK, an enzyme involved in cellular homeostasis, were determined in the present study to examine if the protective effects of the deletion of TNFR1 were associated with alterations of any of the markers stated above. Results are summarized in Figure 5. Hepatic mRNA expression of SREBP-1 and FAS were similar in water fed controls regardless of substrains. However, chronic fructose feeding in wild-type mice was associated with a significant induction of SREBP-1 and FAS mRNA expression by ~3- and ~6-fold in comparison to water controls, respectively. In contrast, a similar effect of fructose feeding was not found in TNFR1 -/- mice, in livers of these animals SREBP-1 mRNA expression was at the level of controls fed plain water whereas expression of FAS was induced by ~3.5-fold in comparison to water controls (Figure 5 A & B).

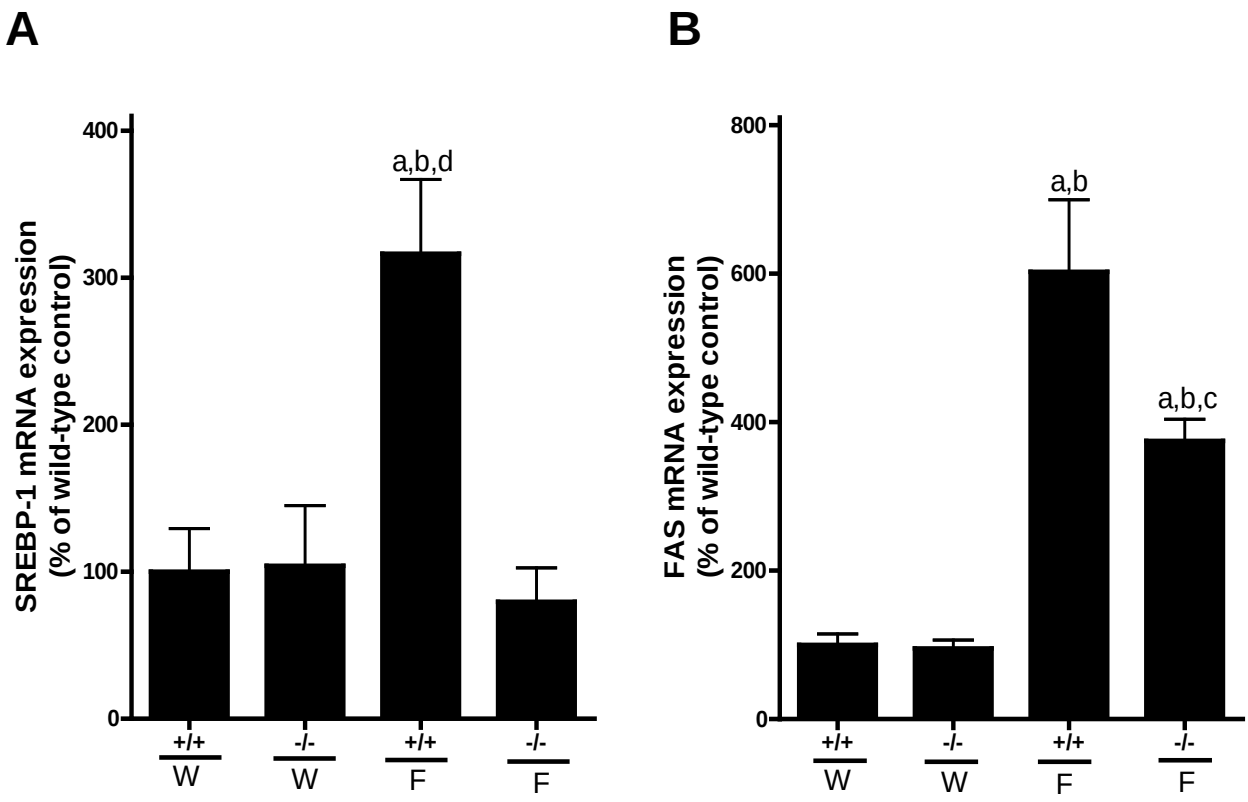

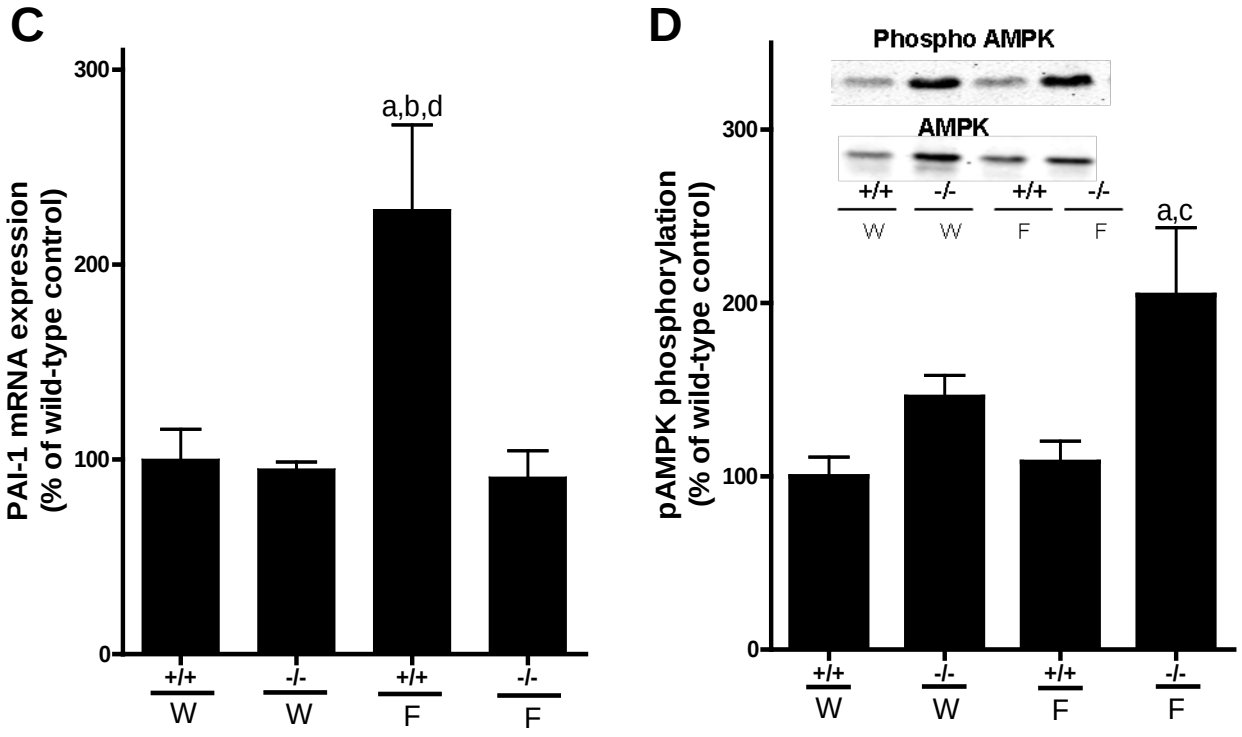

Figure 5 Effect of fructose feeding on SREBP-1, FAS and PAI-1 mRNA levels as well as phosphorylation status of AMPK in livers of TNFR 1-/-mice. (A) SREBP-1, (B) FAS and (C) PAI-1 mRNA expression levels were normalized to 18S expression. (D) Representative photographs of western blots of phospho AMPK and total AMPK and quantitative analysis of blots. Data are expressed as means ± SEM (n=4-6) and are normalized to percent of wild-type control. W – water; F – 30% fructose solution. $^{a}p < 0.05$ compared with wild-type mice fed with plain water. $^{b}p < 0.05$ compared with TNFR1 -/- mice fed with plain water. $^{c}p < 0.05$ compared with wild-type fructose fed mice. $^{d}p < 0.05$ compared with TNFR1 -/- fructose fed mice

PAI-1 mRNA expression in the liver is known to be regulated through TNFα and insulin-dependent mechanisms, moreover, results of our own group and other groups indicate that hepatic PAI-1 mRNA expression is increased in patients with NAFLD ((19, 31, 68). In the present study, hepatic PAI-1 mRNA expression was minimal in water fed mice and did not differ between substrains (Figure 5 C). Conversely, in livers of fructose fed wild-type mice PAI-1 mRNA expression was significantly induced by ~2.2-fold in comparison to water fed controls (Figure 5 C). This effect of fructose feeding was markedly attenuated in the livers of TNFR1-/- mice (Figure 5 C). Phosphorylation of AMPK was similar in livers of water fed mice regardless of substrain as well as fructose fed wild-type mice. In contrast, phosphorylation of AMPK was increased in livers of fructose fed TNFR1-/- mice in comparison to the appropriate controls.

Taken together, results of aim 1 suggest that in fructose-induced NAFLD TNFα through its receptor TNFR1 may cause alterations in hepatic insulin signalling, lipid metabolism and induction of PAI mRNA expression. Therefore, it was further investigated to clarify if PAI-1 is also a critical factor in the onset of fructose-induced hepatic steatosis.

3.2 Studies in PAI-1-/- mice fed fructose

As results of aim 1 suggested that chronic fructose feeding is not only associated with significant increase of triglycerides by +~5.8-fold in the livers of wild-type mice in comparison to controls (see section 3.1) but also with a significant increase in hepatic PAI-1 mRNA expression by ~2.5-fold in comparison to controls (see Table 17). The role of PAI-1 in fructose-induced liver injury was further studied in PAI-1 knockout mice.

3.2.1 Effect of fructose feeding on weight gain and liver to body weight ratio as well as hepatic PAI-1 mRNA expression in PAI-1-/- mice

Body weight of mice was measured weekly. Results are summarized in Table 17. Absolute body weight was slightly higher in PAI-1-/- mice fed water than in controls; however, differences did not reach level of significance. Absolute weight gain did not differ between water fed controls.

Table 17 Effect of fructose feeding on body weight and PAI-1 mRNA expression[1]

	Water		**Fructose**	
	Wild-type	**PAI-1-/-**	**Wild-type**	**PAI-1-/-**
Body weight (in g)	20.48±0.3	22.18±0.5	23.84±0.7 [a]	24.35±0.9 [a]
Liver to body weight ratio (in %)	4.8±0.1	4.7±0.07	5.9±0.1 [a,b]	5.4±0.4
Weight gain (g)	3.1±0.1	2.9±0.4	5.1±0.7 [a,b]	4.6±0.09
PAI-1 (fold-induction)	2.2±0.4	n.d	4.7±0.9 [a]	n.d

[1] Values represent means ± SEM. [a]$p < 0.05$ compared with wild-type mice fed with plain water. [b]$p < 0.05$ compared with PAI-1 -/- mice fed with plain water. [c]$p< 0.05$ compared with wild-type fructose fed mice

When compared with their respective controls, absolute body weight gain of both fructose fed groups were significantly higher (wild-type: +~1.4g, PAI-1-/-: +~1.3g in comparison to respective controls, both $p<0.05$). In both fructose fed groups liver to body weight ratio was significantly higher than their respective controls (wild-type liver to body weight ratio: +~1-fold; PAI-1-/- liver to body weight ratio: +~1-fold) (see Table 17)

3.2.2 Effect of fructose feeding on liver steatosis in PAI-1-/-mice

To determine the effect of the deletion of PAI-1 on liver damage in mice chronically exposed to fructose liver steatosis was assessed by H&E and Oil red O staining. Furthermore, triglyceride accumulation was also assessed in livers of PAI-1 -/- and wild-type mice either fed water, or water sweetened with 30% fructose for 8 weeks. Results are summarized in Figure 6. Triglyceride accumulation, lipid staining and pathological changes were minimal in water fed mice regardless of the strain. Conversely, hepatic triglyceride accumulation was increased by ~5.8-fold in livers fructose fed wild-type mice in comparison to appropriate controls whereas hepatic triglyceride accumulation was only increased by ~2-fold in PAI-1-/- mice exposed to fructose in comparison to PAI-1-/- mice fed water (Figure 6C). Similar results were also found in liver tissue stained with oil red O and H & E staining (Figure 6A & B).

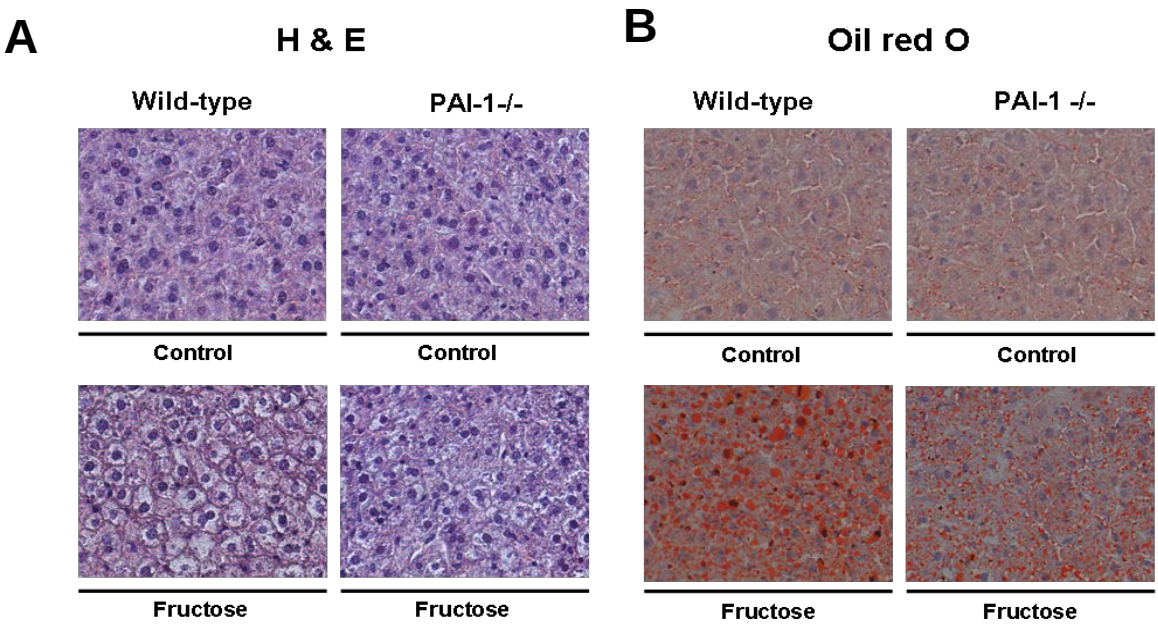

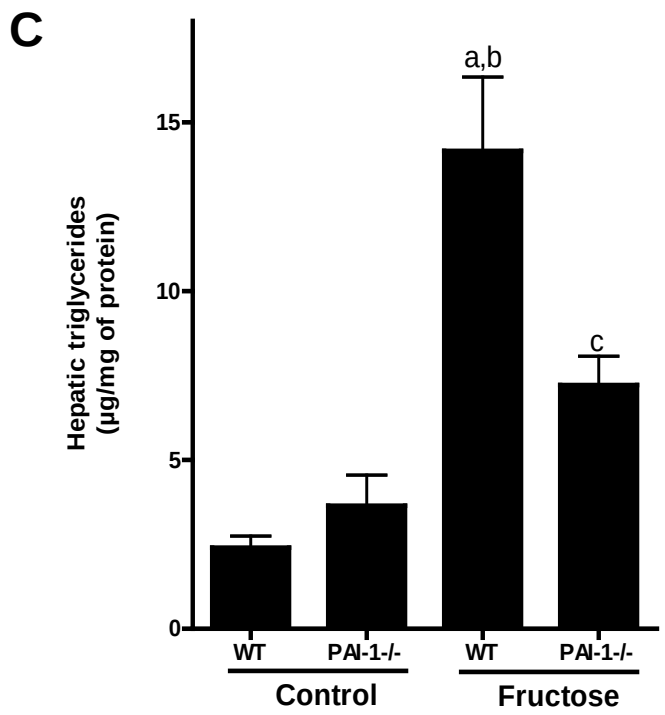

Figure 6 Effect of fructose feeding on hepatic lipid accumulation and histology in PAI-1-/- mice. (A) Representative photomicrographs of hematoxylin and eosin staining of liver sections. (B) Representative photomicrographs of oil red O staining of liver sections. (C) Quantitation of hepatic triglycerides content (n=5-7). Data are expressed as means ± SEM. $^{a}p < 0.05$ compared with wild-type mice fed with plain water. $^{b}p < 0.05$ compared with PAI-1-/- mice fed with plain water. $^{c}p < 0.05$ compared with wild-type fructose fed mice.

3.2.3 Effect of fructose feeding on endotoxin levels and TNFα protein concentration as well as insulin signaling in livers of PAI-1-/- mice

Results of our own group have suggested that chronic fructose feeding in mice is associated with elevated plasma endotoxin levels as well as hepatic TNFα protein concentration (21). Therefore, in PAI-1-/- and wild-type mice fed fructose or water plasma endotoxin levels and hepatic TNFα protein concentration were determined. Results are summarized in Figure 7. Both endotoxin levels in portal plasma and TNFα protein concentration in the liver were minimal and did not differ between water fed mice regardless of strain (Figure 7A & B). Interestingly, chronic fructose feeding led to a significant increase of endotoxin levels in portal plasma as well as TNFα protein levels in the liver in both strains (Figure 7A & B).

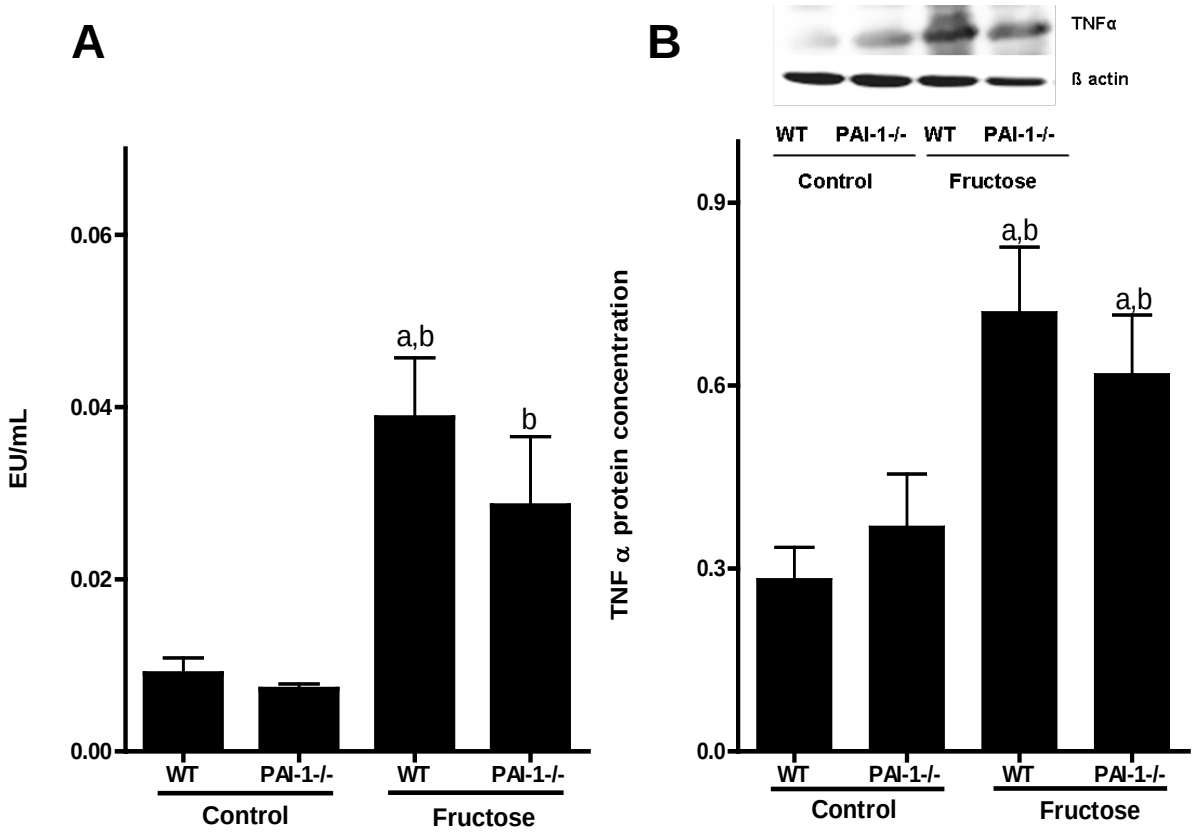

Figure 7 Effect of fructose feeding on portal endotoxin and hepatic TNFα protein levels in PAI-1-/- mice. (A) Endotoxin levels in portal plasma (n=5-6). (B) Representative photographs of Western blots of TNFα and ß-actin in liver tissue (C) quantitative analysis of blots (n=5). Data are expressed as means ± SEM. [a]$p < 0.05$ compared with wild-type mice fed with plain water. [b]$p < 0.05$ compared with PAI-1-/- mice fed with plain water.

In line with these findings, plasma RBP-4 and hepatic RBP-4 mRNA expression, both shown to be markers of insulin resistance (60, 61) were also found to be increased in fructose fed mice regardless of the strain (Table 18). In contrast, in water fed controls these markers did not differ and were minimal. In addition, hepatic GLUT-4 mRNA expression, recently shown to be associated with elevated PAI-1 levels in liver, was also determined (Table 20) (69). Hepatic GLUT-4 mRNA was markedly downregulated in mice fed chronically fructose regardless of strain (Table 18). Furthermore, markers of glucose homeostasis such as PEPCK and glucokinase were also determined. In livers of fructose fed wild-type mice PEPCK mRNA was significantly decreased in comparison to water fed wild-type mice (Table 18).

Table 18 Effect of fructose feeding on the markers of insulin resistance in the liver and in plasma[1]

	Water		Fructose	
	Wild-type	**PAI-1-/-**	**Wild-type**	**PAI-1-/-**
RBP 4 (µg/ml)	28.8±0.8	25.8±1.1	45.5±2.3 [a,b]	42±3.3 [a,b]
RBP 4 mRNA (fold-induction)	1.4±0.2	1.7±0.1	3.3±0.9	4.0±0.9 [a]
GLUT-4 mRNA (fold-induction)	315±50	273±106	6.0±0.7 [a,b]	4.5±1.2 [a,b]
PEPCK mRNA (fold-induction)	32.9±13	22.5±4.4	3.2±0.9 [a]	6.9±2.7
Glucokinase mRNA (fold-induction)	3.9±0.8	4.9±0.6	2.5±0.7	8.7±0.7 [a,b,c]

[1] Values represent means ± SEM. [a]$p < 0.05$ compared with wild-type mice fed with plain water. [b]$p < 0.05$ compared with PAI-1 -/- mice fed with plain water. [c]$p < 0.05$ compared with wild-type fructose fed mice.

Interestingly, expression of glucokinase of mRNA in the liver was significantly higher in fructose fed PAI-1-/- mice than in all other groups ($p<0.05$).

3.2.4 Effect of fructose feeding on c-Met signaling, lipoprotein synthesis and phosphorylation of Akt as well as BCL XL mRNA expression in livers of PAI-1-/- mice

PAI-1 in various etiologies of hepatic steatosis (e.g. alcohol and endotoxin) has been shown to play a crucial role in the activation of the hepatic growth factor (HGF)/Met-depending signaling cascades and subsequently hepatic lipid metabolism (for overview see (34)).

Thus the effect of fructose feeding on cMet phosphorylation, expression of ApoB mRNA and activity of MTTP in livers of PAI-1-/- and wild-type mice was determined. Results are summarized in Figure 8. Phosphorylation of hepatic cMet was minimal in livers of water fed controls regardless of strain and fructose fed wild-type mice. In contrast, chronic feeding of 30 % fructose solution in PAI-1-/- mice was associated with a significant increase of cMet phosphorylation by + ~4-fold in comparison to PAI-1-/- mice fed water (Figure 8A). In line with these findings ApoB mRNA expression was only found to be increased by +~2.3-fold in livers of fructose fed PAI-1-/- mice in comparison to PAI-1-/- mice fed water whereas in livers of fructose fed wild-type mice it remained at level of controls (Figure 8B). In addition, MTTP activity was also only found to be increased in livers of PAI-1-/- mice fed fructose by10% in comparison to PAI-1-/- mice fed water, however as the activity varied considerably between the animals differences did not reach to the level of significance (p=0.06). (Figure 8C).

Results of *in vitro* and *in vivo* studies have shown that phosphorylation of Akt may be regulated through cMet and the cMet dependent-Akt activation may modulate BCL-XL (an anti-apoptotic BCL-2 family protein) (70, 71). Therefore, phosphorylation of Akt and mRNA expression of BCL-XL in livers of fructose and water fed mice were determined. Chronic feeding of 30% fructose solution significantly decreased phosphorylation levels of Akt in livers of fructose fed wild-type mice in comparison to water controls (Figure 8D). Interestingly, this effect of fructose feeding was not found in livers of fructose fed PAI-1-/- mice (Figure 8D). Similar results were also found for BCL-XL mRNA expression in livers of wild-type and PAI-1-/- mice fed. (see Table 19).

Table 19 Effect of fructose feeding on BCL-XL mRNA expression[1]

	Water		**Fructose**	
	Wild-type	**PAI-1-/-**	**Wild-type**	**PAI-1-/-**
BCL-XL mRNA (fold-induction)	5.9±0.9	2.9±0.6	1.8±0.2 [a]	6.8±1.7 [c]

[1] Values represent means ± SEM. [a]$p < 0.05$ compared with wild-type mice fed with plain water. [c]$p < 0.05$ compared with wild-type fructose fed mice.

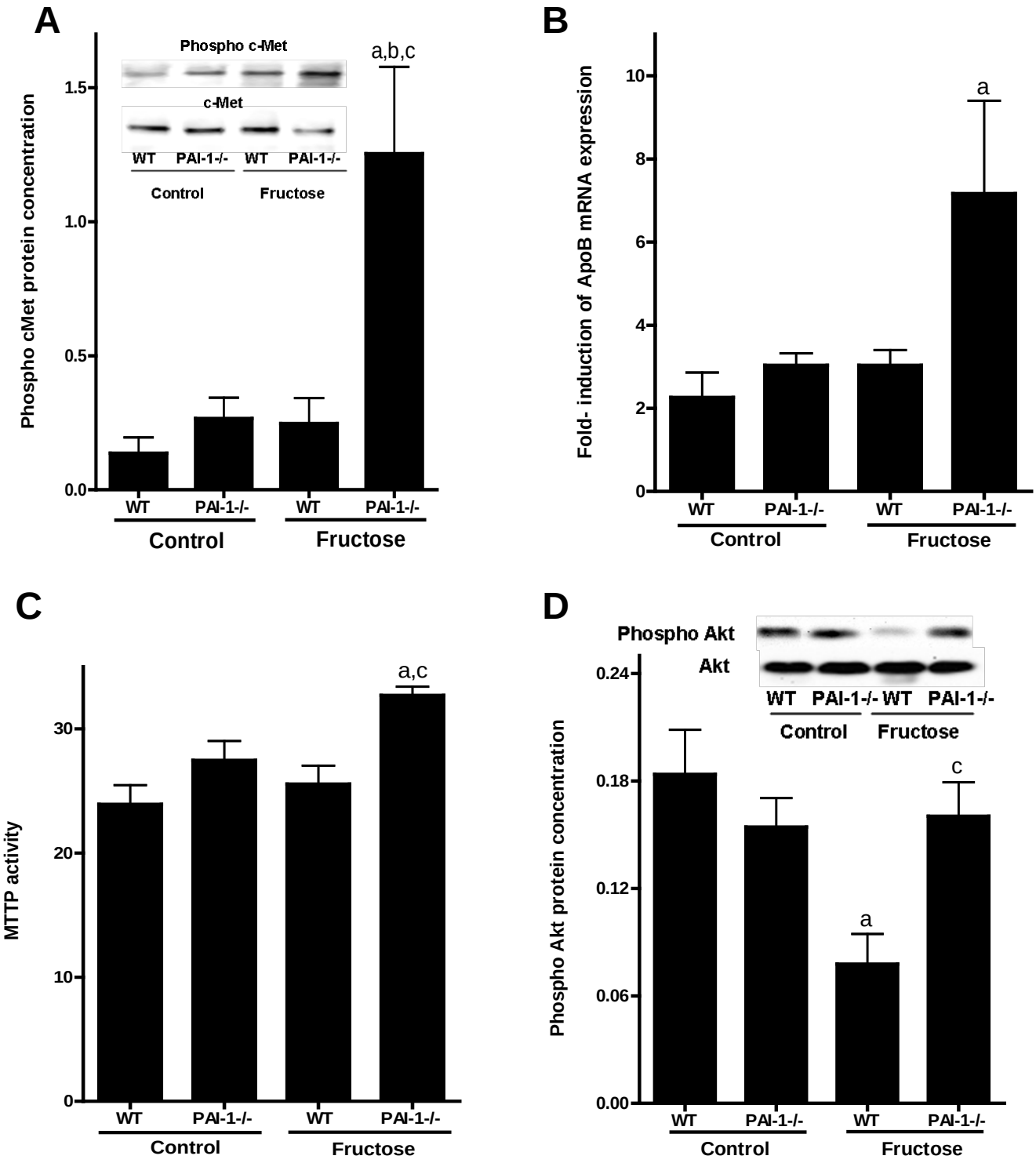

Figure 8 Effect of fructose feeding on phosphorylation of cMet, Akt protein and ApoB mRNA expression as well as MTTP activation in livers of PAI-1-/- mice. (A) Representative photographs of Western blots of phospho c-Met, total c-Met and quantitative analysis of blots (n=4) (B) ApoB mRNA levels normalized to ß-actin expression (n=5) (C) MTTP activity (n=5) and (D) representative photographs of Western blots of phospho Akt and total Akt and quantitative analysis of blots (n=5). Data are expressed as means ± SEM. $^{a}p < 0.05$ compared with wild-type mice fed with plain water. $^{b}p < 0.05$ compared with PAI-1-/- mice fed with plain water. $^{c}p < 0.05$ compared with wild-type fructose fed mice.

Effect of HGF on PAI-1-stimulated AML 12 cells

The role of PAI-1 and HGF in modulating triglyceride export in the liver was further investigated in a cell culture model (e.g. AML12 cells = model of murine hepatocytes). AML 12 cells were challenged with PAI-1 in the presence or absence of HGF as described in section 2.2.4. Results are summarized in Figure 9. HGF alone had no effect on triglyceride content and MTTP activity in AML12 cells (Figure 9 A&B). Conversely, stimulation of cells with PAI-1 resulted in a significant decrease of MTTP activity in comparison to naïve cells (~81%). In line with these findings, triglyceride concentration was significantly increased in these cells (~+ 10-fold in comparison to naïve cells). Interestingly, when cells were treated with HGF while concomitantly being challenged with PAI-1, MTTP activity remained at the level of naïve cells and cells did not accumulate triglycerides (Figure 9 A&B).

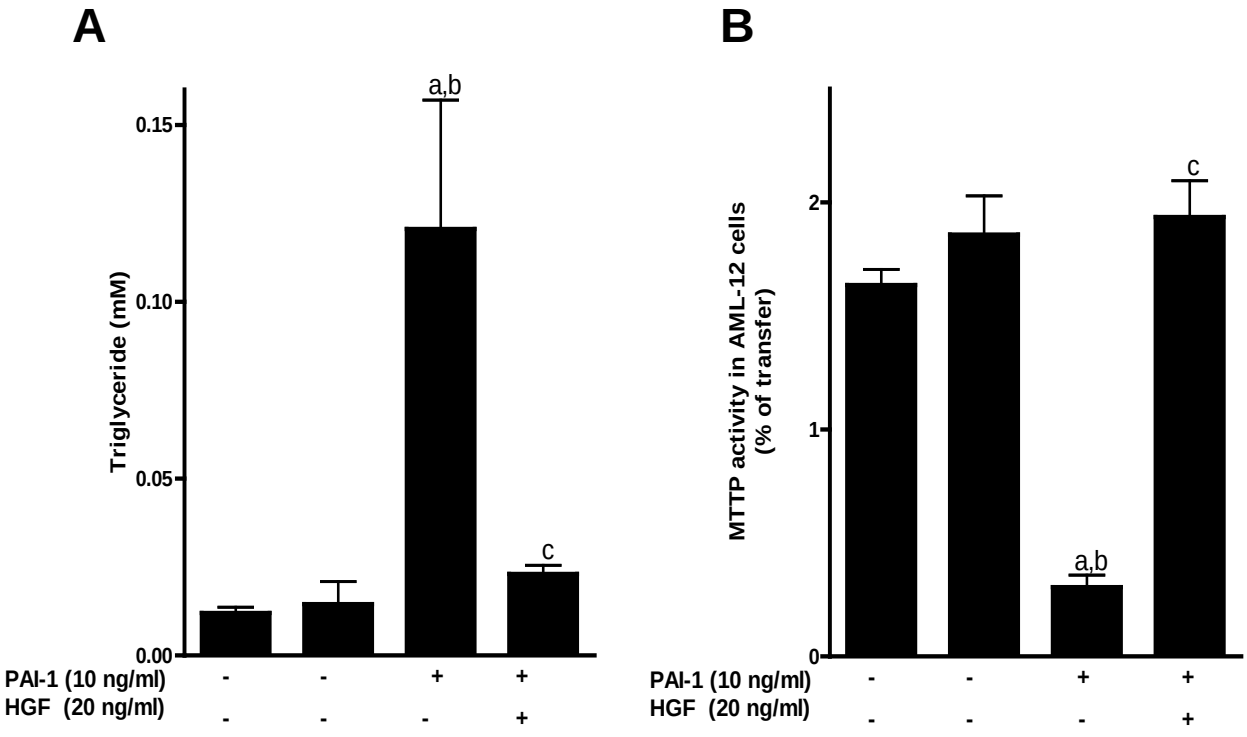

Figure 9 Effect of PAI-1 on triglyceride accumulation and MTTP activity in AML12 cells. (A) Triglyceride accumulation and (B) MTTP activity. Data are expressed as means ± SEM (n=3). [a]$p < 0.05$ compared with naïve cells. [b]$p < 0.05$ compared with HGF treated cells. [c]$p < 0.05$ compared with PAI-1 treated cells.

3.2.5 Effect of fructose feeding on hepatic NKT cells in PAI-1-/- mice

Recently it has been shown that MTTP plays a crucial role in the lipidation of the CD1d receptor, a receptor involved in the regulation of NKT cell viability (72, 73). Therefore, expression of CD1d and markers of iNKT cells as well as iNKT cell activation in livers of PAI-1-/- and wild-type mice fed with water or fructose were determined. Results are summarized in Table 20 and Figure 10. In livers of PAI-1-/- mice CD1d mRNA expression was markedly higher regardless of feeding. (see Table 20).

Table 20 Effect of fructose feeding on expression of CD1d, IL-15,and IFN γ in livers of PAI-1-/- and wild-type mice[1]

	Water		Fructose	
	Wild-type	**PAI-1-/-**	**Wild-type**	**PAI-1-/-**
CD1d (fold-induction)	6.1±0.6	9.5±1.8	4.5±1.1 [b]	11.3±0.7 [a,c]
IL-15 (fold-induction)	3.1±0.3	3.2±0.9	4.5±0.9	7.4±1.2 [a,b]
IFNγ (fold-induction)	4.3±1.0	6.2±1.6	2.3±0.6	10.2±1.2 [a,c]

[1]Values represent means ± SEM. [a]$p < 0.05$ compared with wild-type mice fed with plain water. [b]$p < 0.05$ compared with PAI-1 -/- mice fed with plain water. [c]$p< 0.05$ compared with wild-type fructose fed mice. n.d= not detectable

Furthermore, iNKT cell surface markers CD3ε and NK1.1 were also determined in the liver and the results are summarized in Figure 10. Expression of CD3ε and NK1.1 were found to be increased in PAI-1-/- mice regardless of feeding (CD3ε: +~5.7-fold in comparison to wild-type water controls, +~6.2-fold in comparison to wild-type fructose fed mice. NK1.1: +~4-fold in comparison to wild-type water controls, +~3.5-fold in comparison to wild-type fructose fed mice) In line with these findings, hepatic CD3ζ staining was also found to be increased in PAI-1-/- mice regardless of additional treatments (Figure 10). In contrast, markers of iNKT cells activation (e.g. interleukin 15 (IL-15) and interferon γ (INFγ)) was only found to be significantly increased in fructose fed PAI-1-/- mice (see Table 20).

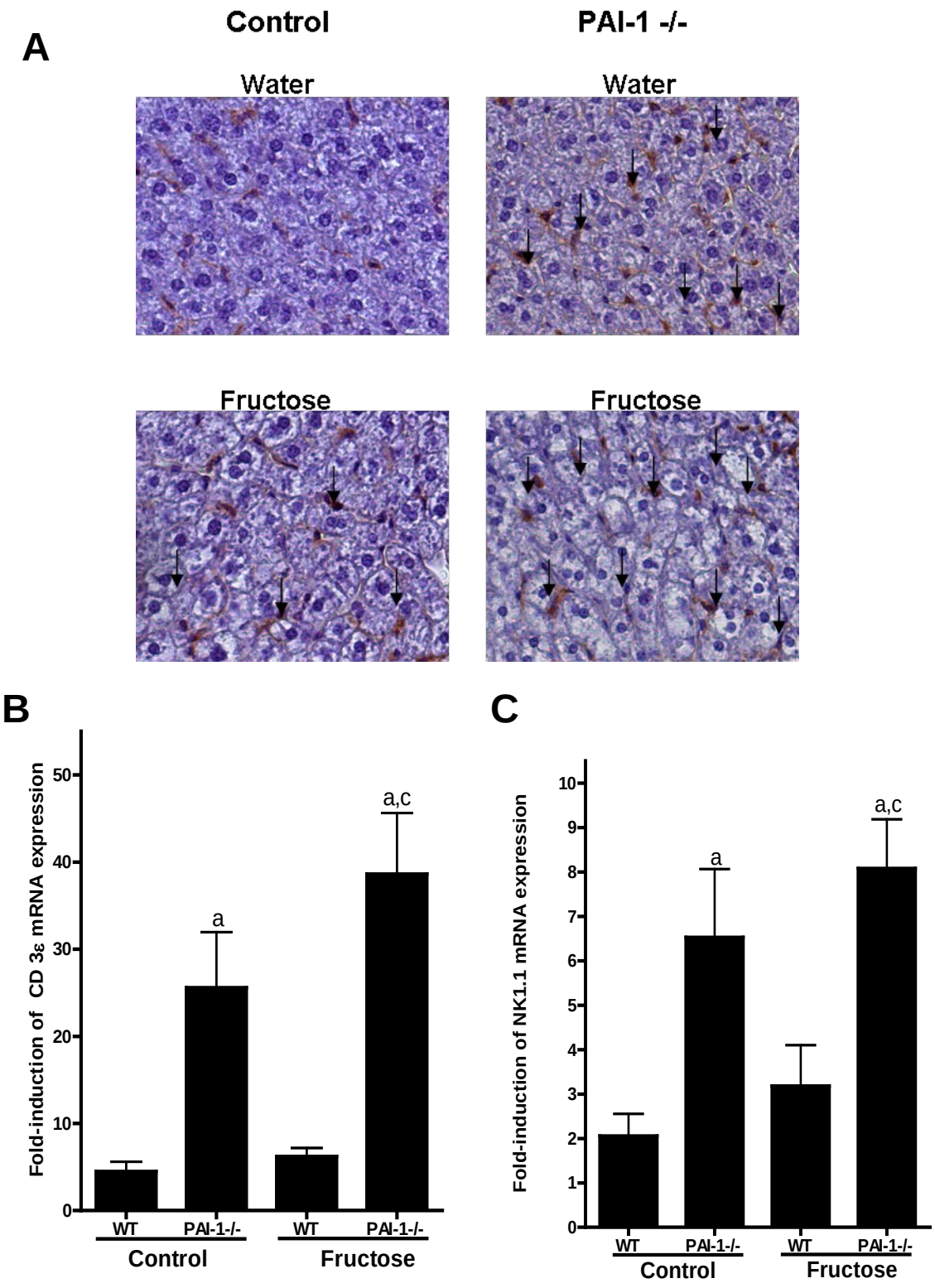

Figure 10 Effect of PAI-1 deletion on iNKT cell markers in livers of fructose fed mice. (A) Representative photographs of CD3ζ staining of liver sections; brown stained parts marked with arrows indicate CD3ζ positive cells (B) CD3ε mRNA levels normalized to 18S expression (n=5) (C) NK1.1 mRNA levels normalized to 18S expression (n=5). Data are expressed as means ± SEM. $^{a}p < 0.05$ compared with wild-type mice fed with plain water. $^{b}p < 0.05$ compared with PAI-1-/- mice fed with plain water. $^{c}p < 0.05$ compared with wild-type fructose fed mice.

3.3 Studies in human liver samples

The results of aim 1 and 2 published before in Kanuri *et al*.2010 (74) and Kanuri *et al.* 2011 (75) suggest that PAI-1 may be a critical factor in the onset of fructose-induced steatosis in mice through mechanisms involving a suppression of the compensatory up regulation of lipid export necessary to protect the liver from the increased amount of lipids resulting from a chronic dietary intake of fructose. In addition, the data also suggest that PAI-1 may also be involved in modulating CD1-reactive NKT cells in the liver. Therefore, it was further investigated in human subjects whether similar mechanisms are also involved in the development of NAFLD. Specifically, to determine if PAI-1, insulin signaling and iNKT cells are also altered in livers of human with NAFLD.

3.3.1 Dietary intake and physical activity of human subjects

Total intake of carbohydrates, fat, protein and the total energy intake did not differ between the controls and NAFLD subjects (Table 21). However, physical activity was less frequent in NAFLD subjects (50%) than in controls (100%). Total glucose and sucrose consumption were higher between NAFLD subjects and controls, however, as the intake varied considerably between the subjects the differences did not reach to the level of significance. Total fructose intake, derived from free fructose and sucrose, was significantly higher by ~10 g/d in subjects with NAFLD than in controls (see Table 21).

Table 21 Nutritional intake of NAFLD subjects and controls[1]

	Control	NAFLD patients
n	6	12
Energy kj/d	9106 ± 670	9387 ± 461
Protein g % Energy	79 ± 6 15 ± 0.4	88 ± 3 16 ± 0.7*
Fat g % Energy	87 ± 10 40 ± 10	89 ± 7 59 ± 12
Carbohydrates g % Energy	256 ± 15 49 ± 3	253 ± 14 49 ± 1
Glucose[2], g/d	37 ± 4	42.8 ± 4.3

Sucrose, g/d	48.3 ± 7.2	57.3 ± 6.3
Fructose[3], g/d	41.0 ± 3.2	51.5 ± 5.2*
Alcohol, g/d	6.5 ± 2.3	4.0 ± 1.2

[1] Values are means ± SEM. *Different from controls, P<0.05. [2] Glucose intake derived from free glucose and sucrose . [3]Fructose intake derived from free fructose and sucrose. (Table adapted from Thuy *et al.* 2008)

3.3.2 Lipid peroxidation in human subjects with NAFLD

As results of our own group and those of other groups in mice suggested that NAFLD in rodents is associated with an increased formation of reactive oxygen species (ROS) and lipid peroxidation (21, 57, 60) 4-hydroxynonenal adducts were determined in the livers of human NAFLD subjects and controls. Levels of 4-hydroxynonenal adducts in livers of human NAFLD subjects were significantly higher by ~2-fold in comparison to controls (Figure 11).

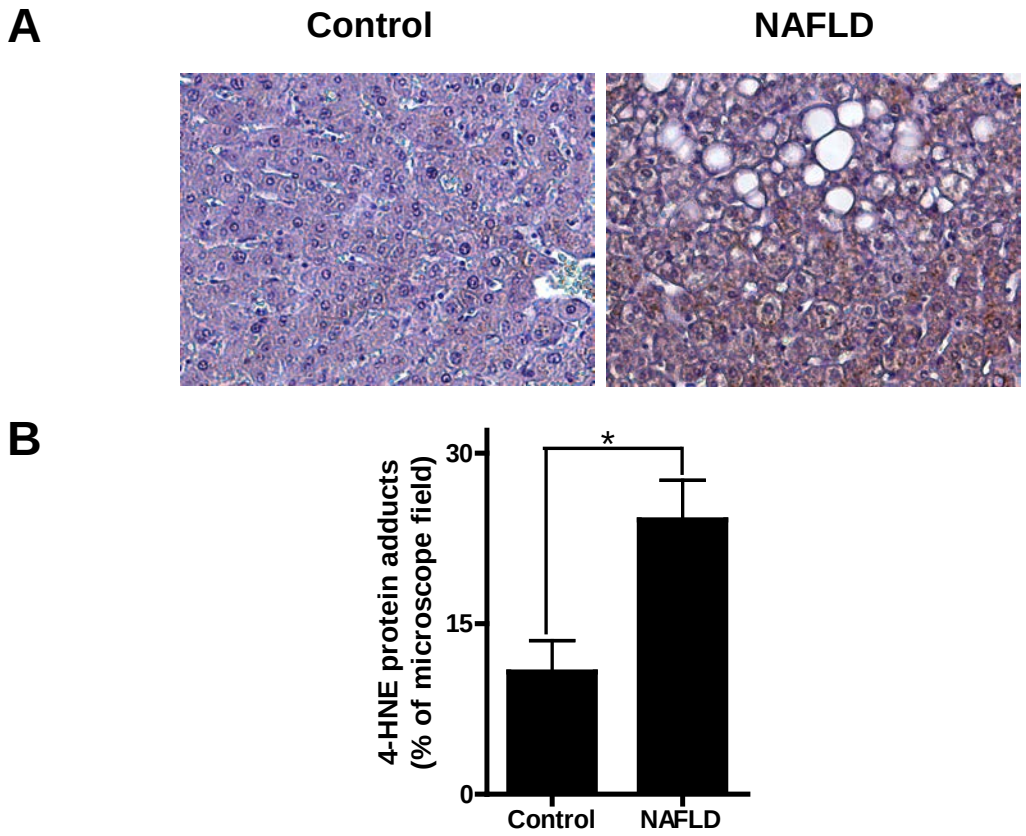

Figure 11 Hepatic 4-hydroxynonenal (4-HNE) protein adducts staining in controls and NAFLD patients (A) Representative photographs of 4-HNE protein adducts staining; brown stained parts indicate 4-HNE protein adducts staining (B) densitometric analysis of the staining.*p< 0.05 compared with controls (n=6 controls; n=8 NAFLD patients).

3.3.3 Hepatic IRS-1 mRNA expression and PAI-1 protein levels in human subjects with NAFLD

Results of animal studies have revealed that NAFLD in rodents is associated with an induction of expression of PAI-1 and altered insulin signaling (74, 75). Therefore, hepatic proteins levels of PAI-1 and IRS-1 mRNA were determined in human NAFLD subjects and controls to investigate whether similar mechanisms are also involved in the development of NAFLD in humans. Hepatic PAI-1 protein concentration localized to hepatocytes was significantly higher by ~2.4-fold in human NAFLD subjects in comparison to controls. In contrast, expression of IRS-1 mRNA was significantly lower by ~80 % in livers of NAFLD patients in comparison to controls (Figure 12)

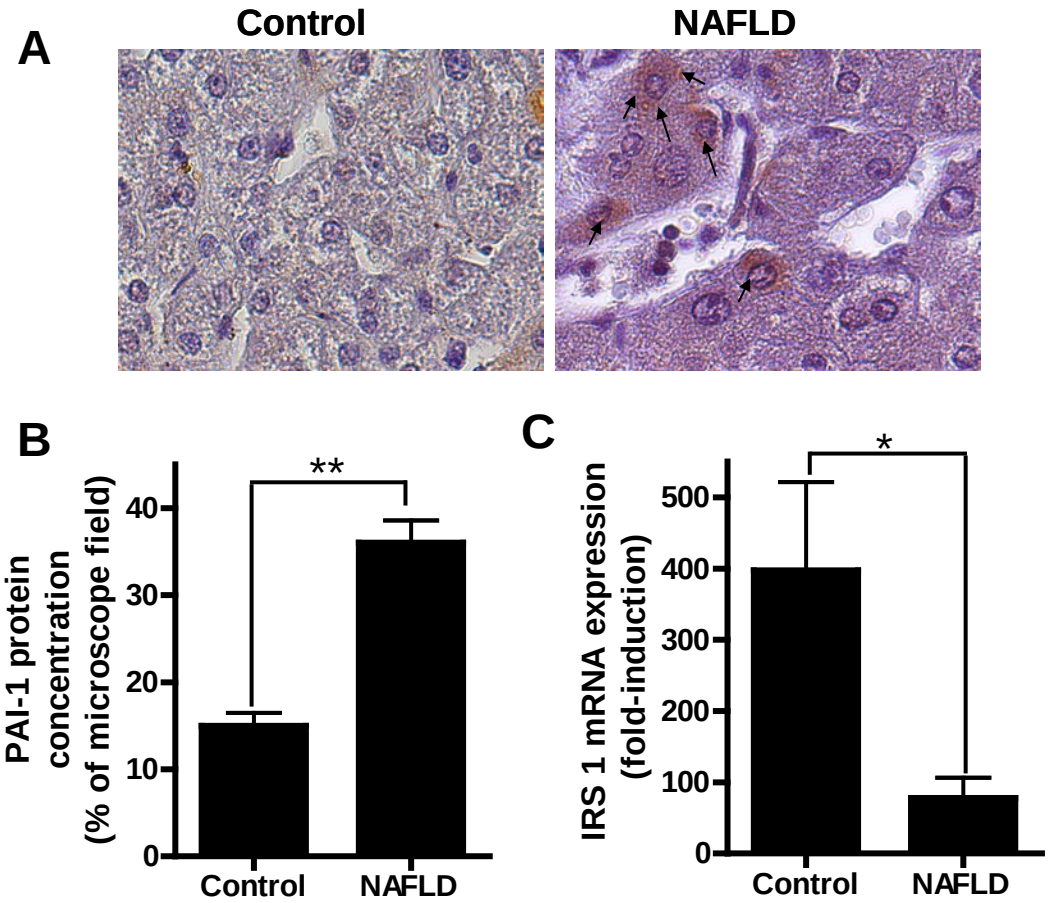

Figure 12 Hepatic PAI-1 protein levels and IRS-1mRNA expression in NAFLD patients (A) Representative photographs of PAI-1 staining; brown stained parts marked with arrows indicate PAI-1 staining and (B) densitometric analysis of the staining (n=6 controls; n=8 NAFLD patients). (C) IRS-1 mRNA expression normalized to ß-actin (n=6 controls; n=11 NAFLD patients). *p< 0.05 compared with controls. **p< 0.001 compared with controls.

3.3.4 Hepatic mRNA expression of cMet, BCL-2l, MTTP and CD1d in human subjects with NAFLD

Hepatic cMet mRNA expression was significantly lower in NAFLD patients in comparison to controls. In line with these findings mRNA expression of BCL 2l was considerably lower by ~71% in NAFLD patients in comparison to controls (Figure 13 A&B). However, no differences were found in the mRNA expression of MTTP and CD1d between the livers of NAFLD patients and those of controls (Figure 13 C&D).

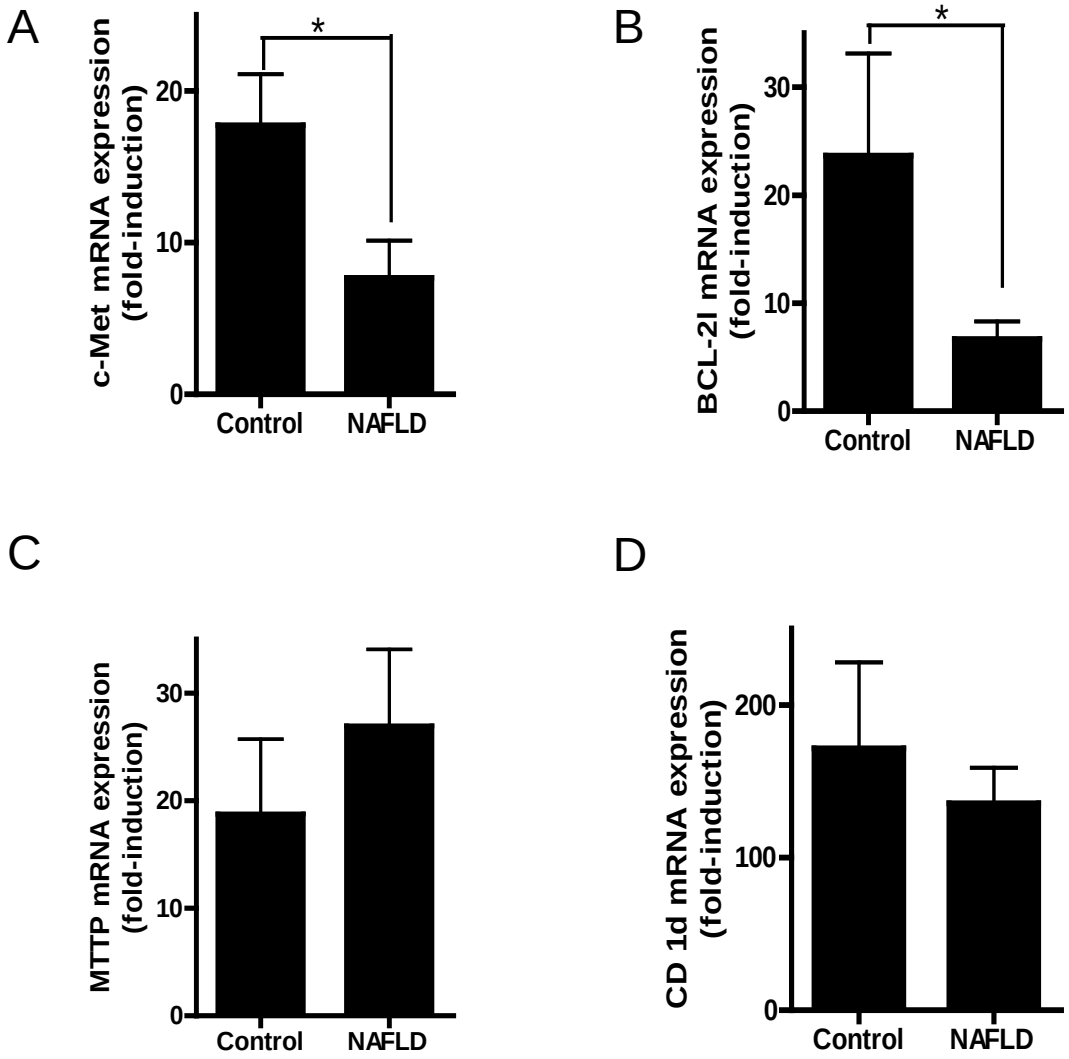

Figure 13 Hepatic mRNA expression of c-Met, BCL 2l, MTTP and CD 1d in NAFLD patients (A) c-Met mRNA expression, (B) BCL2l mRNA expression, (C) MTTP mRNA expression and (D) CD1d mRNA expression normalized to ß-actin. (n=6 controls; n=11 NAFLD patients). *p< 0.05 compared with controls. **p< 0.001 compared with controls.

3.3.5 Hepatic accumulation of iNKT cells and mRNA expression of IL-4 and IL-15 in NAFLD patients

In NAFLD patients number of iNKT cells in the liver was significantly increased in comparison to controls (Figure 14 A&B). Contrary to the increased number of iNKT cells, expression of iNKT cell markers such as IL-4 and IL-15 were significantly lower in livers of patients with NAFLD when compared with controls (Figure 14 C&D).

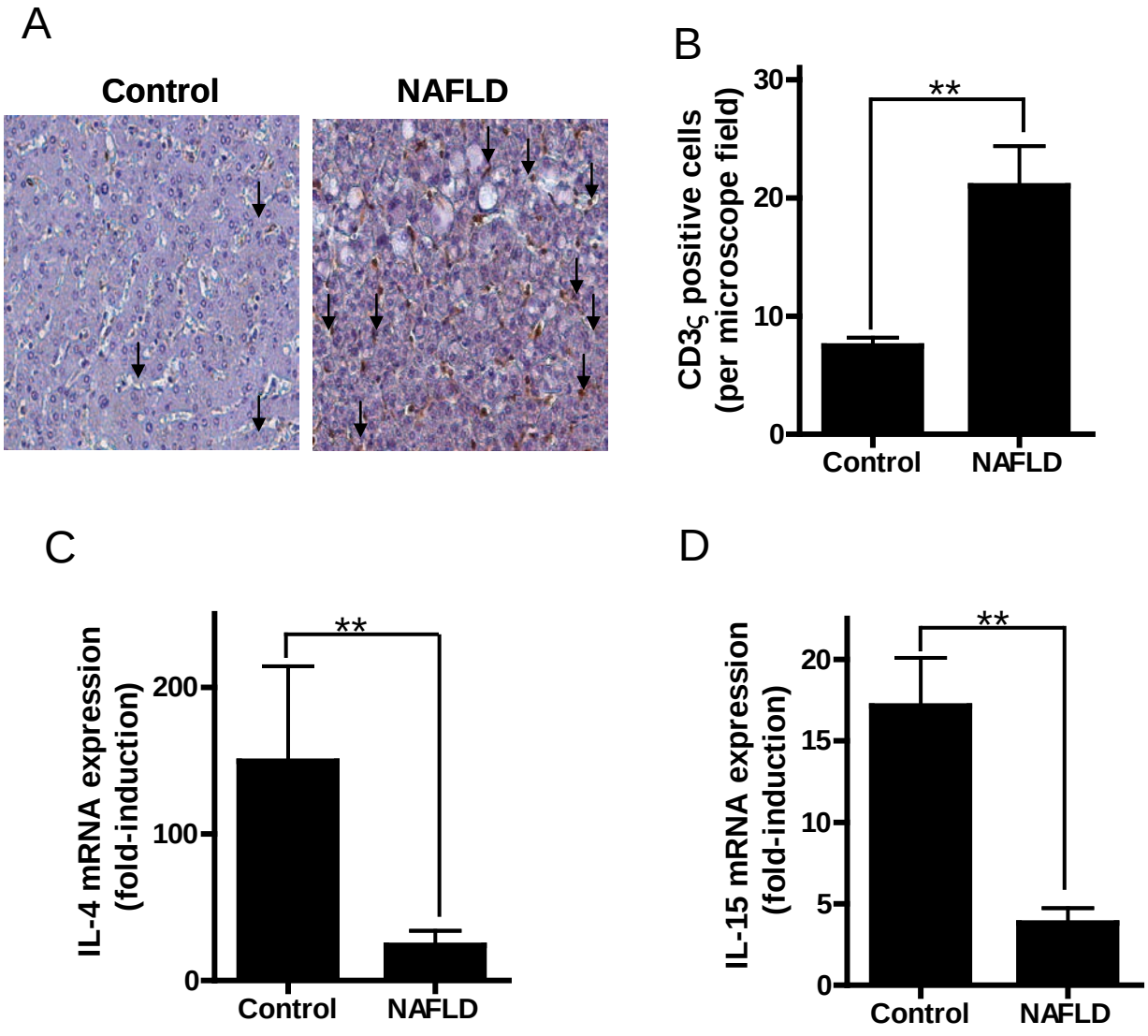

Figure 14 Hepatic CD3ζ staining and mRNA expression of IL-4 and IL-15 in NAFLD patients (A) Representative photographs of CD3ζ staining of liver sections (brown stained parts marked with arrows indicate CD3ζ positive cells) (B) Densitometric analysis of the staining (n=6 controls; n=8 NAFLD patients). (C) IL-4 mRNA expression and (D) IL-15 mRNA expression in the liver normalized to ß-actin. (n=6 controls; n=11 NAFLD patients). *p< 0.05 compared with controls. **p< 0.001 compared with controls.

4 Discussion

Non-alcoholic fatty liver disease with its clinical spectrum spanning from simple fatty liver to cirrhosis is by now one of the major cause for liver related mortality worldwide. The consumption of fructose has enormously increased in the US and in Europe over the last three decades, paralleling the prevalence of obesity and type-2-diabetes (35, 36, 76). Emerging evidences suggest that consumption of a carbohydrate rich diet and herein particularly a diet rich in fructose may also be a risk factor in the development of NAFLD in humans (19, 55, 77). Indeed, results of intervention studies in humans and animals suggest that a diet rich in fructose can result in dyslipidemia, hepatic insulin resistance and fatty liver disease (21, 57, 59, 78). Results of our own group indicate that besides the 'de novo lipogenesis' (also see chapter 1.2) caused by the metabolism of fructose, one of the major events in fructose-induced NAFLD involves the activation of the TLR 4 signalling cascade in the liver due to an increased intestinal translocation of endotoxin from the gut (21, 60). Furthermore, this increased intestinal translocation of bacterial endotoxin from the intestine to the portal vein due to chronic fructose intake was associated with elevated formation of reactive oxygen species and tumor necrosis factor (TNF) α expression in the liver (21). Results of animal studies have repeatedly shown that an increased expression of TNF α is linked with the development of NAFLD (27, 28, 79).

In models of alcoholic liver disease (ALD) the damaging effect of TNF α was associated with an elevated expression of hepatic PAI-1 whereas the genetic deletion of TNFR 1 or PAI-1 was associated with a protection against ALD (32). Results of our own group (19) but also other group (31) suggest that PAI-1 expression is also involved in the development of NAFLD in humans. It has further been suggested by the results of animal studies that PAI-1 is a modulator of hepatic lipid transport in acute and chronic alcoholic liver disease (ALD)(32). Taken together these results suggest that PAI-1 may be a critical factor in the pathogenesis of ALD.

However, if PAI-1 is also critically involved in the onset of NAFLD and if so what the underlying mechanisms involved in the induction of PAI-1 in the liver has not yet been determined. Therefore, the main aim of the PhD thesis was not only to investigate the role of TNF α and it's receptor TNFR1 in the induction of PAI-1 in mouse models of NAFLD as well as in humans but also to further clarify the role of PAI-1 in the development of NAFLD.

4.1 TNFR 1-/- mice are protected from fructose-induced steatosis

Several studies have suggested a role of TNFα in the pathogenesis of NAFLD. For instance, Crespo *et al.,* found elevated levels of TNFα mRNA and TNFα receptor p55 protein in NAFLD patients (80). In rodent studies it was shown that administration of TNF antibodies to ob/ob mice fed high fat diet improved hepatic steatosis, insulin sensitivity and inflammation in the liver (81). However, if TNFα is also a critical factor in the development of fructose-induced NAFLD and if the effects of TNFα are mediated through it's receptor has not been determined. In the present study, TNFR 1-/- mice and wild-type mice were chronically fed 30% fructose solution for 8 weeks to test the hypothesis that TNFα through its receptor 1 plays a casual role in the onset of fructose-induced NAFLD. In TNFR 1-/- mice, hepatic steatosis was markedly less pronounced in fructose fed mice in comparison to wild-type mice. This protective effect was associated with a decreased hepatic inflammation (e.g. infiltrating neutrophils as well as expression of ICAM-1, CCL2 and CCL19) in fructose fed TNFR 1-/- mice. In contrast, no differences were found between fructose fed groups in regards to inducible nitric oxide synthase (iNOS) protein, 4-hydroxynonenal (4-HNE) adducts and ATP levels. In line with our findings, recent studies of other groups have also shown that the deletion of TNFR 1 decreased high fat diet induced hepatic lipid accumulation and inflammation (82). These results suggest that TNFα through its receptor TNFR 1 may not only regulate lipid accumulation but also mediating an induction of chemokine secretion and adhesion molecules (e.g ICAM 1) in the liver. Indeed, studies have shown before that defect in TNFR 1 signalling downregulated hepatic ICAM-1 expression thereby decreasing inflammation (27).

Results of our own group suggest that concomitant antibiotic treatment or deletion of TLR-4 (endotoxin receptor) in fructose fed mice decreased 4-HNE (a marker for ROS formation) and an induction of iNOS levels (21, 60, 83). In line with these findings, iNOS expression but also 4HNE protein adducts levels were markedly high in livers of fructose fed mice regardless of strain. This elevated induction of iNOS and 4HNE protein addcuts was seemed to be resulting from increased translocation of intestinal bacterial endotoxins. Hepatic ATP levels were shown before by Latta M *et al.* to be depleted after an acute intravenous exposure of fructose in mice whereas in this study chronic oral exposure was not associated with a depletion of hepatic ATP levels in fructose fed mice (66). Differences between the results of the present study and those of Latta M *et al.* may have resulted from the different feeding/exposure patterns. Furthermore, earlier *in vitro* studies of Latta M *et al.* have shown that fructose at a concentration of 50mM did not deplete ATP levels in human HepG2 or murine Hepal-6 hepatoma cells (84). Taken together, it cannot be ruled out that fructose may add to the development of NAFLD through its insulin-independent metabolism or through alterations of the bioavailability of ATP but also through increased bacterial endotoxin and intestinal permeability thereby activation of Kupffer cells associated with iNOS induction and reactive oxygen species formation and an induction of TNFα.

TNFR1 mice are protected from fructose-induced alterations of insulin signalling and lipid metabolism

Results of animal and human studies suggest that insulin resistance may also be a critical factor in the development of NAFLD (67). Furthermore, TNFα has been shown before not only to promote insulin resistance but also to be activated by insulin resistance via activation of IKKβ (85). Therefore, in the present study markers of insulin resistance such as phosphorylation of Akt and plasma RBP-4 levels were determined. Chronic fructose feeding in wild-type mice was associated with an altered phosphorylation status of Akt in the liver as well as plasma RBP-4 levels in wild-type mice whereas this effect was not found in fructose fed TNFR1-/- mice, suggesting that TNFα though it’s receptor may play a critical role in fructose-induced insulin resistance.

These results are in accordance with results of our earlier study where we showed that hepatic phospho Akt levels as well as plasma RBP-4 levels were altered in fructose fed mice (60). Interestingly, expression of gluconeogenic enzyme PEPCK mRNA was found to be significantly lower in TNFR1-/- mice regardless of feeding in comparison to wild-type controls, suggesting that wild-types and TNFR 1-/- may have a differential regulation of PEPCK or even gluconeogenesis, These results indicate an adaptive mechanism of TNFR 1-/- mice to the lack of inhibitory effect of TNFα on PEPCK. Indeed Yan *et al.* showed in *in vitro* experiments that PEPCK expression was inhibited by TNFα (86). Furthermore, recent studies of Lim JH *et al.* have shown that an overexpression of PEPCK is associated with mitochondrial dysfunction, a response to endoplasmic reticulum (ER) stress (87). Furthermore, AMPK, which is known as energy sensor that regulates cellular metabolism, has been shown to regulate hepatic lipogenesis through down-regulation of SREBP 1c (88, 89). In line with these findings SREBP1c, FAS and PAI-1 were only induced in livers of wild-type mice whereas in livers of TNFR1 mice phospho AMPK was induced. These results suggest that TNFα plays a vital role in hepatic lipid metabolism through suppression of AMPK which may down regulate SREBP 1c. Moreover, expression of PAI-1, which has been lately linked to hepatic lipid export also see chapter 4.2 and 3 (34) and which is also known to be regulated by insulin-dependent mechanism, was found to be induced in fructose fed wild-type mice. These findings are in accordance with results of Cai D *et al.*(85) where it was shown that TNFα though activation of NFκB may regulate the inflammatory mediators like PAI-1. Taken together, these data suggest that TNFα through its receptor TNFR1 is at least partly responsible for fructose-induced insulin resistance thereby suppressing AMPK and inducing lipogenesis as well as PAI-1 expression.

4.2 PAI-1 -/- mice are protected from the development of hepatic steatosis

The findings of aim 1 and herein particularly the TNFα dependent induction of PAI-1 but also results of studies on the mechanisms of alcohol-induced liver damage (32) suggest that PAI-1 may be a critical factor in the development of liver damage .

In the present study, to further test if PAI-1 is a critical factor in the development of fructose-induced NAFLD, PAI-1-/- mice and wild-type mice were chronically fed 30% fructose solution for 8 weeks. Chronic fructose feeding induced fat accumulation in the livers of wild-type mice whereas fat accumulation was reduced to ~-50% in fructose fed PAI-1 -/- mice, despite similarly elevated endotoxin levels in portal plasma and TNFα protein concentration in the liver of both the strains. These data suggest that PAI-1 may be an essential factor in mediating the effects of the increased translocation of bacterial endotoxin and the subsequent activation of Kupffer cells in livers of fructose fed mice.

On the other hand, PAI-1 has also lately been linked to hepatic lipid export and has shown to inhibit urokinase-type plasminogen activator (uPA), to modulate the activation of prohepatocyte growth factor (proHGF) to HGF (for review see (34)). HGF through its receptor cMet has been shown to stimulate the MTTP-dependent lipoprotein secretion in hepatocytes (32, 90, 91). In support of these results, it has been shown before that acute alcohol exposure is associated with an upregulation of cMet phosphorylation, MTTP activity and ApoB concentration in PA1-/- and TNFR1-/- mice (32). Indeed, in the present study phosphorylation of cMet, ApoB mRNA and MTTP activity was increased in PAI-1-/- mice fed with fructose whereas in wild-type mice fed with fructose all these parameters remained at the level of controls. These results were further bolstered by *in vitro* studies (e.g. AML-12 cells=model of hepatocytes) in which the treatment of hepatocytes (e.g. AML 12 cells) with PAI-1 caused triglyceride accumulation and reduction of MTTP activity whereas this effect of PAI-1 was attenuated by HGF treatment. Taken together, these results suggest that through an inhibition of uPA PAI-1 may alter the activation of pro HGF to HGF, which in turn cannot bind to its receptor cMet thereby suppressing an upregulation of MTTP, which results in an accumulation of triglycerides in hepatocytes that are no longer transported out of the cells via ApoB/VLDL. On the contrary, deletion of PAI-1 may facilitate the cell to increase VLDL synthesis and to transport greater amounts of triglycerides out of the cell.

PAI-1 regulates Akt and apoptosis in the livers of fructose-induced NAFLD mice

A loss of insulin sensitivity has been claimed to be a key factor in the development of NAFLD (for overview see (92)).Furthermore, it has been demonstrated in animal studies that chronic intake of fructose can cause insulin resistance (60, 61). Indeed, in the present study chronic fructose feeding was associated with markedly altered all parameters of insulin resistance in wild-type mice (e.g. RBP-4 plasma concentration, GLUT-4, PEPCK, RBP-4 and glucokinase mRNA expression as well as phosphorylation status of Akt in the liver). Interestingly, chronic fructose feeding also increased RBP-4 levels and decreased hepatic GLUT-4 and PEPCK mRNA expression in PAI-1 -/- mice suggesting that these mice also had impaired insulin signalling or were insulin resistant. However, contrary to the findings in livers of fructose fed wild-type mice phosphorylation status of Akt was similar to that of controls fed water in livers of PAI-1-/- mice. These results suggest that PAI-1 may alter phosphorylation of Akt.

Indeed, cMet has shown to be regulated through PAI-1 dependent signalling pathways may play different roles in cellular functions. For instance, it has been shown that cMet is involved in regulation of PI3K/Akt signalling cascade (70, 93) and HGF-cMet-Akt dependent pathways were shown to modulate the expression of anti-apoptotic BCL2 protein BCL-XL (71). In line with these findings, expression of BCL-XL was upregulated in livers of fructose fed PAI-1-/- mice, whereas a similar effect was not found in fructose fed wild-type mice. These findings are in line with the *in vitro* studies of Bu R *et al.,* where it was shown that cMet activates anti apoptotic markers (e.g BCL XL) through phosphorylation of Akt (94). These findings are also supported by the results of Balsara RD *et al.* where it was shown that PAI-1 may regulate cell survival through modulation PI3K/Akt pathway in endothelial cells (95). Furthermore, a similar effect was also found for mRNA expression levels of glucokinase. Indeed, similar to Akt, it has been suggested by the results of other groups before that glucokinase expression is not solely regulated by insulin (96). For instance, the results of García-Ocaña *et al.* suggest that HGF/ c-Met signalling cascades may also be involved in the regulation of glucokinase expression (96).

Taken together, our results suggest that fructose fed PAI-1-/- mice are protected against the onset of fructose-induced liver steatosis despite displaying signs of insulin resistance (e.g. elevated plasma and hepatic mRNA RBP-4 levels and decreased GLUT-4 and PEPCK expression in the liver). Furthermore, PAI-1 deletion may protect the liver from impaired PI3K/Akt signalling cascade occurred due to fructose intake thereby also promoting an anti-apoptosis status in the liver.

Protection of PAI-1-/- mice from fructose-induced steatosis is associated with an induction of markers of iNKT cell activation

MTTP, besides being a key enzyme in the regulation of hepatic lipid export via VLDL, is also necessary for the transfer of lipids to the iNKT cell receptor CD1d (73, 97). Indeed, in an *in vitro* assay, it was shown that MTTP may transfer phospholipids to CD1d suggesting a vital role of MTTP in lipidation of CD1d and its lipid antigen presentation to CD1d-restricted NKT cells (73, 98). Furthermore, it was also shown that MTTP gene deletion or inhibition may cause significant decrease in CD1d antigen presentation to iNKT cells (73, 97). Recently it was shown that iNKT cells may be involved in metabolic control due to their striking ability to sense lipids (99). For instance, results of Elinav *et al.*, have shown that adoptive transfer of NKT lymphocytes protected ob/ob mice from steatohepatitis and glucose intolerance (100). Additionally, it was suggested that in mouse models of NAFLD (e.g diet-induced NAFLD and ob/ob mice) the progression of the disease was related to a marked decrease in CD1d reactive hepatic iNKT cells (101, 101, 102). Recently it was shown by Kremer *et al.*, that in the steatotic liver Kupffer cells contribute to depletion of iNKT cells (103). In the present study, regardless of feeding, PAI-1-/- mice has increased expression of hepatic CD 1d as well as iNKT cells markers (e.g CD3ε and NK1.1). Conversely, the iNKT cell activation markers (e.g. IL 15 and IFNγ) were only found to be increased in the livers of fructose fed PAI-1-/- mice. In line with earlier findings of other groups (101, 101) the results of the present study also suggest that an upregulation of MTTP due to a PAI-1 deletion is associated with higher number of active CD1d restricted iNKT cells.

Furthermore, these data also suggest that a PAI-1 deletion in mice may also increase the expression of cytokines like IL-15 from NKT cells, which has recently been shown to contribute for liver regeneration in damaged livers (104). In regards to IFNγ expression, it was recently shown that iNKT cells may express untranslated cytokines mRNAs (e.g. IFNγ) in unchallenged or healthy state in mice (105, 106) suggesting that PAI-1 deletion may promote an unstimulated or unchallenged (e.g. healthy) environment in the livers of mice. Altogether, the results of aim 2 suggest that PAI-1 plays a vital role in the onset of fructose-induced hepatic steatosis through suppression the upregulation of hepatic lipid export, which is an essentially adaptive mechanism to protect liver from increased amount of lipids occurred due to excessive consumption of fructose. Furthermore, the data also suggests that through modulating lipid export, PAI-1 is indirectly involved in modulating CD1 reactive iNKT cells in the liver.

4.3 Human studies

PAI-1 and markers of insulin signaling in livers of human patients with NAFLD

The third aim of this PhD thesis was to further investigate if the alterations found in animal models of NAFLD (e.g. increased lipid peroxidation, impaired insulin signalling and alterations of iNKT cells as well as activation markers) are also found in livers of patients with NAFLD. Indeed, levels of 4-HNE protein adducts were markedly higher in the livers of NAFLD patients in comparison controls suggesting that the formation of ROS was elevated in NAFLD patients. These findings are line with the results of our own group where it was shown that chronic fructose intake in mice is associated with higher levels of portal endotoxin and lipid peroxidation in the liver (21, 60, 61). Furthermore, results of Thuy *et al.* indicated that NAFLD patients have higher endotoxin levels in peripheral blood in comparison to controls (19). Results of Seki *et al.* indicated that concentration of 4-HNE protein adducts were significantly higher in NAFLD patients even at early stages (steatosis) in comparison controls (107).

Furthermore, it has also been shown that markers of ROS such as plasma levels of malondialdehyde (MDA) and thiobarbituric acid reactive substances assay (TBARS) were significantly higher in NAFLD patients in comparison to controls (108). Results of *in vitro* and *in vivo* studies have shown that endotoxin may increase the formation of ROS, which is a trigger for the redox sensitive receptor NFκB and subsequently release the TNFα (for review see (83)). In addition, several *in vivo* and *in vitro* studies have shown that increased levels of TNFα may induce insulin resistance (109). Results of aim 1 of this thesis have indicated that TNFα through it's receptor TNFR 1 may add to the development of insulin resistance. Furthermore, results of Li *et al.* have shown that stimulation of Hep G2 cell lines (cells being a model of hepatocytes) with TNFα inhibit phosphorylation of IRS-1 subsequently leading to insulin resistance (110). Furthermore, in settings of alcohol-induced liver damage TNFα has been shown to modulate PAI-1 expression in insulin-dependent manner (32). In the present study, enhanced lipid peroxidation was associated with a decreased expression of IRS-1 mRNA and increased PAI-1 protein levels being localized to hepatocytes, suggesting that insulin signalling may be impaired in NAFLD patients despite no elevated fasting glucose levels. The lower IRS-1 mRNA expression observed in the livers of NAFLD patients in the present study was in contrast with the results of Gracia Monzon *et al.* who observed in the livers of NASH patients (111). The discrepancy between our study and that of Gracia Monzon *et al.* study may be due to the environmental and genetic factors. However, previous studies have shown that insulin resistance was independent of histological severity in livers of HCV patients (112, 113) suggesting that impairment of hepatic insulin signalling might be an early event at NAFLD. The results of PAI-1 protein levels are in accordance with our previous findings where we found an increased PAI-1 mRNA expression in livers of NAFLD patients in comparison to controls (19). Interestingly, staining for PAI-1 concentration revealed that PAI-1 was primarily confined to hepatocytes. Furthermore, results of Alessi *et al.* indicate a strong correlation between steatotic liver and plasma PAI-1 levels in rodents as well as in humans (31). Taken together, the results of this aim suggest that in livers of humans with NAFLD formation of ROS, insulin resistance and formation acute phase protein PAI-1 are increased similar to the findings of animal models of fructose-induced NAFLD.

cMet signalling in human NAFLD patients

Studies in animals and humans have suggested that in addition to an increased de novo lipogenesis, an impaired hepatic lipid export may also contribute to lipid accumulation in NAFLD (31, 32, 75). Indeed, studies of our own group have suggested that PAI-1 may impair hepatic lipid export through altering the activation of HGF-cMet signalling cascade (32, 75). Indeed, results of aim 2 have shown that hepatic cMet phosphorylation is elevated in fructose fed PAI-1-/- mice. In addition, it was also shown that treating rat hepatocytes with HGF resulted in an activation of cMet and subsequently stimulated lipoprotein secretion (114). In the present study mRNA expression of cMet was markedly lower in livers of NAFLD patients. Moreover, the anti-apoptotic protein BCL-2l, a downstream target of cMet (71) was also found to be lower in livers of NAFLD patients suggesting that NAFLD patients may have higher levels of apoptosis. Taken together, these results suggest that in livers of patients with NAFLD cMet signalling may be impaired thereby leading to apoptosis similar to the findings of animal models of fructose-induced NAFLD.

iNKT cells in human NAFLD patients

In the present study expression of MTTP and CD1d did not differ between controls and NAFLD patients. This inconsistency with our results of animal studies may be due to analysis of mRNA expression in humans whereas analysis of protein levels or activity in animal studies. Indeed, studies of others suggest that MTTP activity is not merely regulated at the level of mRNA expression but rather through half-life of MTTP mRNA larger subunit (115). However, as tissue samples in the present study were limited it was not possible to determine if MTTP activity was altered in the livers. This will have to be addressed in future studies. Hence, it cannot be precluded that NAFLD in humans, too, may be associated with impaired lipid export from the liver. Furthermore, another controversial finding to rodent models of NAFLD was that the numbers of CD3ζ positive cells (iNKT cells) was markedly higher in NAFLD patients in comparison to controls. In line with our findings in humans Tajiri *et al.* have shown that in NASH patients number of iNKT cells was markedly higher (116).

Furthermore, the results of Syn *et al.,* suggest that an elevated number of iNKT cells in human NASH patients may be a feature of cirrhosis (117). These data may suggest that the patients in the present study might be on the verge to develop the next stage of liver disease (e.g. cirrhosis). However, the expression of iNKT cell markers (e.g. IL 4 and IL-15) was lower in NAFLD patients, suggesting that iNKT cells may not be active. Taken together, these results suggest that similar to rodents NAFLD in humans is associated with altered iNKT cell numbers. However, the implication of the findings needs to be addressed in future studies.

4.4 Conclusion and outlook

Taken together, the results of the present studies suggest that TNFα through its receptor TNFR1 is casually involved in the development of fructose-induced NAFLD in mice. Furthermore, the results indicate that TNFα through its receptor seems to be involved in the development of hepatic insulin resistance and may thereby add to alterations found in lipogenesis as well as the induction of hepatic PAI-1 expression associated with fructose-induced NAFLD. Indeed, in the present thesis it was shown in studies with PAI-1-/- mice that PAI-1 may be a critical factor in the onset of fructose-induced steatosis through mechanisms involving suppression of the up-regulation of lipid export necessary to protect the liver from the increased amount of lipids resulting from chronic dietary intake of fructose. The present study further suggest that PAI-1 may modulate PI3K/Akt signaling and CD 1 reactive iNKT cells. In Figure 15 the possible mechanism involved in the development of fructose-induced NAFLD in rodents are summarized. The results of aim 3 of this thesis suggest that similar to the alterations found in mouse models of fructose-induced NAFLD, NAFLD in humans is also associated with increased ROS production, impaired insulin signaling leading to PAI-1 induction in hepatocytes. Furthermore, similar to rodents hepatic lipid export was also altered in patients with NAFLD. Altogether, the present study suggests that consumption of carbohydrates rich diet here in particularly fructose may lead to the development of onset of NAFLD. Furthermore, these results also imply that TNFα and PAI-1 may be considered as targets in the therapies but may be also in the prevention of NAFLD. However, this will have to be addressed in future studies.

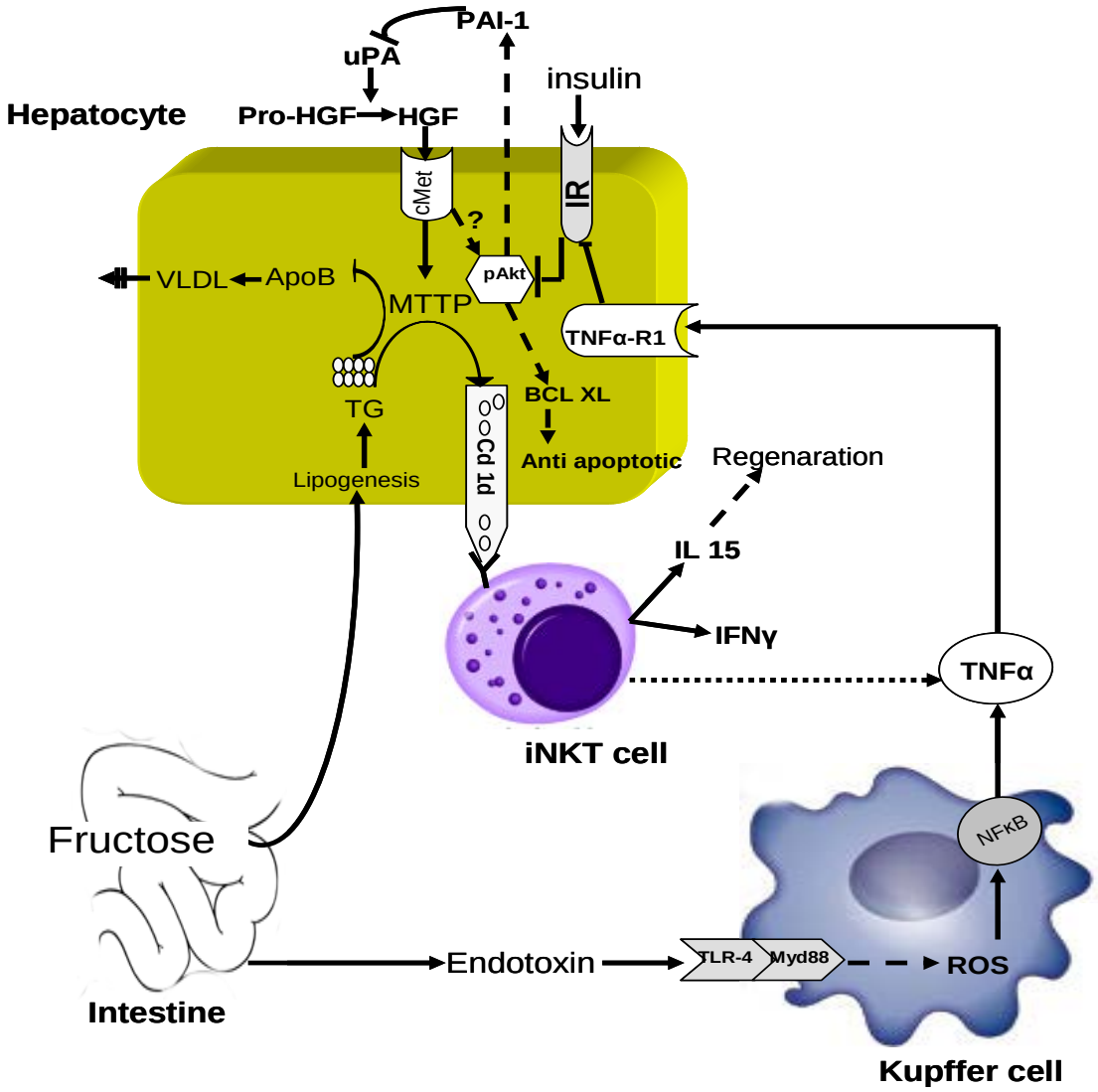

Figure 15 Possible molecular mechanism involved in the development of fructose-induced fatty liver. Chronic intake of fructose may lead to elevated bacterial endotoxin levels in the portal blood and an activation of TLR-4 signaling cascades, subsequently leading to an increased formation of reactive oxygen species (ROS) and an nuclear factor-κB (NFκB)-dependent induction of tumor necrosis factor (TNFα). TNFα through its receptor 1 can then cause insulin resistance (IR) in hepatocytes and an induction of plasminogen activator inhibitor (PAI-1) which in turn may through cMet-hepatocyte growth factor (HGF)-dependent pathways modulate hepatic lipid export, lipidation of cluster of differentiation 1d (CD1d) and NKT cell activation but also apoptosis. (Adapted from Kanuri G 2011)

5 Summary

Non-alcoholic fatty liver disease (NAFLD), a liver disease frequently associated with obesity, type 2 diabetes and dyslipidemia has become a worldwide health problem during the last decades. Results of recent studies suggest that a diet rich in fructose may also be a risk factor for the development of NAFLD. Results of our own group but also other group suggest that TNFα and PAI-1 may be involved in the development of NAFLD in rodents but also humans. Therefore, the aim of the present study was to investigate the role TNFα and PAI-1 in the onset of fructose-induced NAFLD in a mouse model as well as in human NAFLD patients. The specific aims were

1) Are TNFR1-/- mice protected from fructose-induced NAFLD? If yes, what are the molecular mechanisms involved?

TNFR1 -/- and wild-type mice were either fed 30% fructose solution or tap water. Chronic fructose feeding caused a significant ~5-fold increase in triglyceride accumulation and neutrophil infiltration in livers of wild-type mice and an ~8-fold increase in plasma alanine aminotransferase (ALT) levels in comparison to control mice. Similar effects of fructose feeding were not found in TNFR 1-/- mice. Indeed, the protective effect of the tumor necrosis factor receptor 1 (TNFR1) deletion against the onset of fructose-induced steatosis was associated with decreased sterol regulatory element-binding protein 1 (SREBP-1), fatty acid synthase (FAS) and plasminogen activator inhibitor 1 (PAI-1) expression in the liver. Furthermore, the protective effect was also associated with protection against alterations markers of insulin signaling cascade (e.g. adenosine monophosphate-activated protein kinase (AMPK), protein kinase B (Akt) levels). However, markers of hepatic lipid peroxidation, inducible nitric oxide synthase (iNOS) protein and adenosine triphosphate (ATP) levels were similar between wild-type and TNFR1 -/- mice fed fructose. Taken together, these data suggest that TNFα plays a casual role in the onset of fructose-induced liver damage as well as insulin resistance in mice through signaling cascades downstream of TNFR1.

2) Are PAI-1-/- mice protected from fructose-induced NAFLD? And if so, what are the molecular mechanisms involved?

To address if PAI-1 is also a critical factor in the onset of fructose-induced NAFLD, PAI-1-/- and wild-type mice were either fed a fructose solution or tap water. Chronic fructose feeding in wild-type mice caused a marked increase in hepatic triglycerides, PAI-1 expression and plasma ALT levels in comparison to water controls. A similar effect of fructose feeding was not found in PAI-1-/- mice. PAI-1-/- mice fed fructose were protected from hepatic steatosis despite similar portal endotoxin levels, alterations of markers of insulin resistance and hepatic TNFα protein levels between fructose fed groups. The protective effect of the loss of PAI-1 against the onset of fructose-induced steatosis was associated with a significant increase in phospho-cMet, phospho Akt, expression of apolipoprotein B (ApoB) and activity of microsomal triglyceride transfer protein (MTTP) in livers of PAI-1-/- mice in comparison to fructose fed wild-type mice. Moreover, in PAI-1-/- mice expression of CD1d and markers of CD1d-reactive iNKT cells were markedly higher than in wild-type mice; however, expression of markers of activation of CD1d-reactive iNKT cells (e.g. interleukin 15 (IL-15) and interferon γ (INFγ)) were only found to be increased in livers of fructose fed PAI-1-/- mice. Taken together, these data suggest that PAI-1 plays a causal role in mediating the early phase of fructose-induced liver damage in mice through signalling cascades down-stream of Kupffer cells and TNFα.

3) Are molecular mechanisms identified in mouse studies also relevant to human situation?

To determine if the alterations found in livers of animals with NAFLD are also relevant in humans with NAFLD, markers of lipid peroxidation, insulin signaling and number of iNKT cells were determined in 6 controls and 11 NAFLD patients.4-hydroxynonenal (4-HNE) protein adducts levels were significantly higher in livers of NAFLD patients whereas expression of insulin receptor substrate (IRS-1) was reduced by ~80 % in comparison to controls. PAI-1 protein levels primarily found in hepatocytes was significantly higher in NAFLD patients; however, hepatic CD1d and MTTP mRNA expression did not differ between groups.

Hepatic c-Met and BCL-2l mRNA expressions were significantly lower in NAFLD patients in comparison to controls and number of CD3ζ positive cells was higher. In contrast, expression of iNKT cell markers (e.g. IL-4 and IL-15) was significantly lower in livers of patients with NAFLD when compared with controls.Taken together, the present study suggests that the molecular mechanism involved in the progression of NAFLD is similar in both rodents and humans. Furthermore, TNFα and PAI-1 may be considered as therapeutic targets for NAFLD.

Zusammenfassung

Die nicht-alkoholbedingte Fettlebererkrankung (NAFLD) ist eine Lebererkrankung, die häufig mit Übergewicht, Typ-2 Diabetes und Dyslipidämie assoziiert ist und somit in den letzten Jahrzehnten zu einem weltweiten Gesundheitsproblem wurde. Ergebnisse neuer Studien legen nahe, dass eine fruktose reiche Ernährung ein Risikofaktor für die Entwicklung von NAFLD ist. Nicht nur Ergebnisse der eigenen Arbeitsgruppe, sondern auch anderer Arbeitsgruppen legen nahe, dass TNFα und PAI-1 in der Entwicklung von NAFLD in Tiermodell aber auch Menschen beteiligt sein können. Vor diese HIntergrund war es das Ziel der vorliegenden Arbeit, die Rolle von TNFα und PAI-1 in der Entstehung einer fruktose-induzierten NAFLD sowohl im Mausmodell als auch bei Patienten mit NAFLD zu untersuchen.

Die spezifischen Ziele waren:

1) Sind TNFR1-/- Mäuse vor der fruktose-induzierten NAFLD geschützt? Wenn ja, was sind die beteiligten molekularen Mechanismen?

Tumornekrosefaktor-Rezeptor 1 (TNFR1)-/- und Wildtyp-Mäuse wurden entweder mit einer 30%igen Fruktose-Lösung oder Wasser gefüttert. Die chronische Fütterung mit Fruktose führte zu einem signifikanten, ~5-fachen Anstieg der Triglyceridkonzentration und Neutrophileninfiltration in der Leber von Wildtypmäusen, sowie einem ~8-fachen Anstieg der Konzentration der Alanin-Aminotransferase (ALT) im Plasma im Vergleich zu den Kontroll mäusen. Ähnliche Effekte konnten in TNFR1-/- Mäusen nach der Fütterung mit Fruktose nicht nachgewiesen werden. Die protektive Wirkung des Verlustes TNFR1 gegenüber der fruktose-induzierten Steatose mit einer Verminderung der Expression des *sterol regulatory element-binding protein 1* (SREBP-1), der Fettsäure-Synthase (FAS) und von PAI-1 in der Leber assoziiert. Darüber hinaus waren TNFR1-/- Mäuse auch vor veränderungen von

Markern der Insulin-Signalkaskade, wie der Adenosin-monophosphat-aktivierten Proteinkinase (AMPK) und der Proteinkinase B (Akt) geschützt. Jedoch fanden sich nur geringe Unterschiede in der hepatischen Lipidperoxidation, der Konzentration der induzierbaren Stickstoffmonoxid-Synthase (iNOS) und des Adenosintriphosphats (ATP) zwischen Wildtyp- und TNFR1-/- Mäusen nach Fruktosefütterung. Insgesamt, weisen die Ergebnisse darauf hin, dass TNFα eine wasentliche Rolle in der Entstehung von fructose-induzierte Leberschäden sowie der Insulin-Resistenz bei Mäusen über dem TNFR1 nachgeschalteten Signalkaskaden spielt.

2) Sind PAI-1-/- Mäuse vor der fruktose-induzierten NAFLD geschützt? Wenn ja, was sind die beteiligten molekularen Mechanismen?

Um zu untersuchen ob PAI-1 ebenfalls ein kritischer Faktor bei der Entstehung von fruktose-induzierter NAFLD ist, wurden PAI-1-/- sowie Wildtyp-Mäuse entweder mit einer Fruktoselösung oder Wasser gefüttert. Die chronische Fütterung mit Fruktose führte in Wildtyp-Mäusen zu einem deutlichen Anstieg der Triglycerid-Konzentration in der Leber, der Expression von PAI-1 sowie der Plasma ALT-Spiegel im Vergleich zu den Wasserkontrollen. Eine ähnliche Wirkung der Fruktosefütterung auf PAI-1-/- Mäuse wurde nicht gefunden. So waren PAI-1-/- Mäuse vor der Lebersteatose trotz ähnlich hoher portaler Endotoxinspiegel, Insulinresistenz und hepatischer TNFα Konzentrationen geschützt. Die schützende Wirkung des PAI-1-Verlustes gegenüber der Entstehung von fruktose-induzierter Steatose war mit einer signifikanten Zunahme der Konzentration an phospho-c-Met, phospho Akt, der Expression von Apolipoprotein B (ApoB) sowie der Aktivität des mikrosomalen Triglyceridtransferporteins (MTTP) in den Lebern von PAI-1-/- Mäusen im Vergleich zu fruktose-gefütterten Wildtyp-Mäusen assoziert. Darüber hinaus war die Expression von CD1d und Markern von CD1d-reaktiven NKT Zellen in PAI-1-/- Mäusen deutlich höher als in den Wildtyp-Mäusen. Allerdings war die Expression der Aktivierungsmarker von CD1d-reaktiven NKT Zellen (z. B. Interleukin (IL) 15 und Interferon (IFN) γ) nur in den Lebern von fruktose-gefütterten PAI-1-/- Mäusen erhöht. Insgesamt deuten die Daten darauf hin, dass PAI-1 eine kausale Rolle in der Vermittlung der frühen Phase der fructose-induzierten Leberschädigung bei Mäusen über Signalkaskaden „down-stream“ der Kupffer-Zellen und von TNFα spielt.

3) Sind die in Mausstudien identifizierten, molekularen Mechanismen auf den Menschen übertragbar?

Um festzustellen, ob die Veränderungen in der Leber von Tieren mit NAFLD auch für die Entstehung der NAFLD bei Menschen relevant sind, wurden Marker der Lipidperoxidation, Insulin-Signalkaskade und die Anzahl der iNKT-Zellen in 6 Kontrollen und 11 Patienten mit NAFLD bestimmt. Das Niveau an 4-HNE Proteinaddukten war in den Lebern der NAFLD-Patienten signifikant erhöht, wohingegen die Expression von Insulin-Rezeptor-Substrat (IRS-1) im Vergleich zu den Kontrollen um ~80 % reduziert war. Die Konzentration an PAI-1 Protein war in Patienten mit NAFLD signifikant höher wohingegen die mRNA-Expression von hepatischem CD1d und MTTP sich nicht zwischen den verschiedenen Gruppen unterschied. Die Hepatische c-Met sowie die BCL-21 mRNA Expression war bei NAFLD-Patienten signifikant niedriger im Vergleich zu den Kontrollen, wohingegen die Anzahl der CD3ζ-positiven Zellen erhöht war. Im Gegensatz dazu war die Expression der iNKT-Zellmarker IL-4 und IL-15 bei Patienten mit NAFLD signifikant niedriger als in den Lebern der Kontrollen. Insgesamt deuten die Ergebinesse der vorliegende Studie darauf hin, dass die bei der Progression der NAFLD beteiligten molekularen Mechanismen sowohl bei Nagern als auch bei Menschen ähnlich sind. Ferner können TNFα und PAI-1 in der Therapie der NAFLD von Bedeutung sein

6 References

(1) Smith BW, Adams LA. Non-alcoholic fatty liver disease. Crit Rev Clin Lab Sci 2011 May;48(3):97-113.

(2) Adams LA, Lymp JF, St SJ, Sanderson SO, Lindor KD, Feldstein A, et al. The natural history of nonalcoholic fatty liver disease: a population-based cohort study. Gastroenterology 2005 Jul;129(1):113-121.

(3) Gross LS, Li L, Ford ES, Liu S. Increased consumption of refined carbohydrates and the epidemic of type 2 diabetes in the United States: an ecologic assessment. Am J Clin Nutr 2004 May;79(5):774-779.

(4) Browning JD, Szczepaniak LS, Dobbins R, Nuremberg P, Horton JD, Cohen JC, et al. Prevalence of hepatic steatosis in an urban population in the United States: impact of ethnicity. Hepatology 2004 Dec;40(6):1387-1395.

(5) Bedogni G, Miglioli L, Masutti F, Tiribelli C, Marchesini G, Bellentani S. Prevalence of and risk factors for nonalcoholic fatty liver disease: the Dionysos nutrition and liver study. Hepatology 2005 Jul;42(1):44-52.

(6) Luyckx FH, Desaive C, Thiry A, Dewe W, Scheen AJ, Gielen JE, et al. Liver abnormalities in severely obese subjects: effect of drastic weight loss after gastroplasty. Int J Obes Relat Metab Disord 1998 Mar;22(3):222-226.

(7) Fan JG, Zhu J, Li XJ, Chen L, Li L, Dai F, et al. Prevalence of and risk factors for fatty liver in a general population of Shanghai, China. J Hepatol 2005 Sep;43(3):508-514.

(8) Dixon JB, Bhathal PS, O'Brien PE. Nonalcoholic fatty liver disease: predictors of nonalcoholic steatohepatitis and liver fibrosis in the severely obese. Gastroenterology 2001 Jul;121(1):91-100.

(9) Park SH, Jeon WK, Kim SH, Kim HJ, Park DI, Cho YK, et al. Prevalence and risk factors of non-alcoholic fatty liver disease among Korean adults. J Gastroenterol Hepatol 2006 Jan;21(1 Pt 1):138-143.

(10) Karnikowski M, Cordova C, Oliveira RJ, Karnikowski MG, Nobrega OT. Non-alcoholic fatty liver disease and metabolic syndrome in Brazilian middle-aged and older adults. Sao Paulo Med J 2007 Nov 1;125(6):333-337.

(11) Das K, Das K, Mukherjee PS, Ghosh A, Ghosh S, Mridha AR, et al. Nonobese population in a developing country has a high prevalence of nonalcoholic fatty liver and significant liver disease. Hepatology 2010 May;51(5):1593-1602.

(12) Lim JS, Mietus-Snyder M, Valente A, Schwarz JM, Lustig RH. The role of fructose in the pathogenesis of NAFLD and the metabolic syndrome. Nat Rev Gastroenterol Hepatol 2010 May;7(5):251-264.

(13) Brun P, Castagliuolo I, Di L, V, Buda A, Pinzani M, Palu G, et al. Increased intestinal permeability in obese mice: new evidence in the pathogenesis of nonalcoholic steatohepatitis. Am J Physiol Gastrointest Liver Physiol 2007 Feb;292(2):G518-G525.

(14) Nair S, Cope K, Risby TH, Diehl AM. Obesity and female gender increase breath ethanol concentration: potential implications for the pathogenesis of nonalcoholic steatohepatitis. Am J Gastroenterol 2001 Apr;96(4):1200-1204.

(15) Cope K, Risby T, Diehl AM. Increased gastrointestinal ethanol production in obese mice: implications for fatty liver disease pathogenesis. Gastroenterology 2000 Nov;119(5):1340-1347.

(16) Bode C, Kugler V, Bode JC. Endotoxemia in patients with alcoholic and non-alcoholic cirrhosis and in subjects with no evidence of chronic liver disease following acute alcohol excess. J Hepatol 1987 Feb;4(1):8-14.

(17) Wigg AJ, Roberts-Thomson IC, Dymock RB, McCarthy PJ, Grose RH, Cummins AG. The role of small intestinal bacterial overgrowth, intestinal permeability, endotoxaemia, and tumour necrosis factor alpha in the pathogenesis of non-alcoholic steatohepatitis. Gut 2001 Feb;48(2):206-211.

(18) Miele L, Valenza V, La TG, Montalto M, Cammarota G, Ricci R, et al. Increased intestinal permeability and tight junction alterations in nonalcoholic fatty liver disease. Hepatology 2009 Jun;49(6):1877-1887.

(19) Thuy S, Ladurner R, Volynets V, Wagner S, Strahl S, Konigsrainer A, et al. Nonalcoholic fatty liver disease in humans is associated with increased plasma endotoxin and plasminogen activator inhibitor 1 concentrations and with fructose intake. J Nutr 2008 Aug;138(8):1452-1455.

(20) Volynets V, Kuper MA, Strahl S, Maier IB, Spruss A, Wagnerberger S, et al. Nutrition, Intestinal Permeability, and Blood Ethanol Levels Are Altered in Patients with Nonalcoholic Fatty Liver Disease (NAFLD). Dig Dis Sci 2012 Mar 17.

(21) Bergheim I, Weber S, Vos M, Kramer S, Volynets V, Kaserouni S, et al. Antibiotics protect against fructose-induced hepatic lipid accumulation in mice: role of endotoxin. J Hepatol 2008 Jun;48(6):983-992.

(22) Wheeler MD. Endotoxin and Kupffer cell activation in alcoholic liver disease. Alcohol Res Health 2003;27(4):300-306.

(23) Akira S, Hoshino K, Kaisho T. The role of Toll-like receptors and MyD88 in innate immune responses. J Endotoxin Res 2000;6(5):383-387.

(24) Su GL. Lipopolysaccharides in liver injury: molecular mechanisms of Kupffer cell activation. Am J Physiol Gastrointest Liver Physiol 2002 Aug;283(2):G256-G265.

(25) Bode C, Bode JC. Activation of the innate immune system and alcoholic liver disease: effects of ethanol per se or enhanced intestinal translocation of bacterial toxins induced by ethanol? Alcohol Clin Exp Res 2005 Nov;29(11 Suppl):166S-171S.

(26) Iida S, Ohshima H, Oguchi S, Hata T, Suzuki H, Kawasaki H, et al. Identification of inducible calmodulin-dependent nitric oxide synthase in the liver of rats. J Biol Chem 1992 Dec 15;267(35):25385-25388.

(27) Tomita K, Tamiya G, Ando S, Ohsumi K, Chiyo T, Mizutani A, et al. Tumour necrosis factor alpha signalling through activation of Kupffer cells plays an essential role in liver fibrosis of non-alcoholic steatohepatitis in mice. Gut 2006 Mar;55(3):415-424.

(28) Ma X, Hua J, Li Z. Probiotics improve high fat diet-induced hepatic steatosis and insulin resistance by increasing hepatic NKT cells. J Hepatol 2008 Nov;49(5):821-830.

(29) Ruiz AG, Casafont F, Crespo J, Cayon A, Mayorga M, Estebanez A, et al. Lipopolysaccharide-binding protein plasma levels and liver TNF-alpha gene expression in obese patients: evidence for the potential role of endotoxin in the pathogenesis of non-alcoholic steatohepatitis. Obes Surg 2007 Oct;17(10):1374-1380.

(30) Targher G, Bertolini L, Rodella S, Lippi G, Franchini M, Zoppini G, et al. NASH predicts plasma inflammatory biomarkers independently of visceral fat in men. Obesity (Silver Spring) 2008 Jun;16(6):1394-1399.

(31) Alessi MC, Bastelica D, Mavri A, Morange P, Berthet B, Grino M, et al. Plasma PAI-1 levels are more strongly related to liver steatosis than to adipose tissue accumulation. Arterioscler Thromb Vasc Biol 2003 Jul 1;23(7):1262-1268.

(32) Bergheim I, Guo L, Davis MA, Lambert JC, Beier JI, Duveau I, et al. Metformin prevents alcohol-induced liver injury in the mouse: Critical role of plasminogen activator inhibitor-1. Gastroenterology 2006 Jun;130(7):2099-2112.

(33) Kruithof EK. Plasminogen activator inhibitors--a review. Enzyme 1988;40(2-3):113-121.

(34) Arteel GE. New role of plasminogen activator inhibitor-1 in alcohol-induced liver injury. J Gastroenterol Hepatol 2008 Mar;23 Suppl 1:S54-S59.

(35) Hanover LM, White JS. Manufacturing, composition, and applications of fructose. Am J Clin Nutr 1993 Nov;58(5 Suppl):724S-732S.

(36) US Department of Agriculture. The food pyramid. US Dept of Agriculture; 1992.

(37) Vos MB, Kimmons JE, Gillespie C, Welsh J, Blanck HM. Dietary fructose consumption among US children and adults: the Third National Health and Nutrition Examination Survey. Medscape J Med 2008;10(7):160.

(38) Marriott BP, Cole N, Lee E. National estimates of dietary fructose intake increased from 1977 to 2004 in the United States. J Nutr 2009 Jun;139(6):1228S-1235S.

(39) Bray GA, Nielsen SJ, Popkin BM. Consumption of high-fructose corn syrup in beverages may play a role in the epidemic of obesity. Am J Clin Nutr 2004 Apr;79(4):537-543.

(40) Leclercq C, Arcella D, Piccinelli R, Sette S, Le DC, Turrini A. The Italian National Food Consumption Survey INRAN-SCAI 2005-06: main results in terms of food consumption. Public Health Nutr 2009 Dec;12(12):2504-2532.

(41) Tappy L, Le KA. Metabolic effects of fructose and the worldwide increase in obesity. Physiol Rev 2010 Jan;90(1):23-46.

(42) Jalal DI, Smits G, Johnson RJ, Chonchol M. Increased fructose associates with elevated blood pressure. J Am Soc Nephrol 2010 Sep;21(9):1543-1549.

(43) Welsh JA, Sharma A, Abramson JL, Vaccarino V, Gillespie C, Vos MB. Caloric sweetener consumption and dyslipidemia among US adults. JAMA 2010 Apr 21;303(15):1490-1497.

(44) Montonen J, Jarvinen R, Knekt P, Heliovaara M, Reunanen A. Consumption of sweetened beverages and intakes of fructose and glucose predict type 2 diabetes occurrence. J Nutr 2007 Jun;137(6):1447-1454.

(45) Dhingra R, Sullivan L, Jacques PF, Wang TJ, Fox CS, Meigs JB, et al. Soft drink consumption and risk of developing cardiometabolic risk factors and the metabolic syndrome in middle-aged adults in the community. Circulation 2007 Jul 31;116(5):480-488.

(46) Anderson JW, Story LJ, Zettwoch NC, Gustafson NJ, Jefferson BS. Metabolic effects of fructose supplementation in diabetic individuals. Diabetes Care 1989 May;12(5):337-344.

(47) Perez-Pozo SE, Schold J, Nakagawa T, Sanchez-Lozada LG, Johnson RJ, Lillo JL. Excessive fructose intake induces the features of metabolic syndrome in healthy adult men: role of uric acid in the hypertensive response. Int J Obes (Lond) 2010 Mar;34(3):454-461.

(48) Stanhope KL, Schwarz JM, Keim NL, Griffen SC, Bremer AA, Graham JL, et al. Consuming fructose-sweetened, not glucose-sweetened, beverages increases visceral adiposity and lipids and decreases insulin sensitivity in overweight/obese humans. J Clin Invest 2009 May;119(5):1322-1334.

(49) Le KA, Ith M, Kreis R, Faeh D, Bortolotti M, Tran C, et al. Fructose overconsumption causes dyslipidemia and ectopic lipid deposition in healthy subjects with and without a family history of type 2 diabetes. Am J Clin Nutr 2009 Jun;89(6):1760-1765.

(50) Castello A, Guma A, Sevilla L, Furriols M, Testar X, Palacin M, et al. Regulation of GLUT5 gene expression in rat intestinal mucosa: regional distribution, circadian rhythm, perinatal development and effect of diabetes. Biochem J 1995 Jul 1;309 (Pt 1):271-277.

(51) Cheeseman CI. GLUT2 is the transporter for fructose across the rat intestinal basolateral membrane. Gastroenterology 1993 Oct;105(4):1050-1056.

(52) Colville CA, Seatter MJ, Jess TJ, Gould GW, Thomas HM. Kinetic analysis of the liver-type (GLUT2) and brain-type (GLUT3) glucose transporters in Xenopus oocytes: substrate specificities and effects of transport inhibitors. Biochem J 1993 Mar 15;290 (Pt 3):701-706.

(53) Rutledge AC, Adeli K. Fructose and the metabolic syndrome: pathophysiology and molecular mechanisms. Nutr Rev 2007 Jun;65(6 Pt 2):S13-S23.

(54) Abdelmalek MF, Suzuki A, Guy C, Unalp-Arida A, Colvin R, Johnson RJ, et al. Increased fructose consumption is associated with fibrosis severity in patients with nonalcoholic fatty liver disease. Hepatology 2010 Jun;51(6):1961-1971.

(55) Zelber-Sagi S, Nitzan-Kaluski D, Goldsmith R, Webb M, Blendis L, Halpern Z, et al. Long term nutritional intake and the risk for non-alcoholic fatty liver disease (NAFLD): a population based study. J Hepatol 2007 Nov;47(5):711-717.

(56) Ouyang X, Cirillo P, Sautin Y, McCall S, Bruchette JL, Diehl AM, et al. Fructose consumption as a risk factor for non-alcoholic fatty liver disease. J Hepatol 2008 Jun;48(6):993-999.

(57) Armutcu F, Coskun O, Gurel A, Kanter M, Can M, Ucar F, et al. Thymosin alpha 1 attenuates lipid peroxidation and improves fructose-induced steatohepatitis in rats. Clin Biochem 2005 Jun;38(6):540-547.

(58) Jurgens H, Haass W, Castaneda TR, Schurmann A, Koebnick C, Dombrowski F, et al. Consuming fructose-sweetened beverages increases body adiposity in mice. Obes Res 2005 Jul;13(7):1146-1156.

(59) Faeh D, Minehira K, Schwarz JM, Periasamy R, Park S, Tappy L. Effect of fructose overfeeding and fish oil administration on hepatic de novo lipogenesis and insulin sensitivity in healthy men. Diabetes 2005 Jul;54(7):1907-1913.

(60) Spruss A, Kanuri G, Wagnerberger S, Haub S, Bischoff SC, Bergheim I. Toll-like receptor 4 is involved in the development of fructose-induced hepatic steatosis in mice. Hepatology 2009 Oct;50(4):1094-1104.

(61) Spruss A, Kanuri G, Uebel K, Bischoff SC, Bergheim I. Role of the inducible nitric oxide synthase in the onset of fructose-induced steatosis in mice. Antioxid Redox Signal 2011 Jun;14(11):2121-2135.

(62) Spruss A, Bergheim I. Dietary fructose and intestinal barrier: potential risk factor in the pathogenesis of nonalcoholic fatty liver disease. J Nutr Biochem 2009 Sep;20(9):657-662.

(63) Towbin H, Staehelin T, Gordon J. Electrophoretic transfer of proteins from polyacrylamide gels to nitrocellulose sheets: procedure and some applications. 1979. Biotechnology 1992;24:145-149.

(64) Folch J, LEES M, SLOANE STANLEY GH. A simple method for the isolation and purification of total lipides from animal tissues. J Biol Chem 1957 May;226(1):497-509.

(65) Lalor PF, Faint J, Aarbodem Y, Hubscher SG, Adams DH. The role of cytokines and chemokines in the development of steatohepatitis. Semin Liver Dis 2007 May;27(2):173-193.

(66) Latta M, Kunstle G, Lucas R, Hentze H, Wendel A. ATP-depleting carbohydrates prevent tumor necrosis factor receptor 1-dependent apoptotic and necrotic liver injury in mice. J Pharmacol Exp Ther 2007 Jun;321(3):875-883.

(67) Malaguarnera M, Di RM, Nicoletti F, Malaguarnera L. Molecular mechanisms involved in NAFLD progression. J Mol Med 2009 Apr 8;87:679-695.

(68) Arteel GE. Oxidants and antioxidants in alcohol-induced liver disease. Gastroenterology 2003 Mar;124(3):778-790.

(69) Kotani K, Peroni OD, Minokoshi Y, Boss O, Kahn BB. GLUT4 glucose transporter deficiency increases hepatic lipid production and peripheral lipid utilization. J Clin Invest 2004 Dec;114(11):1666-1675.

(70) Taher TE, Tjin EP, Beuling EA, Borst J, Spaargaren M, Pals ST. c-Cbl is involved in Met signaling in B cells and mediates hepatocyte growth factor-induced receptor ubiquitination. J Immunol 2002 Oct 1;169(7):3793-3800.

(71) Suzuki H, Toyoda M, Horiguchi N, Kakizaki S, Ohyama T, Takizawa D, et al. Hepatocyte growth factor protects against Fas-mediated liver apoptosis in transgenic mice. Liver Int 2009 Nov;29(10):1562-1568.

(72) Kaser A, Hava DL, Dougan SK, Chen Z, Zeissig S, Brenner MB, et al. Microsomal triglyceride transfer protein regulates endogenous and exogenous antigen presentation by group 1 CD1 molecules. Eur J Immunol 2008 Aug;38(8):2351-2359.

(73) Dougan SK, Salas A, Rava P, Agyemang A, Kaser A, Morrison J, et al. Microsomal triglyceride transfer protein lipidation and control of CD1d on antigen-presenting cells. J Exp Med 2005 Aug 15;202(4):529-539.

(74) Kanuri G, Spruss A, Wagnerberger S, Bischoff SC, Bergheim I. Role of tumor necrosis factor alpha (TNFalpha) in the onset of fructose-induced nonalcoholic fatty liver disease in mice. J Nutr Biochem 2011 Jun;22(6):527-534.

(75) Kanuri G, Spruss A, Wagnerberger S, Bischoff SC, Bergheim I. Fructose-induced steatosis in mice: role of plasminogen activator inhibitor-1, microsomal triglyceride transfer protein and NKT cells. Lab Invest 2011 Jun;91(6):885-895.

(76) Forshee RA, Storey ML, Allison DB, Glinsmann WH, Hein GL, Lineback DR, et al. A critical examination of the evidence relating high fructose corn syrup and weight gain. Crit Rev Food Sci Nutr 2007;47(6):561-582.

(77) Assy N, Nasser G, Kamayse I, Nseir W, Beniashvili Z, Djibre A, et al. Soft drink consumption linked with fatty liver in the absence of traditional risk factors. Can J Gastroenterol 2008 Oct;22(10):811-816.

(78) Lewis GF, Murdoch S, Uffelman K, Naples M, Szeto L, Albers A, et al. Hepatic lipase mRNA, protein, and plasma enzyme activity is increased in the insulin-resistant, fructose-fed Syrian golden hamster and is partially normalized by the insulin sensitizer rosiglitazone. Diabetes 2004 Nov;53(11):2893-2900.

(79) Kudo H, Takahara T, Yata Y, Kawai K, Zhang W, Sugiyama T. Lipopolysaccharide triggered TNF-alpha-induced hepatocyte apoptosis in a murine non-alcoholic steatohepatitis model. J Hepatol 2009 Jul;51(1):168-175.

(80) Crespo J, Fernandez-Gil P, Hernandez-Guerra M, Cayon A, Mayorga M, Dominguez-Diez A, et al. Are there predictive factors of severe liver fibrosis in morbidly obese patients with non-alcoholic steatohepatitis? Obes Surg 2001 Jun;11(3):254-257.

(81) Li Z, Yang S, Lin H, Huang J, Watkins PA, Moser AB, et al. Probiotics and antibodies to TNF inhibit inflammatory activity and improve nonalcoholic fatty liver disease. Hepatology 2003 Feb;37(2):343-350.

(82) Park EJ, Lee JH, Yu GY, He G, Ali SR, Holzer RG, et al. Dietary and genetic obesity promote liver inflammation and tumorigenesis by enhancing IL-6 and TNF expression. Cell 2010 Jan 22;140(2):197-208.

(83) Han D, Ybanez MD, Ahmadi S, Yeh K, Kaplowitz N. Redox regulation of tumor necrosis factor signaling. Antioxid Redox Signal 2009 Sep;11(9):2245-2263.

(84) Latta M, Kunstle G, Leist M, Wendel A. Metabolic depletion of ATP by fructose inversely controls. J Exp Med 2000 Jun 5;191(11):1975-1985.

(85) Cai D, Yuan M, Frantz DF, Melendez PA, Hansen L, Lee J, et al. Local and systemic insulin resistance resulting from hepatic activation of IKK-beta and NF-kappaB. Nat Med 2005 Feb;11(2):183-190.

(86) Yan J, Gao Z, Yu G, He Q, Weng J, Ye J. Nuclear corepressor is required for inhibition of phosphoenolpyruvate carboxykinase expression by tumor necrosis factor-alpha. Mol Endocrinol 2007 Jul;21(7):1630-1641.

(87) Lim JH, Lee HJ, Ho JM, Song J. Coupling mitochondrial dysfunction to endoplasmic reticulum stress response: a molecular mechanism leading to hepatic insulin resistance. Cell Signal 2009 Jan;21(1):169-177.

(88) Zhou G, Myers R, Li Y, Chen Y, Shen X, Fenyk-Melody J, et al. Role of AMP-activated protein kinase in mechanism of metformin action. J Clin Invest 2001 Oct;108(8):1167-1174.

(89) Woods A, zzout-Marniche D, Foretz M, Stein SC, Lemarchand P, Ferre P, et al. Characterization of the role of AMP-activated protein kinase in the regulation of glucose-activated gene expression using constitutively active and dominant negative forms of the kinase. Mol Cell Biol 2000 Sep;20(18):6704-6711.

(90) Naldini L, Vigna E, Bardelli A, Follenzi A, Galimi F, Comoglio PM. Biological activation of pro-HGF (hepatocyte growth factor) by urokinase is controlled by a stoichiometric reaction. J Biol Chem 1995 Jan 13;270(2):603-611.

(91) Taniyama Y, Morishita R, Nakagami H, Moriguchi A, Sakonjo H, Shokei K, et al. Potential contribution of a novel antifibrotic factor, hepatocyte growth factor, to prevention of myocardial fibrosis by angiotensin II blockade in cardiomyopathic hamsters. Circulation 2000 Jul 11;102(2):246-252.

(92) Marchesini G, Babini M. Nonalcoholic fatty liver disease and the metabolic syndrome. Minerva Cardioangiol 2006 Apr;54(2):229-239.

(93) Ye M, Hu D, Tu L, Zhou X, Lu F, Wen B, et al. Involvement of PI3K/Akt signaling pathway in hepatocyte growth factor-induced migration of uveal melanoma cells. Invest Ophthalmol Vis Sci 2008 Feb;49(2):497-504.

(94) Bu R, Uddin S, Bavi P, Hussain AR, Al-Dayel F, Ghourab S, et al. HGF/c-Met pathway has a prominent role in mediating antiapoptotic signals through AKT in epithelial ovarian carcinoma. Lab Invest 2011 Jan;91(1):124-137.

(95) Balsara RD, Castellino FJ, Ploplis VA. A novel function of plasminogen activator inhibitor-1 in modulation of the AKT pathway in wild-type and plasminogen activator inhibitor-1-deficient endothelial cells. J Biol Chem 2006 Aug 11;281(32):22527-22536.

(96) Garcia-Ocana A, Vasavada RC, Cebrian A, Reddy V, Takane KK, Lopez-Talavera JC, et al. Transgenic overexpression of hepatocyte growth factor in the beta-cell markedly improves islet function and islet transplant outcomes in mice. Diabetes 2001 Dec;50(12):2752-2762.

(97) Brozovic S, Nagaishi T, Yoshida M, Betz S, Salas A, Chen D, et al. CD1d function is regulated by microsomal triglyceride transfer protein. Nat Med 2004 May;10(5):535-539.

(98) Dougan SK, Rava P, Hussain MM, Blumberg RS. MTP regulated by an alternate promoter is essential for NKT cell development. J Exp Med 2007 Mar 19;204(3):533-545.

(99) Kotas ME, Lee HY, Gillum MP, Annicelli C, Guigni BA, Shulman GI, et al. Impact of CD1d deficiency on metabolism. PLoS One 2011;6(9):e25478.

(100) Elinav E, Pappo O, Sklair-Levy M, Margalit M, Shibolet O, Gomori M, et al. Adoptive transfer of regulatory NKT lymphocytes ameliorates non-alcoholic steatohepatitis and glucose intolerance in ob/ob mice and is associated with intrahepatic CD8 trapping. J Pathol 2006 May;209(1):121-128.

(101) Li Z, Oben JA, Yang S, Lin H, Stafford EA, Soloski MJ, et al. Norepinephrine regulates hepatic innate immune system in leptin-deficient mice with nonalcoholic steatohepatitis. Hepatology 2004 Aug;40(2):434-441.

(102) Yang L, Jhaveri R, Huang J, Qi Y, Diehl AM. Endoplasmic reticulum stress, hepatocyte CD1d and NKT cell abnormalities in murine fatty livers. Lab Invest 2007 Sep;87(9):927-937.

(103) Kremer M, Thomas E, Milton RJ, Perry AW, van RN, Wheeler MD, et al. Kupffer cell and interleukin-12-dependent loss of natural killer T cells in hepatosteatosis. Hepatology 2010 Jan;51(1):130-141.

(104) Suzuki A, McCall S, Choi SS, Sicklick JK, Huang J, Qi Y, et al. Interleukin-15 increases hepatic regenerative activity. J Hepatol 2006 Sep;45(3):410-418.

(105) Zeng J, Howard JC. Spontaneous focal activation of invariant natural killer T (iNKT) cells in mouse liver and kidney. BMC Biol 2010;8:142.

(106) Stetson DB, Mohrs M, Reinhardt RL, Baron JL, Wang ZE, Gapin L, et al. Constitutive cytokine mRNAs mark natural killer (NK) and NK T cells poised for rapid effector function. J Exp Med 2003 Oct 6;198(7):1069-1076.

(107) Seki S, Kitada T, Yamada T, Sakaguchi H, Nakatani K, Wakasa K. In situ detection of lipid peroxidation and oxidative DNA damage in non-alcoholic fatty liver diseases. J Hepatol 2002 Jul;37(1):56-62.

(108) Das KS, Balakrishnan V, Mukherjee S, Vasudevan DM. Evaluation of blood oxidative stress-related parameters in alcoholic liver disease and non-alcoholic fatty liver disease. Scand J Clin Lab Invest 2008;68(4):323-334.

(109) Hotamisligil GS. Mechanisms of TNF-alpha-induced insulin resistance. Exp Clin Endocrinol Diabetes 1999;107(2):119-125.

(110) Li L, He Q, Huang X, Man Y, Zhou Y, Wang S, et al. NOX3-derived reactive oxygen species promote TNF-alpha-induced reductions in hepatocyte glycogen levels via a JNK pathway. FEBS Lett 2010 Mar 5;584(5):995-1000.

(111) Garcia-Monzon C, Lo IO, Mayoral R, Gonzalez-Rodriguez A, Miquilena-Colina ME, Lozano-Rodriguez T, et al. Hepatic insulin resistance is associated with increased apoptosis and fibrogenesis in nonalcoholic steatohepatitis and chronic hepatitis C. J Hepatol 2011 Jan;54(1):142-152.

(112) Moucari R, Asselah T, Cazals-Hatem D, Voitot H, Boyer N, Ripault MP, et al. Insulin resistance in chronic hepatitis C: association with genotypes 1 and 4, serum HCV RNA level, and liver fibrosis. Gastroenterology 2008 Feb;134(2):416-423.

(113) Romero-Gomez M, Del M, V, Andrade RJ, Salmeron J, Diago M, Fernandez-Rodriguez CM, et al. Insulin resistance impairs sustained response rate to peginterferon plus ribavirin in chronic hepatitis C patients. Gastroenterology 2005 Mar;128(3):636-641.

(114) Kaibori M, Kwon AH, Oda M, Kamiyama Y, Kitamura N, Okumura T. Hepatocyte growth factor stimulates synthesis of lipids and secretion of lipoproteins in rat hepatocytes. Hepatology 1998 May;27(5):1354-1361.

(115) Lin MC, Gordon D, Wetterau JR. Microsomal triglyceride transfer protein (MTP) regulation in HepG2 cells: insulin negatively regulates MTP gene expression. J Lipid Res 1995 May;36(5):1073-1081.

(116) Tajiri K, Shimizu Y, Tsuneyama K, Sugiyama T. Role of liver-infiltrating CD3+CD56+ natural killer T cells in the pathogenesis of nonalcoholic fatty liver disease. Eur J Gastroenterol Hepatol 2009 Jun;21(6):673-680.

(117) Syn WK, Oo YH, Pereira TA, Karaca GF, Jung Y, Omenetti A, et al. Accumulation of natural killer T cells in progressive nonalcoholic fatty liver disease. Hepatology 2010 Jun;51(6):1998-2007.

Acknowledgements

I wish my extreme thanks to Prof. Dr. med. Stephan C. Bischoff, Head, Institute of Nutritional Medicine and Prevention (180) for allowing and guiding me to do this thesis in his reputed laboratory.

I would also extend my sincere thanks to Prof. Dr. Lutz Graeve Institute of Biological chemistry and Nutrition (140c) for his guidance.

I express my deep sense of gratitude to PD Dr. Ina Bergheim, Institute of Nutritional Medicine and Prevention (180) for her excellent guidance and moral support during my thesis.

I would like to convey my special thanks to all my colleagues for their help and encouragement.

I convey my special thanks to my family for their continuous support in pursuing my work successfully.

My special thanks to Elsevier and Nature publishing group for publishing the work and allowing me reuse in the thesis.

I would also like to extend my deep sense of gratitude to all my friends, who made my social life better in Hohenheim.

Giridhar Kanuri

Declaration

I here by declare that this work has been originally carried out by me under the supervision of Prof. Dr. med. Stephan C. Bischoff, Head, Department of Nutritional Medicine and Prevention (180) and co-guided by Prof. Dr. Lutz Graeve. I have written this thesis by my own. Furthermore, I confirm that no other sources have been used than those specified in the thesis itself.

I further assure that this work has not been submitted either in whole or part for any other degree at any other university.

Giridhar Kanuri